Study of metal-metal bonds in transition metal compounds using quantum chemical methods

La Macchia, Giovanni

UNIVERSITÉ DE GENÈVE
Section de chimie et biochimie
Département de chimie physique

FACULTÉ DES SCIENCES
Professeur L. Gagliardi
Docteur T. A. Wesolowski

Study of metal-metal bonds in transition metal compounds using quantum chemical methods

THÈSE

présentée à la Faculté des sciences de l'Université de Genève
pour obtenir le grade de Docteur ès sciences, mention chimie

par
Giovanni LA MACCHIA
de
Genève (GE)

Thèse N° 4171

GENÈVE
Atelier d'impression ReproMail
2010

UNIVERSITÉ
DE GENÈVE

FACULTÉ DES SCIENCES

Doctorat ès sciences
mention chimie

Thèse de *Monsieur Giovanni LA MACCHIA*

intitulée :

" Study of Metal-Metal Bonds in Transition Metal Compounds Using Quantum Chemical Methods "

La Faculté des sciences, sur le préavis de Monsieur T.A. WESOLOWSKI, docteur et directeur de thèse (Département de chimie), de Madame L. GAGLIARDI, professeure et codirectrice de thèse (Department of Chemistry, University of Minnesota, Minneapolis, United States of America) et de Monsieur Ch. J. CRAMER, professeur (Department of Chemistry and Supercomputer Institute, University of Minnesota, Minneapolis, United States of America), autorise l'impression de la présente thèse, sans exprimer d'opinion sur les propositions qui y sont énoncées.

Genève, le 12 janvier 2010

Thèse - 4171 -

Le Doyen, Jean-Marc TRISCONE

N.B.- La thèse doit porter la déclaration précédente et remplir les conditions énumérées dans les "Informations relatives aux thèses de doctorat à l'Université de Genève".

Nombre d'exemplaires à livrer par colis séparé à la Faculté : - 4 -

Remerciements

Je remercie le Prof. C. J. Cramer et le Dr. T. A. Wesolowski pour avoir accepté de faire partie du jury de cette thèse. Je remercie le Prof. Laura Gagliardi pour m'avoir accueilli dans son groupe de recherche. Son comportement exemplaire, ses qualités humaines et scientifiques ont été d'une grande aide tout au long de ma thèse. Cela a été un plaisir d'avoir été le témoin de la naissance de son groupe de recherche en 2005 et de son développement au cours des années.

Je ne remercierai jamais assez mes parents pour leur soutien et leur affection durant toutes ces années. Ils m'ont toujours soutenu dans mon cursus scolaire et universitaire. Grâce à eux, j'ai pu traverser mes années d'étude avec calme et sérénité.

Mes remerciements s'adressent également à tous mes collègues et amis qui font et ont fait partie du groupe de recherche de Laura. Je remercie Juraj et Eugeniusz, notamment pour leurs compétences très utiles en informatique. Je remercie le prof. B. O. Roos et Marcin pour leurs connaissances dans le domaine de la chimie des métaux de transition. Je remercie Ivan pour m'avoir enseigné les bases de la chimie des actinides. Francesco et sa familiarité avec le programme Molcas m'ont permis de surmonter à plusieurs reprises des problèmes d'ordre technique. Je n'oublie pas les autres membres du groupe et leur amitié: Abdul, Daniel, César, Stephan, Helena. Je n'oublie pas le clan des Siciliens, Giovanni et Enza, pour leur bonne humeur et leur sympathie. Un merci particulier à Tanya, pour son amitié, sa simplicité et sa joie de vivre. Elle est et a été un élément fédérateur du groupe. Je remercie également les membres du groupe Wesolowski, Kuba et Georgios. Je tiens également à remercier Tatyana, pour sa bonne humeur et sa sympathie. Mes remerciements s'adressent aussi aux personnes que j'ai connues au cours de mes années universitaires.

Je remercie particulièrement Alfredo et Marcin pour leur amitié. C'est grâce à Alfredo que j'ai fait mes premiers pas en chimie computationnelle en m'incitant à faire un stage sous la supervision de Clémence. Je remercie le prof. Weber pour m'avoir accepté dans son groupe

de recherche dans le cadre d'un stage de diplôme. Je tiens également à remercier Pierre-Yves Morgantini que j'ai sollicité à maintes reprises au cours de ma thèse. Je n'oublie pas les amis que j'ai connus en dehors de l'université. Un clin d'oeil à Fariborz et à nos heures de révisions durant nos années de Collège. Un salut amical à Joël, pour sa passion pour le bon vin et la Sicile.

Résumé en français

Introduction

L'étude *des liaisons multiples entre métaux de transition* est une branche récente de la chimie [**1**]. Avant son avènement, la chimie des métaux de transition se basait essentiellement sur le schéma d'Alfred Werner [**2**] introduit au 19ème siècle. Selon ce modèle, les métaux de transition ne sont entourés que par des ligands, excluant ainsi la possibilité d'avoir des interactions métal-métal directes. Toujours selon le même modèle, seules des interactions indirectes par l'intermédiaire de ligands peuvent avoir lieu. Cette description est tout à fait correcte mais ne raconte pas la réactivité des métaux de transition dans son entier et par conséquent, elle nécessite d'être complétée.

Dans les années 1960, deux découvertes majeures ont permis de mettre en lumière les interactions métal-métal. La mise en évidence de ce genre d'interactions a eu un important impact dans la communauté scientifique. En effet, différents concepts liés à la définition de la *liaison chimique* et à sa *multiplicité*, qui étaient alors considérés comme acquis, ont dû subir une réévaluation. En 1963, la mise en évidence d'une triple double liaison dans la molécule de $[Re_3Cl_{12}]^{3-}$ par A. Cotton et ses collaborateurs [**3, 4**], a permis de mettre à jour la capacité des métaux de transition à interagir entre eux. En 1964, les mêmes chercheurs ont mis en évidence une liaison quadruple entre deux atomes de rhénium dans le composé $K_2[Re_2Cl_8]\bullet 2H_2O$ [**5-8**]. Cette dernière découverte a eu l'effet d'un tremblement de terre étant donné qu'elle redessinait la frontière de la liaison chimique, et plus spécifiquement, des liaisons multiples. Ainsi, la triple liaison gouvernée par les éléments du groupe p n'était plus la limite supérieure. L'implication des métaux de transition dans la chimie des liaisons multiples a permis d'ouvrir une brèche dans la quête d'ordres de liaison élevés.

En regardant de plus près le tableau périodique, il apparaît clairement que les éléments appartenant aux différents blocs qui le constituent ne sont pas égaux dans la formation des liaisons multiples. Ainsi, les éléments du bloc p peuvent former au mieux une triple liaison. La situation est totalement différente dans le cas des éléments du groupe d, dont la couche de

valence contient des orbitales s et d. Ces derniers ont donc un plus grand nombre d'orbitales à disposition pour former des liaisons multiples. Ainsi, les éléments du groupe 6, avec leur six électrons de valence, peuvent former des liaisons d'ordre six. Le franchissement de la barrière de la triple liaison s'accompagne d'une nouvelle interrogation: Quelle est l'ordre de liaison maximum entre deux atomes? La réponse à cette question est difficile étant donné que différents paramètres tels que le nombre d'électrons de valence et le type d'orbitales qui entrent en jeu doivent être pris en considération. De plus, la complexité à interpréter l'ordre de liaison est d'autant plus grande si les deux atomes considérés sont différents.

Depuis les années 1960, la chimie des liaisons multiples s'est concentrée sur les métaux de transition. Cependant, le tableau périodique a d'autres choix à proposer. Par exemple, il est judicieux de penser que des dimères formés par des atomes du groupe f, comme les actinides, puissent réaliser des ordres de liaisons élevés étant donné qu'ils ont une couche de valence plus étendue. Des études ont été menées afin de confirmer cette hypothèse. Ces dernières sont malheureusement peu nombreuses, ces éléments étant difficile à étudier en laboratoire.

L'ordre de liaison dans la chimie des dimères des métaux de transition

La liaison multiple d'ordre 4

La chimie des dimères des métaux de transitions a été dominée pendant près de quarante ans par la liaison d'ordre 4. $K_2[Re_2Cl_8]\bullet 2H_2O$, qui est le symbole de cette classe de molécules, a été étudié expérimentalement [**8, 9**] et théoriquement [**10**], ceci dans le but de mettre en évidence les différents types de liaison qui entrent en jeu et leur force relative. Une des caractéristiques de ce composé est sa conformation éclipsée. Cette dernière ne peut pas être expliquée si uniquement les répulsions Cl-Cl sont prises en considération. La raison de cette géométrie est à chercher dans la configuration électronique de la liaison multiple, qui est $\sigma^2\pi^4\delta^2$. Les liaisons de type σ et π sont fortes et par conséquent ne sont pas affectées par une quelconque rotation autour de l'axe Re-Re. La situation est différente lorsque les orbitales d_{xy} sont impliquées. Ces dernières forment la quatrième liaison, de type δ, entre les

deux métaux de transition uniquement quand elles sont toutes les deux alignées. Ainsi le gain en énergie résultant de la conformation éclipsée est plus important que les effets stériques résultant de la répulsion entre les atomes de chlore.

Etant donné qu'une grande partie des processus chimiques ont lieu en solution, les efforts se sont concentrés dans la synthèse de molécules capables de protéger la liaison multiple contre toutes interactions avec l'environnement qui pourrait affaiblir l'unité bimétallique. Dans ce contexte, l'utilisation d'une architecture de type "roue à aube" semble offrir une protection adéquate. De nombreuses molécules ont été synthétisées en suivant ce modèle:

Les *tetracarboxylates* de chrome sont un des plus vieux composés contenant l'unité $Cr_2{}^{4+}$, comme l'atteste la synthèse en 1844 par E. Peligot de l'acétate de chrome [**11**]. Cependant, la nature véritable de ce composé, qui contient une quadruple liaison Cr-Cr, lui était alors inconnue. De nos jours, plus de quarante structures de type $Cr_2(O_2CR)_4L_{(ax)_2}$ ont été étudiées. Une particularité de ces composés est la présence, dans la plupart des cas, de ligands le long de l'axe Cr-Cr. L'occupation de cette position a des effets importants sur la longueur de liaison bimétallique. En effet, une telle situation entraîne une augmentation de la densité électronique dans les orbitales anti-liantes de type σ^* ou π^*, qui s'accompagne par une élongation de la distance Cr-Cr.

Les *tetracarboxylates* [**1**] réussissent à stabiliser la liaison multiple métal-métal (M-M) mais ne permettent pas d'obtenir des longueurs de liaison Cr-Cr en dessous du seuil de 1.95 Å. A titre de comparaison, la longueur de liaison dans la molécule de Cr_2 est de 1.68 Å. L'utilisation de ligands de type *oxophenyl* permet de palier à ce problème. Cette stratégie a permis à F. A. Cotton de synthétiser en 1978 le composé $Cr_2(2\text{-}MeO\text{-}5\text{-}MeC_6H_3)_4$ [**12**], caractérisé par une liaison bimétallique de 1.828 Å et qui a détenu pendant près de trente ans le records de la liaison Cr-Cr la plus courte. Différentes tentatives ont été menées afin de repousser la limite établie par Cotton. Dans cette perspective, des composés tels que les *2-oxopyridinates* et *les carboxamidates* ont été étudiés, sans grand succès. La capacité d'un ligand à accueillir une liaison M-M courte dépend de ses propriétés intrinsèques mais également du type d'architecture dans lequel il est impliqué. Ce dernier point est clairement

démontré par l'étude des *guanidinates* et des *amidinates* [**13**]. Ces deux ligands peuvent former une structure de type roue à aube, sans guère de progrès du point de vue de la longueur de liaison bimétallique. Cependant, leur utilisation dans le cadre de l'isolation de l'unité Cr_2^{2+} permet d'obtenir des liaisons Cr-Cr qui se rapprochent de plus en plus de la distance caractérisant la molécule de Cr_2 isolée.

La liaison multiple d'ordre 5

Pendant plus de quarante ans, l'attention s'est portée principalement sur les liaisons d'ordre quatre. La stratégie pour synthétiser des liaisons quadruples ou des liaisons d'ordre plus élevé consiste à choisir correctement le métal de transition ainsi que le ligand. Le choix du métal est assez aisé dans le cas des éléments du bloc d. Par exemple, ce dernier doit avoir six électrons de valence, distribués dans les orbitales nd et (n+1)s, pour pouvoir former une liaison sextuple. Tout l'art consiste à maintenir le plus grand nombre d'électrons de valence mobilisé dans la formation de la liaison multiple. Pour ce faire le choix du ligand est crucial. Ce dernier doit être suffisamment volumineux pour protéger l'unité bimétallique contre toutes interactions avec l'environnement pouvant la déstabiliser. De plus, le ligand doit permettre de maintenir le métal dans un état d'oxydation le plus bas possible, de façon à permettre au plus grand nombre possible d'électrons de valence de former la liaison multiple.

Malgré les efforts mis en oeuvre, il a fallu attendre 2005 avant de pouvoir isoler un composé contenant une liaison quintuple. Ce composé, l' Ar'CrCrAr' [**14**] (Ar'=C_6H_3-2,6(C_6H_3-2,6-Pr^i_2)$_2$), synthétisé par le groupe de P. P. Power, se base sur le ligand terphenyl et est caractérisé par une longueur de liaison Cr-Cr de 1.835 Å. L'utilisation de ligands de type terphenyl a suscité un grand intérêt. Par la suite, différentes études ont été effectuées dans le but de mieux comprendre l'effet de ce ligand sur l'unité bimétallique. Une des particularités des composés ArMMAr est leur conformation de type trans. Des calculs computationnels menés sur différentes molécules HM-MH ont démontré que cette géométrie est préférée parce qu'elle permet d'établir une liaison σ forte [**15**].

La découverte de P. P. Power a donné un second souffle à la chimie des dimères de métaux de transition, ouvrant ainsi une nouvelle voie dans la quête de la liaison Cr-Cr la plus courte.

En effet, seulement deux ans après la découverte de Ar'CrCrAr', Kreisel synthétisa un nouveau composé, le Cr_2-diazadiène [**16**]. Ce dernier est caractérisé par une distance Cr-Cr de 1.803 Å, battant ainsi le record jusqu'alors détenu par le composé de type roue à aube isolé en 1978 par Cotton.

Les années 2008 et 2009 ont également été fructueuses comme en témoigne la synthèse de nouveaux composés se basant sur des ligands tels que les *amidinates* [**17**], *lantern amidinates* [**18**], *aminopyridinates* [**19**] et *guanidinates* [**20**]. Les *amidinates* sont connus pour avoir des propriétés stériques et électroniques qui peuvent facilement être modifiées en changeant les groupes liés à l'atome de carbone ou d'azote. C'est une des raisons pour laquelle ce type de ligand a été utilisé dans le but d'isoler des liaisons Cr-Cr très courtes. Dans cette optique, Tsai et ses collaborateurs ont décidé d'utiliser ce genre d'architecture afin d'obtenir différentes structures de type $Cr_2(\mu\text{-}\eta^2\text{-ArNC(R)NAr})_2$ [**17**]. Ce genre de molécules permet l'isolation de longueurs de liaison Cr-Cr se situant aux alentours de 1.74 Å. Dans la section dédiée à la liaison quadruple, nous avons vu que les amidinates pouvaient être utilisés dans des structures de type roue à aube, où l'unité centrale Cr-Cr est entourée par quatre ligands. Ce genre de composés ne permet pas d'isoler des distances bimétalliques très courtes. Cependant, si un des ligands est enlevé, une architecture qui ressemble à une lanterne chinoise peut être créée, d'où la dénomination de "*lantern amidinates*". La forme neutre paramagnétique et celle réduite permettent d'obtenir respectivement des distances Cr-Cr de 1.817 Å et de 1.740 Å [**18**]. Par la suite, d'autres composés tels que les aminopyridinates [**19**] et les guanidinates [**20**] ont été synthétisés. Les premiers sont caractérisés par une distance Cr-Cr de 1.749 Å et les seconds par une distance de 1.729 Å, qui correspond actuellement à la distance Cr(I)-Cr(I) la plus courte.

Le ligand a pour fonction de protéger l'unité bimétallique et de maintenir le métal de transition dans un état d'oxydation le plus bas possible. Cependant, on ne peut pas comprendre la variation de la longueur de liaison Cr-Cr dans les différents composés ayant une liaison quintuple si on ne tient pas compte de l'effet du ligand sur la distance bimétallique. Dans le cas du chrome, la valeur de cette dernière se situe entre 1.835 Å (Ar'CrCrAr') et 1.729 Å (Cr_2-guanidinate). Le composé isolé par P. P. Power, l'Ar'CrCrAr', constitue la limite supérieure. Ceci s'explique aisément en regardant la nature du ligand utilisé. En effet,

chaque centre métallique est relié à un terphenyl (Ar') dont la fonction est, comme cela a été mentionné précédemment, de protéger l'unité Cr-Cr. Cependant, les deux terphenyls ne sont pas reliés entre eux et par conséquent, ils ne peuvent pas vraiment imposer de contraintes stériques sur la liaison bimétallique. L'utilisation de *ligands pontés* permet de moduler plus facilement la longueur de liaison métal-métal. Les diazadiènes, amidinates, aminopyridinates et guanidinates font partie de cette famille de ligand. Leur capacité à exercer une contrainte sur les deux métaux de transition, à l'instar d'une pince, dépend étroitement de leur architecture:

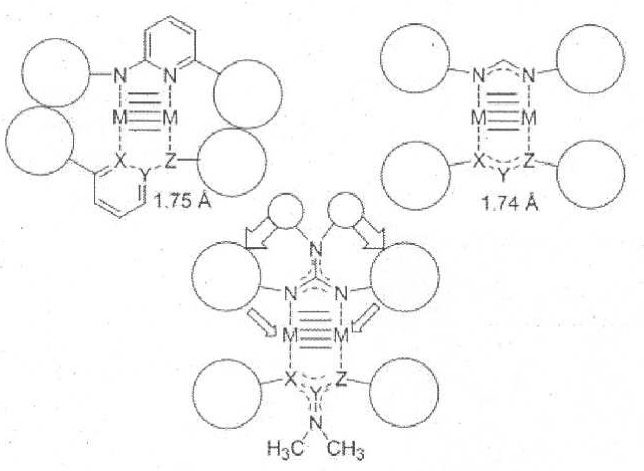

Figure 1: aminopyridinate (en haut à gauche), amidinate (en haut à droite) et guanidinate (en bas)

L'utilisation de groupes encombrés permet tout d'abord d'éviter d'avoir une liaison Cr-N trop courte, évitant ainsi une élongation de la distance Cr-Cr, les deux longueurs de liaison étant étroitement connectées. Cette fonction est parfaitement remplie par les amidinates et les aminopyridinates. De plus, les groupes se trouvant dans la partie externe de l'édifice moléculaire permettent également de moduler l'angle du fragment NC(R)N, qui fait office de pince. Dans ce contexte, les guanidinates sont particulièrement adaptés étant donné que le fragment NC(N)N est planaire. Ainsi, l'utilisation de groupes plus encombrés, connectés à l'atome d'azote périphérique, permet d'exercer une contrainte beaucoup plus efficace, avec à la clef une distance Cr-Cr très courte.

La liaison multiple d'ordre 6

Avant la synthèse en 2005 de Ar'CrCrAr', l'unique évidence de l'existence d'un ordre de liaison supérieur à quatre était l'isolation de dimères de métaux de transition comme la molécule de Cr_2. Cependant, leur isolation a été très difficile à cause de leur instabilité. Néanmoins leur étude est nécessaire afin de mieux comprendre la configuration électronique de ces dimères, une fois inclus dans des molécules plus complexes.

☛ Cr_2: la pièce maîtresse de la chimie des dimères de chrome

En 1974 [**21**] et 1975 [**22**], Efremov et Kündig ont mis en évidence le dimère de chrome à travers deux expériences différentes. Depuis lors, d'autres études ont été menées. De nos jours, les valeurs les plus précises sont 1.68 Å [**23, 24**] et 1.53 eV [**25, 26**], correspondant respectivement à la longueur de liaison bimétallique et à l'énergie de dissociation. Une des caractéristiques de Cr_2 est la complexité de sa configuration électronique, qui a pour origine la différence entre la distribution radiale des orbitales 4s et 3d. Ainsi, à la distance d'équilibre, la liaison entre les deux centres métalliques est dû principalement aux orbitales 3d, étant donné que les interactions entre les orbitales 4s sont plus répulsives. Une élongation de la liaison Cr-Cr est accompagnée par l'apparition d'un plateau dans la courbe d'énergie potentielle, qui a pour origine l'interaction entre les deux orbitales 4s. A cette distance, les orbitales 3d ne participent plus à la liaison chimique et les électrons correspondant sont couplés de manière antiferromagnétique.

☛ Cr_2: un défi pour la chimie computationnelle

Parmi les différents dimères de métaux de transition, la molécule de Cr_2 a souvent été utilisée comme standard afin de tester les performances d'une méthode donnée, le but étant

d'essayer de reproduire les valeurs expérimentales pour la longueur de liaison (1.68 Å) et l'énergie de dissociation (1.53 eV). Différentes techniques, correspondant à différents niveaux de complexité, ont été testées. Le succès ou l'échec d'un modèle théorique dépend de sa capacité à décrire le caractère multiconfigurationnelle de la fonction d'onde et la corrélation électronique. Etant donné qu'au sein de chaque méthode différents paramètres peuvent être réglés, le choix de ces derniers est également important pour l'obtention de résultats en accord avec les valeurs de référence. Ainsi, lorsque la théorie de la fonctionnelle de la densité (DFT) est utilisée, le choix de la fonctionnelle joue un rôle non négligeable dans la qualité des résultats obtenus.

Au-delà de la liaison sextuple: chimère ou réalité?

De nos jours, l'existence de la liaison d'ordre six ne fait plus aucun doute. Maintenant, il s'agit de savoir si l'on doit considérer cet ordre de liaison comme la limite supérieure ou si des ordres de liaisons supérieurs à six sont possibles. La couche de valence étendue des éléments du bloc f laisse penser que ces derniers soient autant capables, si ce n'est de faire mieux, que les atomes du bloc d. Ce dernier point reste encore à démontrer. Malgré la complexité de leur configuration électronique et de la difficulté à les manipuler en laboratoire, la chimie des dimères de lanthanides et d'actinides est encore un domaine qui demande à être exploré. Par exemple, dans la famille des actinides, seulement des interactions directes entre deux atomes d'uranium ont pu être mis en évidence. Ceci a pu être possible à travers l'étude de la molécule d'U_2 [**27**], de H_2UUH_2 [**28**] et d'OUUO [**27**]. La manipulation de ces composés est difficile en laboratoire mais est tout à fait abordable dans le cadre de calculs computationnels.

Lors de l'étude de dimères d'actinides, la connaissance du nombre d'électrons de valence disponible ne peut pas, à lui seul, permettre une évaluation sûre de l'ordre de liaison, étant donné que ce dernier requiert la prise en considération de différents facteurs. La configuration électronique de l'atome d'uranium, $(5f)^3(6d)^1(7s)^2$, est un exemple représentatif. Malgré le fait que l'orbitale 7s soit doublement occupée, la formation d'orbitales hybrides avec les orbitales 6d et 7p rend la formation d'une liaison sextuple possible. Cependant, la situation est plus complexe qu'elle ne paraît. Premièrement, 16 orbitales, incluant les orbitales 5f, 6d, 7s et 7p, sont suffisamment proches en énergie et sont donc susceptibles d'être impliquées

dans la liaison multiple. De plus, étant donné que ces orbitales ont des distributions radiales différentes, leur degré de superposition sera également différent, selon le type d'orbitale considéré.

Les différents points mentionnés auparavant rendent l'évaluation de l'ordre de liaison difficile. Par exemple, contrairement aux apparences, la molécule de U_2 est une liaison quintuple et non une liaison sextuple, comme cela a été démontré dans une précédente étude computationnelle. De plus, la liaison multiple dans cette molécule diatomique est assez complexe. En effet, elle se décompose en trois liaisons covalentes, deux liaisons à un électron, deux liaisons faibles à un électron et deux électrons non-liants [**29**].

A cause de sa stabilité et de son habilité à former une liaison multiple, l'atome d'uranium pourrait être à la base d'une nouvelle chimie ayant comme pièce maîtresse la molécule d'U_2, comme le démontre l'étude de différents composés tels que des chlorures et des carboxylates, qui a mis en évidence la stabilité et le caractère multiple de la liaison U-U [**30**]. Des calculs effectués sur l'unité ${U_2}^{2+}$ [**31**] ont montré que sa configuration électronique était $\sigma^2\pi^4\delta_g^1\delta_u^1\varphi_u^1\varphi_g^1$, ce qui correspond à une triple liaison. Par analogie, on pourrait s'attendre à ce que des composés du type RU(I)-U(I)R, qui incluent des ligands, soient également décrits par cette configuration électronique. Cependant, ce genre d'extrapolation n'est pas si évident. Par exemple, la configuration électronique du composé PhUUPh est $\sigma^2\sigma^2\pi^4\delta^2$ et correspond à une liaison quintuple plutôt que à une triple liaison.

Introduction aux méthodes computationnelles

La théorie de la fonctionnelle de la densité

La théorie de la fonctionnelle de la densité (DFT) se base sur la densité électronique ρ. Hohenberg et Kohn [**32**] ont démontré en 1964 que ρ est suffisante pour décrire l'état électronique fondamental. La densité électronique $\rho(\vec{r}) = \int \psi^*(\vec{r}_1, \vec{r}_2, \ldots \vec{r}_N)\psi(\vec{r}_1, \vec{r}_2, \ldots \vec{r}_N)d\vec{r}_2, d\vec{r}_3, ..., d\vec{r}_N$ est décrite seulement par trois coordonnées, indépendamment du nombre d'électrons, contrairement à la fonction d'onde ψ qui dépend de 3N coordonnées. ρ est donc moins compliquée

que ψ et par conséquent permet la description de systèmes plus grands avec un bon rapport précision/coût. L'énergie dépend de la densité électronique:

$$E[\rho] = T[\rho] + E_{ne}[\rho] + E_{ee}[\rho]$$

Etant donné qu'il est difficile de déterminer exactement les fonctionnelles décrivant l'énergie cinétique et l'énergie d'échange, Kohn et Sham ont élaboré une stratégie en 1965 **[33]**, qui consiste à résoudre un problème d'électrons indépendants évoluant dans un potentiel externe. Ce système simplifié est décrit par un déterminant de Slater construit à partir d'un set d'orbitales qui sont solutions des équations de Kohn-Sham. Ces orbitales sont utilisées pour définir l'énergie cinétique $T_s[\rho]$:

$$T_s[\rho] = -\tfrac{1}{2}\sum_{j=1}^{N}\langle\chi_j|\nabla_j^2|\chi_j\rangle \qquad \rho_s(\overrightarrow{r}) = \sum_{j=1}^{N}|\chi_j|^2$$

Ce terme apparaît dans la définition de l'énergie, qui tient en compte également d'une nouvelle fonctionelle, $E_{xc}[\rho]$, qui inclue les corrections concernant l'énergie cinétique et l'énergie de répulsion entre les électrons:

$$E[\rho] = T_s[\rho] + J[\rho] + E_{en} + E_{nn} + E_{xc}[\rho]$$

$$E_{xc}[\rho] = T[\rho] - T_s[\rho] + E_{ee}[\rho] - J[\rho]$$

Pour un système simplifié considérant des électrons indépendants évoluant dans un potentiel externe, l'énergie peut être définie en tenant compte des orbitales Kohn-Sham:

$$E[\rho] = -\tfrac{1}{2}\sum_{j=1}^{N}\langle\chi_j|\nabla_j^2|\chi_j\rangle + \tfrac{1}{2}\sum_{j=1}^{N}\sum_{i=1}^{N}\int\int\langle\chi_j\chi_i|\tfrac{1}{r_{12}}|\chi_j\chi_i\rangle - \sum_{a=1}^{M}\sum_{j=1}^{N}Z_a\langle\chi_j|\tfrac{1}{r_{12}}|\chi_j\rangle$$

$$+\sum_{a=1}^{M}\sum_{b=1}^{M}\frac{Z_aZ_b}{r_{ab}} + E_{xc}[\rho]$$

Les orbitales Kohn-Sham sont les solutions du système d'équations différentielles couplées suivant:

$$\left\{-\frac{1}{2}\nabla_1^2 - \sum_{a=1}^{M}\frac{Z_a}{r_{aj}} + V_{KS}(r_1)\right\}\chi_j = \varepsilon_j\chi_j$$

$$V_{KS}(\overrightarrow{r_1}) = \int \frac{\rho(\overrightarrow{r_2})}{r_{12}} d\overrightarrow{r_2} + V_{xc}(\overrightarrow{r_1})$$

$$V_{xc}(r) = \frac{\delta E_{xc}[\rho]}{\delta\rho(r)}$$

V_{KS} est ajusté de façon à ce que la même densité soit obtenue pour le système hypothétique avec des électrons indépendants et le système réel. Une des difficultés consiste à déterminer le potentiel d'échange-corrélation. De nos jours différents modèles sont à disposition, tels que LDA (approximation de la densité locale), GGA (approximation des gradients généralisée) et les méthodes hybrides.

La méthode CASSCF/CASPT2

La seule possibilité afin de décrire de manière exacte la corrélation électronique consiste à prendre en considération *une configuration d'interaction complète*, ce qui est impossible. Une solution abordable consiste soit à limiter le nombre de déterminants dans le développement la fonction d'onde, en fixant un seuil pour le nombre d'excitations possibles, soit utiliser la méthode CASSCF [**34**] (*champ auto-cohérent dans l'espace actif complet*), qui est plus élégante. La force de cette dernière réside dans le choix des orbitales utilisées dans l'expansion de la fonction d'onde. Ce choix est déterminé par des critères chimiques et donc requiert des connaissances préliminaires de la configuration électronique du composé qui est à l'étude. Cette méthode se base sur le partitionnement des orbitales moléculaires en trois différents groupes: les *orbitales inactives*, qui sont toujours doublement occupées; les *orbitales actives*, dont le nombre d'occupation peut varier entre 0 et 2; *les orbitales externes*, qui englobent les orbitales restantes et qui ne sont pas occupées.

La fonction d'onde CASSCF tient en compte la corrélation non-dynamique mais ne décrit pas correctement la corrélation dynamique. Afin de palier à ce problème, la théorie de

la perturbation de l'espace actif complet ou CASPT2 peut être utilisée. Afin de mieux comprendre la théorie de la perturbation, nous allons voir le cas simple pour lequel la fonction d'onde est un simple déterminant de Slater **[35]**. L'Hamiltonien total du système est divisé en deux parties: l'Hamiltonien d'ordre zéro, H_0, dont les valeurs propres et fonctions propres sont connues, et une perturbation V. L'équation aux valeurs propres devient:

$$\hat{H}\,|\Phi_i\rangle=(\hat{H}_0+\hat{V})|\Phi_i\rangle=\varepsilon_i\,|\Phi_i\rangle$$

Les fonctions propres et valeurs propres de $\hat{H}_0$ sont connues:

$$\hat{H}_0\left|\psi_i^{(0)}\right\rangle=E_i^{(0)}\left|\psi_i^{(0)}\right\rangle$$

Si la perturbation $\hat{V}$ est petite, on s'attend à ce que $|\Phi_i\rangle$ et ε_i soient respectivement proches de $\left|\psi_i^{(0)}\right\rangle$ et $\mathrm{E}_i^{(0)}$. Le but consiste à amméliorer $|\Phi_i\rangle$ et ε_i de manière à ce qu'ils deviennent le plus proche possible des fonctions propres et valeurs propres de l'Hamiltonien total. Afin de parvenir à ce résultat, $|\Phi_i\rangle$ et ε_i sont exprimés sous la forme de séries de Taylor. Un paramètre λ, dont la valeur est comprise entre 0 (pas de perturbation) et 1 (perturbation totale), est également introduit.

$$\hat{H}=\hat{H}_0+\lambda\hat{V}$$

$$\varepsilon_i=E_i^{(0)}+\lambda E_i^{(1)}+\lambda^2 E_i^{(2)}+\ldots$$

$$|\Phi_i\rangle=\left|\psi_i^{(0)}\right\rangle+\lambda\left|\psi_i^{(1)}\right\rangle+\lambda^2\left|\psi_i^{(2)}\right\rangle+\ldots$$

$\mathrm{E}_i^{(n)}$ sont les énergies d'ordre n. Si l'on considère les fonctions propres de $\hat{H}_0$ comme normalisées et si l'on choisit la normalisation de $|\Phi_i\rangle$ de telle sorte que l'égalité $\left\langle\psi_i^{(0)}\,|\Phi_i\right\rangle=1$ se

vérifie, on peut substituer les expressions pour $|\Phi_i\rangle$ et ε_i dans l'équation aux valeurs propres et ensuite l'égalisation des facteurs λ^n permet d'obtenir les équations d'ordre n (n=0,1,2,...):

$$\hat{H}_0 \left|\psi_i^{(0)}\right\rangle = E_i^{(0)} \left|\psi_i^{(0)}\right\rangle \text{n=0}$$

$$\hat{H}_0 \left|\psi_i^{(1)}\right\rangle + \hat{V} \left|\psi_i^{(0)}\right\rangle = E_i^{(0)} \left|\psi_i^{(1)}\right\rangle + E_i^{(1)} \left|\psi_i^{(0)}\right\rangle \text{n=1}$$

$$\hat{H}_0 \left|\psi_i^{(2)}\right\rangle + \hat{V} \left|\psi_i^{(1)}\right\rangle = E_i^{(0)} \left|\psi_i^{(2)}\right\rangle + E_i^{(1)} \left|\psi_i^{(1)}\right\rangle + E_i^{(2)} \left|\psi_i^{(0)}\right\rangle \text{n=2}$$

$$\hat{H}_0 \left|\psi_i^{(3)}\right\rangle + \hat{V} \left|\psi_i^{(2)}\right\rangle = E_i^{(0)} \left|\psi_i^{(3)}\right\rangle + E_i^{(1)} \left|\psi_i^{(2)}\right\rangle + E_i^{(2)} \left|\psi_i^{(1)}\right\rangle + E_i^{(3)} \left|\psi_i^{(0)}\right\rangle \text{n=3}$$

En multipliant chacune de ces équations par $\left\langle\psi_i^{(0)}\right|$, on obtient les expressions suivantes pour les énergies d'ordre n:

$$E_i^{(0)} = \left\langle\psi_i^{(0)}\right| \hat{H}_0 \left|\psi_i^{(0)}\right\rangle$$

$$E_i^{(1)} = \left\langle\psi_i^{(0)}\right| \hat{V} \left|\psi_i^{(0)}\right\rangle$$

$$E_i^{(2)} = \left\langle\psi_i^{(0)}\right| \hat{V} \left|\psi_i^{(1)}\right\rangle$$

$$E_i^{(3)} = \left\langle\psi_i^{(0)}\right| \hat{V} \left|\psi_i^{(2)}\right\rangle$$

Dans la plupart des cas, seules les corrections du deuxième ordre sont incluses. L'utilisation de la fonction d'onde CASSCF comme fonction d'onde de référence pour le traitement perturbatif ajoute de nouvelles difficultés [**36, 37**].

La chimie quantique et l'étude de la liaison métal-métal dans différents composés

Les métaux de transition ont pendant plus de cinquante ans dominé la chimie des liaisons multiples. L'isolation en 2005 d'une liaison quintuple dans la molécule Ar'CrCrAr' a fait renaître un regain d'intérêt dans ce domaine de recherche. Ces efforts ont aboutit à la synthèse de différents composés du type RM(I)-M(I)R contenant l'unité bimétallique $(M_2)^{2+}$. Des progrès considérables ont été effectués afin de stabiliser et isoler des liaisons métal-métal courtes. La réactivité et les domaines d'application de ce genre de composé sont à l'heure actuelle à l'étude et les résultats préliminaires obtenus semblent prometteurs. A titre d'exemple, il a été démontré en 2009 que la liaison multiple Cr-Cr est impliquée dans un processus de carbométallation. Cette découverte est très intéressante, car elle montre que la chimie des liaisons multiples partage des points communs avec la chimie du carbone.

Ce manuscrit s'inscrit dans le cadre de l'étude des liaisons multiples entre métaux de transition et propose une analyse de la structure électronique de différents composés contenant l'unité bimétallique (M_2), en utilisant des méthodes computationnelles, dites *ab initio*, se basant sur une fonction d'onde de type CASSCF à laquelle on applique une perturbation de second ordre (CASPT2). Cette thèse est organisée de la manière suivante: La **partie II** a pour objectif d'introduire *la chimie des liaisons multiples impliquant des métaux de transition* en abordant différents thèmes: le *chapitre 1* de la partie II traitera brièvement du rôle des métaux de transition en chimie. Etant donné que la liaison chimique sera traitée tout au long du manuscrit, le *chapitre 2* sera consacré à sa description et à l'évolution de sa définition au cours du temps. De plus, différentes méthodes de quantification de la multiplicité de la liaison chimique seront discutées. Dans le *chapitre 3*, les différentes étapes qui ont menées à la naissance de la chimie des liaisons multiples entre les métaux de transitions seront décrites. Les différents ordres de liaison que cette classe d'atome peut atteindre seront décrits dans le *chapitre 4*. Le dernier chapitre de la partie II introduira brièvement les différentes méthodes computationnelles actuellement utilisées dans l'étude de composés contenant l'unité M-M faisant intervenir les métaux de transition du bloc d. L'accent sera porté sur la méthode CASSCF et CASPT2 qui se base sur l'espace actif complet, et également sur la théorie de la

fonctionnelle de la densité (DFT).

La **partie III** se propose de décrire les résultats obtenus dans le cadre de l'étude de composés caractérisés par une liaison d'ordre 5 et contenant le chrome comme métal de transition (chapitres 1 à 3) ou l'atome d'uranium (chapitre 4):

Dans le premier chapitre [**38**], il sera question de mettre en évidence les effets du ligand terphenyl sur la liaison bimétallique. Les méthodes DFT et CASPT2 seront utilisées afin d'étudier des modèles simplifiés: MeMMMe, PhMMPh, (MeMMMe)(C_6H_6)$_2$, Ar§MMAr§, Ar$^{\#}$MMAr$^{\#}$ (M = Cr, Fe, Co; Ar§= C_6H_4-2(C_6H_5), Ar$^{\#}$ = C_6H_3-2,6(C_6H_3-2,6-Me_2)$_2$). Le but est de mettre en évidence l'importance des interactions métal-arène à travers l'étude de systèmes plus simples tels que MeMMMe et PhMMPh. Les calculs effectués indiquent que dans le cas du chrome ces interactions sont faibles et n'ont pas un impact important sur la liaison quintuple. La situation est différente quand le fer et le cobalt sont impliqués. En effet, quand l'unité bimétallique contient un de ces deux métaux de transition, des interactions très fortes de type η^6-arène sont mis en évidence. Par conséquent, il y a un affaiblissement de la liaison bimétallique.

Le deuxième chapitre [**39**] se consacre à l'étude de la configuration électronique du composé Cr_2-diazadiène. Ce composé, synthétisé en 2007 par Kreisel, est caractérisé par une longueur de liaison Cr-Cr de 1.803 Å. Dans le but d'étudier de manière précise la configuration électronique de cette molécule, des calculs CASPT2 ont été effectués sur une structure simplifiée, où les groupes isopropyles ont été substitués par des méthyles. La distance bimétallique obtenue, 1.799 Å, est en accord avec la valeur expérimentale. Le point le plus important concerne la nature de la configuration électronique de la liaison multiple. En effet, dans le cas présent une interaction de type π avec le ligand est mise en évidence. Ce genre d'interaction n'a pas lieu avec Ar'CrCrAr' et PhCrCrPh, où seulement une interaction de type σ est observée. La configuration électronique dans le cas du Cr_2-diazadiène est (Cr-Cr)σ^2(Cr-Cr)π^4(Cr-Cr)δ^2(Cr-N)π^4. Ce composé est donc caractérisé par une liaison quadruple et non une liaison quintuple [**39**].

Le troisième chapitre [**13**] se propose d'étudier différents composés qui se sont succédés après la synthèse du Cr_2-diazadiène. Le but est d'étudier la relation entre l'ordre de liaison effectif (EBO), qui donne une bonne analyse de l'ordre de liaison dans la molécule, et la distance de liaison Cr-Cr dans différents composés tels que les amidinates, aminopyridinates et guanidinates. Une des conclusions de cette étude est qu'il y a une corrélation linéaire entre la longueur de liaison bimétallique et l'EBO, pour autant que les différents composés étudiés appartiennent à la même famille. Ainsi un composé contenant le terphenyl (Ar') ne peut pas être comparé avec des composés contenant des ligands différents tels que les ligands pontés. De plus, il s'agit d'être attentif à la nature de la configuration électronique de la liaison multiple. Par exemple, le Cr_2-diazadiène est associé à une longueur bimétallique courte. Cependant la distance Cr-Cr de ce dernier ne peut pas être comparée avec celle associée aux autres structures contenant des ligands pontés, étant donné que contrairement au Cr_2-diazadiène, les composés tels que les amidinates, aminopyridinates et guanidinates sont caractérisés par la configuration électronique $\sigma^2\pi^4\delta^4$. En tenant compte des contraintes citées précédemment, l'EBO peut être utilisé pour avoir une idée de la force de la liaison multiple.

Le quatrième chapitre [**40**] de la partie III sera dédié à l'étude de la configuration électronique d'un composé à l'architecture similaire à celle du composé terphenyl, le PhU-UPh. Dans le cas présent le chrome est remplacé par un atome d'uranium. Deux isomères de PhUUPh, la conformation linéaire et trans, ont été étudiés au niveau DFT et CASPT2. Les résultats obtenus indiquent que la conformation trans est la plus basse en énergie et correspond à un singulet ^1A_g. Le premier état excité correspond à un triplet ^3A_g de la conformation trans et se situe à moins de 1 kcal mol^{-1} de l'état fondamental. La configuration électronique de ce dernier est $\sigma^2\sigma^2\pi^4\delta^2$. L'étude théorique de ce composé a été menée afin de vérifier la possibilité d'inclure l'unité diuranium dans des structures plus complexes permettant l'isolation de liaisons multiples d'ordre élevé.

Bibliography

[1] Cotton, F.A., Murillo, C.A. and Walton, R.A. Multiple bond between metal atoms 3rd ed. Berlin : Springer, 2005.

[2] Kauffman, G.B. 1973, *Coord. Chem. Rev.* 9, p. 339.

[3] Bertrand, J.A., Cotton, F.A., Dollase, W.A. 1963, *J. Am. Chem. Soc.* 85, p. 1349.

[4] Bertrand, J.A., Cotton, F.A., Dollase, W.A. 1963, *Inorg. Chem.* 2, p. 1166.

[5] Cotton, F. A., Curtis, N. F., Harris, C. B., Johnson, B. F. G., Lippard, S. J., Mague, J.T, Robinson, W.R. and Wood, J.S. 1964, *Science* 145, p. 1305.

[6] Cotton, F. A., Curtis, N. F., Johnson, B. F. G., Robinson, W. R. 1965, *Inorg. Chem.* 4 , p. 326.

[7] Cotton, F. A., Harris, C. B. 1965, *Inorg. Chem.* 4, p. 330.

[8] Cotton, F.A. 1965, *Inorg. Chem.* 4, p. 334.

[9] Trogler, W.C. and Gray, H.B. 1978, *Acc. Chem. Res.* 11, p. 232.

[10] Gagliardi, L. and Roos, B.O. 2003, *Inorg. Chem.* 42, p. 1599.

[11] Peligot, E. 1844, *C.R. Hebd. Seances Acad. Sci.* 19, p. 609.

[12] Cotton, F. A., Koch, S. A., Millar, M. 1978, *Inorg. Chem.* 17, p. 2084.

[13] La Macchia, G., Li Manni, G., Todorova, T. K., Brynda, M. , Roos, B. O. and Gagliardi, L. *submission stage*

[14] Nguyen, T., Sutton, A. D., Brynda, M., Fettinger, J.C., Long, G. J., Power, P. P. 2005, *Science* 310, p. 844.

[15] Landis, C. R., Weinhold, F. 2006, *J. Am. Chem. Soc.* 128, p. 7335.

[16] Kreisel, K. A., Yap, G. P. A., Dmitrenko, O., Landis, C. R., Theopold, K. H. 2007, *J. Am. Chem. Soc.* 129, p. 14162.

[17] Hsu, C.-W., Yu, J.-S. K., Yen, C.-H., Lee, G.-H., Wang, Y., Tsai, Y.-C. 2008, *Angew. Chem. Int. Ed.* 47, p. 9933.

[18] Tsai, Y.-C.; Hsu, C.-W.; Yu, J.-S. K.; Lee, G.-H.; Wang, Y.; Kuo, T.-S. *Angew. Chem., Int. Ed.* 2008, 47, 7250.

[19] Noor, A., Wagner, F. R., Kempe, R. 2008, *Angew. Chem. Int. Ed.* 47, p. 7246.

[20] Noor, A., Glatz, G., Müller, R., Kaupp, M., Demeshko, S. and Kempe, R. 2009, *Z. Anorg. Allg. Chem.* 635, p. 1149.

[21] Efremov, Y.M., Samoilova, A.N. and Gurvich, L.V. 1974, *Opt. Spectry.* 36, p. 381.

[22] Kündig, E. P., Moskovits, M., Ozin, G. A. 1975, *Nature* 254, p. 503.

[23] Bondebey, V. E., English, J. H. 1983, *Chem. Phys. Lett.* 94, p. 443.

[24] Michalopoulos, D.L. Geusic, M.E., Hansen, S.G., Powers, D.E. and Smalley, R.E. 1982, *J. Phys. Chem.* 86, p. 3914.

[25] Simard, B., Lebeault-Dorget, M.-A., Marijnissen, A., ter Meulen, J. J. 1998, *J. Chem. Phys.* 108, p. 9668.

[26] Hilpert, K. and Ruthardt, K. 1987, *Ber. Bunsenges. Physik. Chem.* 91, p. 724.

[27] Gorokhov, L.N., Emelyanov, A.M., Khodeev, Y.S. 1974, *Teplofiz. Vys. Temp.* 12, p. 1307

[28] Souter, P.F., Kushto, G.P., Andrews, L. and Neurock, M. 1997, *J. Am. Chem. Soc.* 119, p. 1682

[29] Gagliardi, L. and Roos, B. O. 2005, *Nature* 433, p. 848

[30] Roos, B.O. and Gagliardi, L. 2006, *Inorg. Chem.* 45, p. 803

[31] Gagliardi, L., Pykkö, P. and Roos, B.O. 2005, *Phys. Chem. Chem. Phys.* 7, p. 2415

[32] Hohenberg, P. and Kohn, W. 1964, *Phys. Rev.* 136, p. B864.

[33] Kohn, W. and Sham, L.J. 1965, *Phys. Rev.* 140, p. A1133.

[34] Roos., B.O. [ed.] Chichester, England, chap. 69 K.P. Lawley (John Wiley & Sons Ltd. 1987, Advances in Chemical Physics; Ab Initio Methods in Quantum Chemistry-II, p. 399.

[35] Bartlett, R.J. 1981, *Ann. Rev. Phys. Chem.* 32, p. 359.

[36] Andersson, K., Malmqvist, P.-A., Roos, B.O., Sadlej, A.J. and Wolinski, K. 1990, *J. Phys. Chem.* 94, p. 5483.

[37] Andersson. K., Malmqvist, P.-A. and Roos, B.O. 1992, *J. Chem. Phys.* 96, p. 1218.

[38] La Macchia, G., Gagliardi, L., Power, P. P., Brynda, M. 2008, *J. Am. Chem. Soc.* 130, p. 5104.

[39] La Macchia, G., Aquilante, F., Veryazov, V., Roos, B.O. and Gagliardi L. 2008, *Inorg. Chem.* 47, p. 11455.

[40] La Macchia, G., Brynda, M. and Gagliardi L. 2006 (45), *Angew. Chem. Int. Ed.*, p. 6210

Contents

"It is nice to know that the computer understands the problem but I would like to understand it too."

E.P. Wagner

Part 1

This Thesis

The purpose of this thesis is to present the state of the art of multicenter transition metal chemistry. We will describe several molecules presenting high order multiple bonds with a special focus on dichromium compounds, which are good candidates for quintuple and higher order multiple bonds. The electronic configuration of these compounds has been investigated using highly acurrate *ab initio* methods such as CASSCF and CASPT2.

The **part II** will be a general introduction to the multiple bond involving transition metals. The *first chapter* will give a flavour about the role of transition metal in chemistry. Since the discussion will be centred on the chemical bond, the *second chapter* will be dedicated to its description and its definition throughout the time. The different ways to assess bond multiplicity will be also discussed. Before going further in the presentation of the various multiply bonded compounds, we will describe in the *third chapter* the origin of multicenter transition metal chemistry. In the *fourth chapter* we will go through the different bond multiplicities that d-block transition metals can afford, from the quadruple to the sextuple bond. The Cr_2 unit, in its bare form and within different ligand architectures will be analysed. The importance of the ligand for the isolation of molecules featuring high order multiple bonds and exhibiting increasingly shorter bimetallic distances will be discussed. The *fifth chapter* will give a brief introduction to the computational methods currently used in the di-metal multicenter chemistry, with special focus on the complete active space SCF (CASSCF) and CASPT2 methods, and also density functional theory (DFT).

The **part III** will be dedicated to the description of the results of the investigation performed on different compounds featuring a quintuple bond. The center of attention will be mainly the chromium atom, although other elements such as Co, Fe and U will be discussed:

In the *first paper* we will highlight the effects of the terphenyl ligand on the bimetallic unit. DFT and CASPT2 methods will be applied to investigate several simplified models: MeMMMe, PhMMPh, (MeMMMe)$(C_6H_6)_2$, $Ar^{\S}MMAr^{\S}$, $Ar^{\#}MMAr^{\#}$ (M = Cr, Fe, Co; $Ar^{\S}$= C_6H_4-2(C_6H_5), $Ar^{\#}$ = C_6H_3-2,6(C_6H_3-2,6-Me_2)$_2$). In smaller models such as MeMMe and PhMMPh no arene-metal interactions are occurring. Therefore, looking at the changes of some parameters such as the bimetallic bond distance, going from simpler to more complicate models, will allow to underline these interactions. The performed calculations showed that

the terphenyl ligand has only feeble effects on the bimetallic quintuple bond when chromium is involved. Unlike the former transition metal, cobalt and iron are featuring strong η^6-arene interactions which are associated with a weakening of the multiple bond.

The *second paper* will be dedicated to the investigation of the electronic configuration of Cr_2-diazadiene. This compound was synthesized in 2007 by Kreisel and co-workers and is featuring a dichromium bond distance of 1.803 Å. According to the DFT calculations they have performed, the electronic configuration is a singlet closed shell and the bond order is 4.3. The reported bond order is matter of debate and will be discussed farther in the paper. Since the dichromium diazadiene was opening a new path in the synthesis of increasingly shorter Cr-Cr unit, it is worth to investigate how the bond multiplicity compares to the one observed in Ar'CrCrAr' and in its related model PhCrCrPh using highly accurate computational method such as DFT and CASPT2. The latter calculations were performed on a slightly modified model, where the eight isopropyl ligands were replaced by methyl groups. The reported results clearly highlight that the multiple bond is better described by a $\sigma^2\pi^4\delta^2$ electronic configuration than the $\sigma^2\pi^4\delta^4$ one.

The *third paper* will focus on the study of different compounds featuring nitrogen-metal coordination which have been synthesized after Cr_2-diazadiene isolation in 2007. The aim is to look at the relationship between the effective bond order (EBO) and the Cr-Cr bond distance. We investigated different structures such as amidinates, lantern amidinates, aminopyridinates and guanidinates. This work allowed to demonstrate that there is a linear correlation between the Cr-Cr bond length and the effective bond order (EBO), provided that one compares dichromium compounds belonging to the same class of supporting ligands. Therefore compounds containing terphenly and bridging ligands should not be compared. Moreover the electronic configuration of the multiple bond has to be taken into account. For example, Cr_2-diazadiene as well as amidinates, aminopyridinates, guanidinates belongs to the same class of ligands and therefore according to the first rule they could be compared. However, the electronic configuration of Cr_2-diazadiene, $\sigma^2\pi^4\delta^2$, differs from the $\sigma^2\pi^4\delta^4$ electronic configuration featured by the other reported compounds. Having in mind the aforementioned constraints, one can use the EBO as a comparison tool to assess the stability of the multiple

bond.

The *fourth paper* of part III will consider other compounds where the transition metal is replaced by uranium in the diatomic unit. The U_2 molecule was reported to be stable and to exhibit a multiple bond character. Therefore, it seems that the diuranium unit could be the key element for the synthesis of more elaborate compounds featuring high order multiple bond. Since the terphenyl ligand is suitable to isolate and stabilise the diatomic unit, we decided here to investigate a simpler model, PhU-UPh. The linear and the trans isomer were studied at the DFT and CASPT2 level. The results showed that the trans configuration is the lowest in energy and corresponds to a ^1A_g state. The first excited state, ^3A_g, is trans as well and is only 1 kcal mol^{-1} higher in energy. The electronic configuration of the ground state is $\sigma^2\sigma^2\pi^4\delta^2$ and corresponds to a formal quintuple bond.

Part 2

Introduction

1. The role of transition metals in chemistry

Transition metals of the d-block are fascinating because of the variety of the chemical processes they take part into. For example, catalytic converters based on platinum, palladium and rhodium change poisonous molecules like carbon monoxide and various nitrogen oxides produced by cars into more harmless molecules like carbon dioxide and nitrogen. Since these metals are very expensive, other routes involving cobalt are investigated and seem to give promising results [**1**]. Transition metals are also employed in organic chemistry synthesis, like, for example, nickel based catalysts in double bond hydrogenation and chromium in ethylene polymerization [**2-7**]. The abovementioned examples represent only a part of the range of applications of metal catalysts. However, many of them are costly and environmentally unfriendly and therefore there is nowadays a rising interest in organic catalyzed reactions involving cheaper and less polluting metals such as copper and iron [**8**].

Catalysis is not the only area in which d-block transition metals are employed. Indeed, the sixties witnessed the birth of a new kind of chemistry involving these elements: the transition metal multicenter chemistry [**9**], which for the first time revealed the existence of compounds featuring direct metal-metal interactions and high order multiple bonds. For 40 years the metal-metal quadruple bond was considered the highest bond order. The isolation of a Cr-Cr quintuple bond in 2005 [**10**] using a terphenyl ligand was a new breakthrough and resulted in a resurrection of interest for metal-metal multiple bonds chemistry. This discovery was followed by the isolation of other compounds involving diazadienes, amidinates, aminopyridinates and guanidinates. All these structures exhibit very short metal-metal bond distances and high order multiple bonds. In Theopold's words, who synthesized the dichromium diazadiene compound [**11**],*"This molecule is probably not practically useful. We are not going to get a patent here or cure cancer"*. This statement is obsolete nowadays. Already in 2007 it was thus reported that a compound containing the M_2 unit (M=Mo,W) within a specific ligand architecture is featuring interesting electroluminescence properties [**12**]. More recently, in 2009, the carboalumination of a Cr-Cr multiple bond was reported [**13**]. There are only few examples but their existence clearly highlights the potential of the reactivity of the metal-metal multiple bonds and opens new perspectives.

2. The chemical bond and its quantification

2.1 The chemical bond throughout the time

The interactions between atoms are the foundation of all chemistry. They cannot be reduced to simple lines linking atoms one to another because they involve all kinds of interplays between electrons and nuclei that hold atoms together. How has the concept of chemical bond evolved throughout time? The first models, such as those proposed by Kekulé and others in the 19th century were quite simplistic because the nature of the atom itself was unknown. The discovery of the electron by J.J.Thompson in 1897 [**14**] and the experiment of E. Rutherford in 1909 [**15**], lead to the formulation of the Bohr's atom in 1913 [**16-18**]. With full knowledge of these facts, Lewis introduced the concept of shared electron pair in 1916 [**19**]. For the first time the valence electrons, which are the essence of the chemical bond, were taken into account. Although Lewis's formulation is chemically intuitive, it is physically incomplete since the wave-like property of the electron, developed in those days [**20-22**], is missing. The chemical bond represents the interplay between electrons and therefore a quantum treatment is required to describe it accurately. In this perspective, Heitler and London solved exactly the Schrödinger's equation (1926) [**23**] for the H_2 molecule [**24**]. The combination of Lewis-dot diagram and Heitler-London's ansatz merged in the valence bond theory formulated by Pauling [**25**]. The bond formed by two electrons is described by a localized wave function arising from the linear combination of atomic orbitals. Although valence bond theory is chemically intuitive, it lacks in accuracy in computing spectroscopic properties.

2.2 The chemical bond quantification

Although high level computational methods are giving an accurate qualitative description of the chemical bond, its quantification is still challenging since it does not refer to a physical observable [**26-28**]. Therefore, appropriate models have to be developed to describe properly the bond order, which is related to the electronic configuration of the system in exam. In the following subsections we will go briefly through the most known models to estimate bond orders, that have been available since the first part of the 20th century, namely the formal,

the effective, the natural and the Coulson bond order. Natural resonance theory, Wiberg bond index and formal shortness ratio will be also treated.

The molecular orbital (MO) or formal bond order was proposed by Herzberg in 1929 [**29**]. In his words, it is calculated as half the difference between the number of bonding and loosening electrons. This definition can be refined and reformulated as half the difference between the occupation number of the bonding orbital and the corresponding antibonding orbital. In case of Hartree-Fock wave functions, the occupation numbers can take only integer values and the corresponding bond order is defined as the formal bond order. In case of multiconfigutational wave functions such as CASSCF, the antibonding orbital can have a non zero occupation number. Based on the natural orbital occupation number, the concept of *effective bond order* (EBO) was introduced. For each pair of bonding and antibonding orbitals, it is calculated as half the difference between the occupation number of the bonding orbital minus the occupation number of the corresponding antibonding orbital. When there are several bonding/antibonding pairs of orbitals the sum of all these contributions for each pairs gives the total EBO [**30**]. *The natural bond order* [**31**] is part of the natural bond orbital analysis. The idea of such theory consists in building natural bond orbitals (NBO) which are linear combination of natural hybrid orbitals (NHO) which in turn are built from a set of effective valence shell atomic orbitals (NAOs). NHOs take into account the hybridization phenomena (sp^2, sp^3,...). NBOs are labelled as core, bond, valence lone pair or extra-valence Rydberg orbitals. Once determined, NBOs allow to build up the "natural Lewis structure" which can be connected to the standard Lewis representation. Suppose we have four h_i hybrid orbitals (NHOs) (i=A,B,C and D) on four different atoms. A Lewis-type A-B bond and a non-Lewis C-D antibond can be defined:

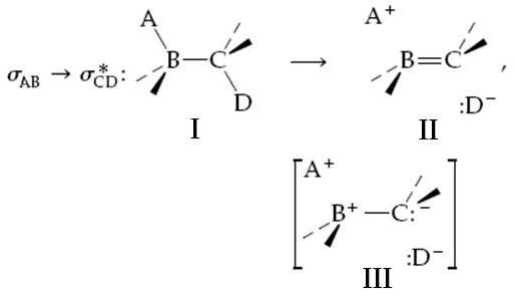

$$Bonding : \sigma_{AB} = c_A h_A + c_B h_B$$

$$Antibonding : \sigma^*_{CD} = c_C h_C - c_D h_D$$

The antibonding orbital has little to do here with the usual definition of such kind of orbitals, which by definition is associated to a bonding counterpart. In the present case, the antibonding orbital can be defined as an empty orbital within a given resonance form. In the idealized Lewis picture σ^*_{CD} should be empty although it is not the case. Such feature is the consequence of the delocalization effects. The occupation of σ^*_{CD} is the result of the coexistence of another Lewis structure with less probability to occur, characterized by two electrons on the D center (II) in the present example. In the knowledge of these effects, natural semi-localized molecular orbitals (NLMOs) can be defined as:

$$\Omega_i = c_{ii}\sigma_i + \sum_j^{NL} c_{ji}\sigma^*_j$$

Each semi-localized NLMO Ω_i can be expressed as a linear combination of the parent Lewis-type NBO σ_i and the residual weak contributions from the non-Lewis (NL) NBOs σ^*_j. At the end of the process the bond order can be defined since the occupation numbers are available. *The Natural Resonance Theory*, like the natural bond order, is part of the Natural Bond Orbital analysis. The electronic configuration of a molecule can be viewed as the result of the superposition of the different resonance forms. In this perspective, Pauling and Wheland [**32**] proposed a model based on the resonance theory. Actually, the idea is that any molecular property $\langle P \rangle$ can be expressed as the weighted average ω_α of idealized values $\langle P \rangle_\alpha$ corresponding to the different structural resonance forms α:

$$\langle P \rangle = \sum_\alpha \omega_\alpha \langle P \rangle_\alpha , \, \omega_\alpha \geq 0 \;\; and \;\; \sum_\alpha \omega_\alpha = 1$$

The bond order can also be described using the same scheme:

$$b_{AB} = \sum_{\alpha} \omega_{\alpha} b_{AB}^{(\alpha)}, \text{ where AB is the bond between A and B}$$

Furthermore, Pauling and Wheland employed valence bond (VB) wave functions to determine the bond order:

$$\psi = \sum_{\alpha} c_{\alpha} \psi_{\alpha} \quad \text{and} \quad \omega_{\alpha} = |c_{\alpha}|^2$$

The use of VB wave functions reveals to be inappropriate in describing efficiently polar molecules such as H_2O. Therefore wavefunctions based on natural bond orbitals (NBO)[**33**] and 1^{st}-order reduced density matrices are preferred for a more accurate description. Such choice is at the basis of natural resonance theory (NRT)[**34, 35**]:

$$\hat{\Gamma} = N \int \psi^*(1, 2...N)\psi(1, 2...N)d2...dN \quad \text{and} \quad \hat{\Gamma} = \sum_{\alpha} \omega_{\alpha} \hat{\Gamma}_{\alpha}$$

$\hat{\Gamma}$ is the first order reduced density matrix and $\hat{\Gamma}_{\alpha}$ are those for the idealized localized Lewis structures.

Once their values are known, the natural resonance weights $\omega_{\alpha}^{(N)}$ as well as the bond order can be determined:

$$b_{AB}^{(N)} = \sum_{\alpha}^{n_{RS}} \omega_{\alpha}^{(N)} b_{AB}^{(\alpha)}$$

Where $b_{AB}^{(\alpha)}$ takes an integer value and corresponds to the A-B bond order for the α^{th} natural Lewis structure. *The Coulson bond order* [**36**] was the first one to propose a way to define the bond order applicable to delocalized orbitals in the framework of the Hückel model. The bonder order b_{AB} can be determined as follow:

$$b_{AB} \propto P_{AB} = 2 \sum_{i}^{occ} c_{iA} c_{iB}$$

Where c_{iA} is the coefficient of the atomic orbital χ_A (on atom A) in the i^{th} occupied molecular orbital ϕ_i:

$$\phi_i = \sum_{A} c_{iA} \chi_{iA}$$

The molecular orbital is made of linear combination of atomic orbitals and all the χ_r centered on the atoms A and B have to be taken into account in the bond order evaluation:

$$b_{AB} = \sum_{r}^{on\,A} \sum_{s}^{on\,B} P_{rs}$$

The Wiberg bond index [**37**] was proposed in the framework of semiempirical molecular orbital theory, based on orthonormal atomic orbitals basis. Its definition is closely related to the Coulson bond order and it is calculated as the sum of squared density matrix elements:

$$b_{AB}^{(W)} = \sum_{r}^{on\ A} \sum_{s}^{on\ B} P_{rs}^2$$

Since its first formulation in 1968, the Wiberg bond index has been several times revisited. All the aforementioned models are suitable to compare bond orders within different kind of structures for a given transition metal. However they don't allow an evaluation of the bond's strength when comparing different kinds of transition metals. To allow such kind of mapping, Cotton introduced in 1978 the concept of 'formal shortness ratio' FSR [**38**]. It is calculated as the absolute metal-metal distance divided by twice the Pauling's single bond radii [**39**]. Although this mathematical treatment can give a flavour of the shortness of the bimetallic unit in comparison to the bond distances featured in other compounds, the notion of bond multiplicity is missing.

3. Transition Metal (TM) multicenter chemistry:

For a long time transition metal chemistry was ruled by the scheme of Alfred Werner [**40**] developed at the end of the 19^{th} century. This theory was describing quite well the coordination chemistry of these elements although the metal ion was considered as an isolated unit surrounded by ligands, precluding any direct metal-metal bonding. At best, only indirect transition metal interactions through shared ligands were taken into account. $Fe_2(CO)_9$ [**41**] is one of such example even if the use of carbonyl as bridging group doesn't exclude the possibility to form a direct chemical bond [**42**]. The delay in the investigation of new types of bonding can be explained by the lack of tools able to give a direct mapping between a given empirical formula and its corresponding structure. Indeed, compounds containing the bonded bimetallic unit were already studied before the sixties and Cotton's discovery. As

far as we can look backward, Eugène Peligot in 1844 was the first one successful in synthesizing a compound containing a metal-metal multiple bond, namely the chromium acetate $Cr_2(O_2CCH_3)_4(H_2O)_2$ [**43**]. The advent of the X-ray crystallography reduced the gap between the structure of the molecule and its empirical formula. In 1925 a study highlighted that the Mo-Mo bond distance in molybdenum chlorides was shorter (∼2.6 Å) than the one observed in metallic molybdenum (2.725 Å) [**44**]. However such observations were not able to reveal the nature of the chemical bond between the transition metals: all the pieces of the multicenter chemistry were available, only their assembly was required.

The first assessment of direct metal-metal interactions took place in 1963 through the isolation of $[Re_3Cl_{12}]^{3-}$ by Cotton and co-workers [**45, 46**]. This compound contains a $Re(III)_3^{9+}$ core unit made of three double bonds. The remaining doubts vanished in 1964 when the Re(III)-Re(III) unit was isolated in the $K_2[Re_2Cl_8]\bullet 2H_2O$ complex [**47-50**] showing a Re-Re distance of 2.24 Å, which was shorter than the one found in the metallic rhenium (2.75 Å). Interestingly, at that time this kind of compounds was also studied by other research groups but they were not able to assign correctly the Re(III) oxidation state and were giving erroneous interpretation of the crystal structure [**51, 52**]. However, in the knowledge of the nature of the multiple bonds in $Re(III)_3^{9+}$ and aware of the other studies performed in those days, Cotton succeeded to merge all the available fragmentary results into the description of the Re-Re quadruple bond in $[Re_2Cl_8]^{2-}$. Such a discovery had the effect of introducing the concept of transition metal multiple bond and of overcoming the common knowledge that the triple bond based on the p-block elements was the highest bond order. This new feature of d-block transition metals gave birth to the transition metal multicenter chemistry and was at the origin of a new challenge: the quest of the highest multiple bond. Since then a lot of effort has been dedicated to isolate compounds featuring high order transition metal multiple bond. About one thousand of these compounds have been synthesized and characterized up to now.

4. Bond order in transition metal dimer chemistry

4.1 The quadruple bond:

4.1.1 The $[Re_2Cl_8]^{2-}$ compound

Figure 1: $[Re_2Cl_8]^{2-}$

It is the keystone of this class of molecules. In analogy to it, Cotton and co-workers were successful in isolating the $[Mo_2Cl_8]^{4-}$ [**53**] and $[Tc_2Cl_8]^{3-}$ [**54**] ion. They are featuring an eclipsed conformation, which cannot be explained if only steric effects arising from the Cl-Cl repulsion are taken into account. It was found that such feature originates from the nature of the orbitals involved in the bonding which gives rise to the $\sigma^2\pi^4\delta^2$ electronic configuration. The σ and π bonds are strong and are not affected by the rotation around the M-M axis. The situation is different for the d_{xy} orbitals which can form the fourth bond between the two centers only when both are aligned. The gain in energy arising from such eclipsed conformation is higher than the sterical effects due to the Cl-Cl repulsion. The weakness of the δ bond was demonstrated performing optical absorption spectrums [**50, 55**] and looking at the energy of the δ-δ* transition band. Such transition was found to occur at a frequency of 14700 cm^{-1} and was characterized by low oscillator strength. Such observation was confirmed by computational calculations [**56**] and clearly highlights the poor δ orbital overlap.

4.1.2 The paddlewheel structure for bimetallic unit isolation

The paddlewheel architecture was widely used to isolate transition metals in their lower oxidation state. Their utilisation started about 150 years ago and such kind of ligand was shown to be able to isolate the dichromium unit in its Cr_2^{4+} form. In the purpose to have a clear idea of the potential of such structures, we will go through the different members of this class of molecules:

☛ Dichromium tetracarboxylates

The dichromium tertacarboxylates are one of the oldest compounds known to contain the Cr_2^{4+} unit. Indeed, in 1844 Peligot synthesized for the first time the well known chromium acetate. Nowadays, about 40 molecules of the type $Cr_2(O_2CR)_4L_{(ax)2}$ have been investigated. An interesting feature of these compounds is that most of them have their axial position filled by either separated ligands L (Figure 2a) or by the oxygen atoms of others $Cr_2(O_2CR)_4$ molecules (Figure 2b).

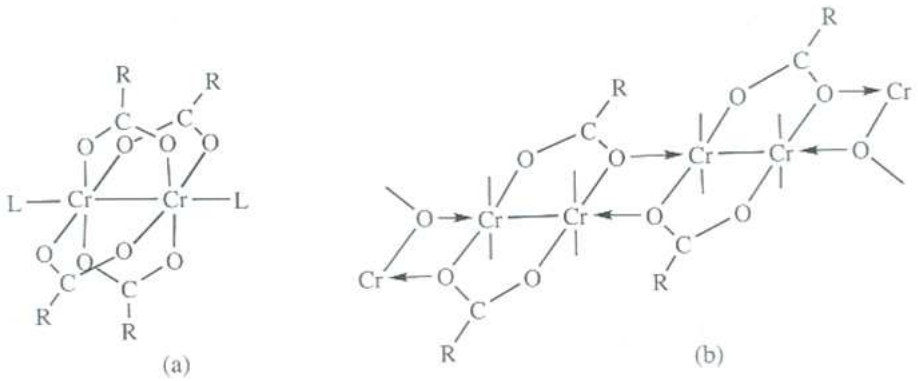

Figure 2

The formation of chains occurs when R is CH_3 [**57**], $C(CH_3)_3$ [**58**] or 2-PhC_6H_4 [**59**]. The presence in the axial position of either an external or internal ligand which is covalently

bound to the bridging ligands has an important effect on the bimetallic bond distance. Indeed such situation is featuring an increased electron density in the σ* or π* orbitals [**60**](Figure 3). The isolation of bare $Cr_2(O_2CR)_4$ molecules is rare because of the strong tendency of this class of molecules to coordinate electron pair donors in the axial position. However such situation is possible using CH_3 [**61**] and 2,4,6-$(Me_2CH)_3C_6H_2$ [**62**] for R.

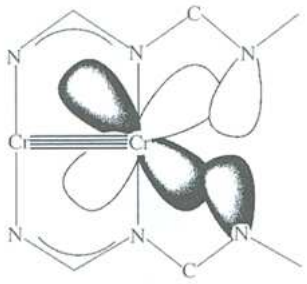

Figure 3

☛ Oxophenyl-type ligands

Although tetracarboxylate ligands are suitable for isolating the Cr_2 unit, they all exhibit quite long M-M bond distances which are in the range of 1.95-2.50 Å. Therefore, another path must be investigated to isolate paddlewheel structures featuring increasingly shorter bimetallic unit. Such goal was achieved by Cotton and co-workers [**63, 64**], who were successful in synthesizing $Cr_2(DMP)_4$ (DMP = 2,6-dimethoxyphenyl), $Cr_2(TMP)_4$ (TMP = 2,4,6-trimethoxyphenyl) and Cr_2(2-MeO-5-$MeC_6H_3)_4$ (Figure 4) which are exhibiting a Cr-Cr bond length of 1.847 Å, 1.849 Å and 1.828 Å, respectively.

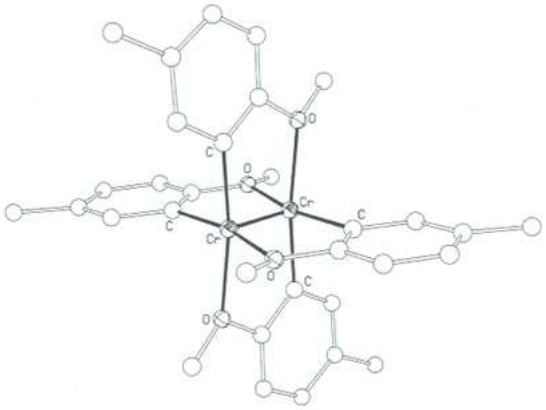

Figure 4: Cr_2(2-MeO-5-$MeC_6H_3)_4$

It appears that oxophenyl-type ligands such as Cr_2(2-MeO-5-$MeC_6H_3)_4$ can accommodate very short M-M unit. Such property was confirmed studying an oxophenyl-carboxyl hybrid [**65**] (Figure 5) whose Cr-Cr bond length of 1.862 Å is in the midway between the value characterizing both class of paddlewheel structures, namely ∼1.83 Å for oxophenyl and ∼1.97 Å for carboxyl type of ligand.

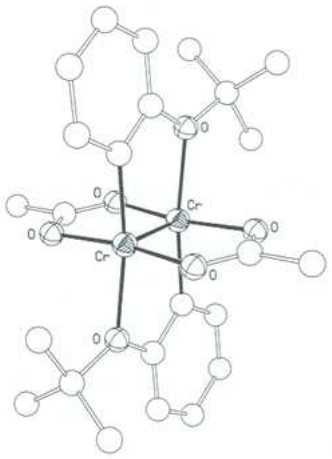

Figure 5: $Cr_2(O_2CCH_3)_2$(2-$Me_3COC_6H_4)_2$ [**65**]

☛ 2-oxopyridinate and carboxamidate type of ligands

Since oxophenyl and carboxyl-type ligands are suitable for stabilizing the transition metal diatomic unit, it was proposed to investigate similar structural compounds involving nitrogen-containing ligands such as 2-oxopyridinate (Figure 6a) and carboxamidate (Figure 6b). However such complexes weren't able to achieve Cr-Cr bond length shorter than Cr_2(2-MeO-5-$MeC_6H_3)_4$. $Cr_2(map)_4$ (map: 2-amino-6-methylpyridine) [**66**] and $Cr_2(PhNC(CH_3)O)_4$ [**67**] are representative of both type of complexes and are featuring a bond distance of 1.870 Å and 1.873 Å, respectively.

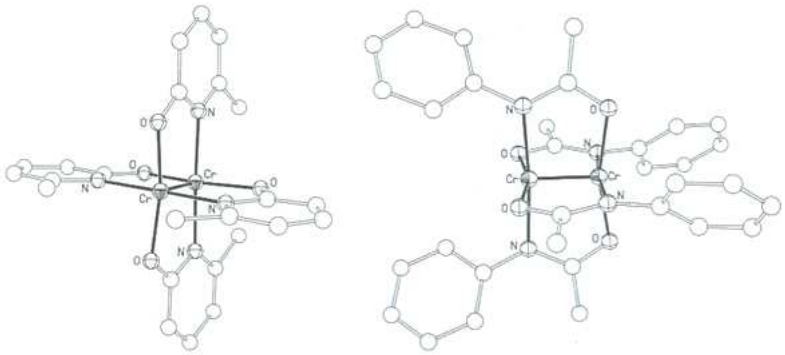

Figure 6: $Cr_2(mhp)_4$ [**68**] (a) $Cr_2(PhNC(CH_3)O)_4$ [**69**] (b)
mhp: 6-methyl-2-hydroxypyridine

☛ Amidinates and guanidinates

Before knowing their potential in achieving extremely short Cr-Cr bond distances, amidinates (Figure 7a) and guanidinates (Figure 7b) were widely used in the paddlewheel architecture. Although such complexes were able to stabilize the Cr_2^{4+} unit, no real breakthrough in the bimetallic bond length was occurring.

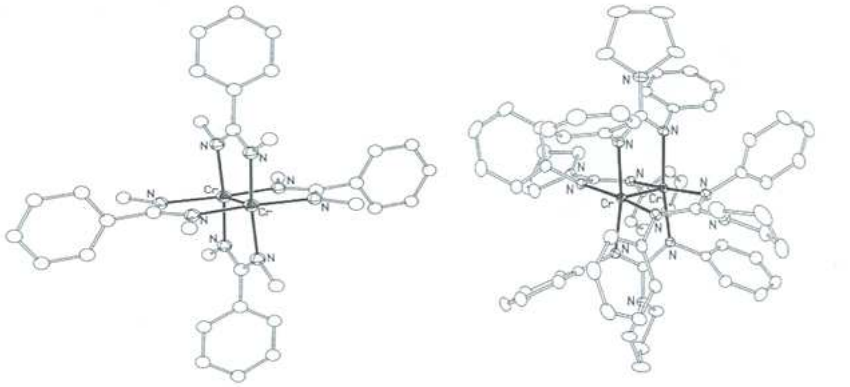

Figure 7: $Cr_2[MeNC(Ph)Nme]_4$ (a) Tetrakis (guanidinate) dichromium (b)

4.2 The quintuple bond

For 40 years the attention was mainly focused on the synthesis and characterization of bimetallic quadruply bonded structures. The main difficulty in studying these compounds is related to the nature of the metal and the choice of the ligand. The art of isolating high order multiple bonds is based to a large extent on the choice of the metal and especially on the number of available valence electrons. The transition metals have the nd and (n+1)s orbitals in their valence shell and therefore they have 6 orbitals available for the bond formation. Cr, Mo and W, with their 6 valence electrons, are the best candidates for the isolation of high order multiple bonds. Since most of the chemistry is occurring in solution, the isolation of compounds featuring high order multiple bond in such environment is more difficult and requires to take into account the aspect of the ligand. The latter has to be enough bulky to avoid any interactions with the environment which could destabilize the metal diunit. The other important aspect is that the transition metal has to be kept in the lowest possible oxidation state to make a maximum number of valence electrons available for the formation of the multiple bond.

In spite of the effort made to go beyond the quadruple bond limit, no real innovation was achieved. At the time when the hope of breaking the record established by Cotton in 1964 was

vanishing, the group of P. Power succeeded, in 2005, in synthesizing Ar'CrCrAr' (Ar'=C_6H_3-2,6(C_6H_3-2,6-Pr^i_2)$_2$) [**10**] which is characterized by a formal quintuple bond. In spite of its very short dichromium bond distance (1.835 Å), the record of the shortest Cr-Cr bond still belonged to the Tetrakis(2-methoxy-5-methylphenyl)dichromium compound reported by Cotton and co-workers in 1978 and exhibiting a Cr-Cr bond length of 1.828 Å [**63**]. This discovery was followed by a resurrection of interest in finding new bonding patterns featuring high order and shorter multiple bonds. In a very short period of time the transition metal multicenter chemistry witnessed the isolation of increasingly shorter bimetallic units lowering the threshold established by Cotton in 1978. Such structures are involving diazadienes, amidinates, aminopyridinates and guanidinates. All the aforementioned molecules will be described in the following subsections.

4.2.1 Historical Overview

Terphenyl ligands include all the compounds consisting of benzene rings linked to each other in either ortho, meta or para position. The use of such class of ligands is part of the quest for isolating main group elements in their lowest oxidation state [**70**]. One of the aims consists in protecting the core unit against destabilizing interactions with the environment and preventing oligomerization. Such property was illustrated by the isolation of the doubly bonded Mes*P=PMes* compound (Mes*=2,4,6-tri-tert-butylphenyl) [**71**](Figure 8).

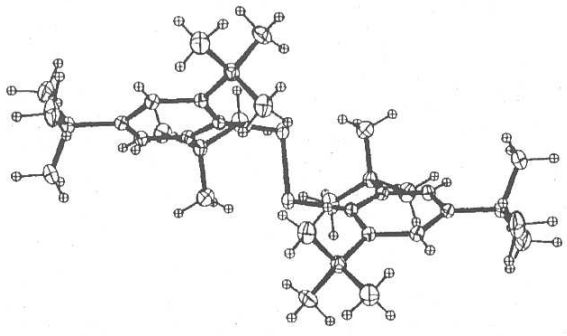

Figure 8

Besides Mes*, other ligands such as $(SiMe_3)_2CH$ [**72**], Trip (tri-iso-propylphenyl) [**73**], Dipp (di-iso-propylphenyl) and Bmt (4-tert-butyl-2,6-bis[2,2",6,6"-tetramethyl-m-terphenyl-2'-yl)methyl]phenyl) [**74**] have been employed to isolate unusual bonding modes. The terphenyl ligand was shown to be suitable for the isolation of compounds featuring low coordination numbers as reported by Schiemenz and co-workers, who isolated σ-bonded aryllithium compound stabilized by a weak Li-benzene π interaction [**75**](Figure 9).

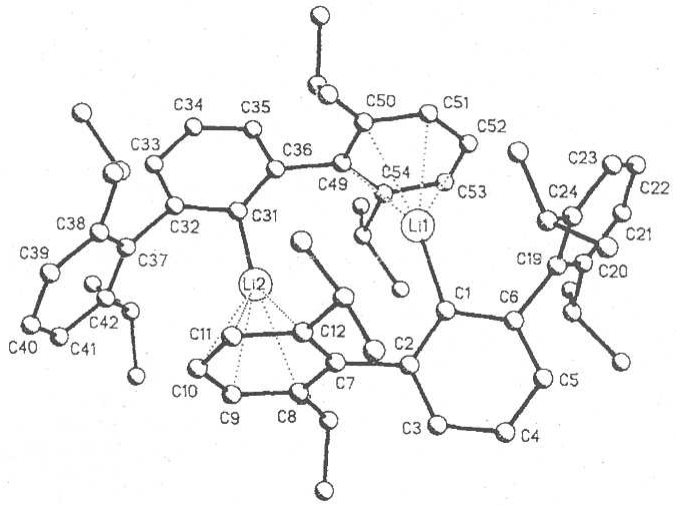

Figure 9

The step before applying terphenyl ligands to d-block transition metals was the study of multiple bonds between heavy main group elements. The synthesis of $Na_2[Mes^*_2C_6H_3$-Ga≡Ga- $C_6H_3Mes^*_2]$ is one of such example involving group 13 elements and was the first time that a gallyne was isolated [**76**]. It is characterized by a Ga-Ga bond distance of 2.319 Å and a C_{aryl}-Ga-Ga angle of about 130 degrees. DFT calculations [**77**] performed on this structure questioned the bond order in the aforementioned molecule, stating that there was the possibility that an extra hydrogen was bound to each Gallium centre. However, both experimental [**76**] and theoretical [**77**] works agreed with the non-linearity of R-Ga≡Ga-R although acetylene, the carbon analogue, has a linear structure.

Group 14 elements such as Sn and Ge are behaving as well differently from their carbon analogues. Such trend was verified in the case of R_2MMR_2 compounds, whose structures were

reported to be nonplanar and trans-bent [**78**]. Such feature originates from the s-p orbital hybridization which is less pronounced for heavier elements within a group. It appears going down group 14 elements that the ns orbital is more stable than the np orbital and therefore s electrons will be excluded from the bonding, having more a lone pair character (Figure 10).

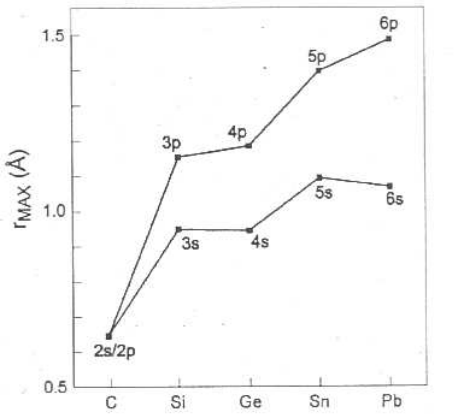

Figure 10

Although group 14 alkene analogues were very well studied, the study of alkyne analogues wasn't so obvious from the experimental point of view. Nonetheless, Olmstead and Pu succeeded in isolating $[Ar^*MMAr^*]^{\cdot-}$ and $[Ar^*MMAr^*]^{2-}$ ($Ar^* = C_6H_3$-2,6-$Trip_2$ and M = Ge or Sn) [**79, 80**]. Both structures are featuring trans-bent geometry and the formal M-M bond order was reported to be 1.5 and 2, for the singly and doubly reduced species respectively [**81**]. The neutral [Ar*PbPbAr*] [**82**] and [Ar'MMAr'] (M = Ge [**83**], Sn [**84**] ; Ar'= C_6H_3-2,6-$Dipp_2$; Dipp = C_6H_3-2,6-Pr^i_2) species were also investigated. For example, the neutral Ar*PbPbAr* was reported to be more a diplumbylene rather than a diplumbyne, the 6s orbital having more a lone pair character and therefore not involved in the bonding. Its trans-bent configuration is more the result of steric constraints than electronic effects. The same trend was observed for the Sn and Ge analogues.

The reason of the trans-bent conformation was analysed studying simpler models based on R-M≡M-R (M = Si, Ge, Pb) and using a broad choice of ligands going from hydrogen to more bulky ligands featuring either electron-donating or electron-accepting character [**85-88**]. Different structures such as the linear (1), the trans-bent (2), the 1,2-R-shifted (3) and the dibridged (4) isomers were investigated (Figure 11).

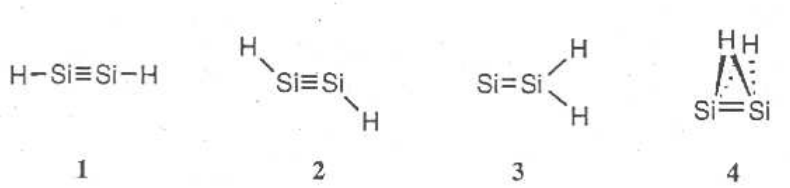

Figure 11

All the performed DFT calculations using hydrogen as ligand are exhibiting the same trend: the linear structure (1) is not a minima and the trans-bent structure (2) is preferred. The latter easily undergoes isomerisation into the most stable 1,2-H shifted (3) or dibridged isomers (4). The use of increasingly bulky ligands results in changes in the energy ranking, the trans-bent compound becomes lower in energy in comparison to isomer 3 and 4 because of the steric effects. One other feature of the potential energy surface is the reduction of the gap between the trans-bent and the linear compound when electron-donating ligands are used. Such behaviour is explained by the reduction of the s-p orbital size difference. The change of shape arises from the increased negative charges on the triply-bonded silicons which results in improved s-p hybridization.

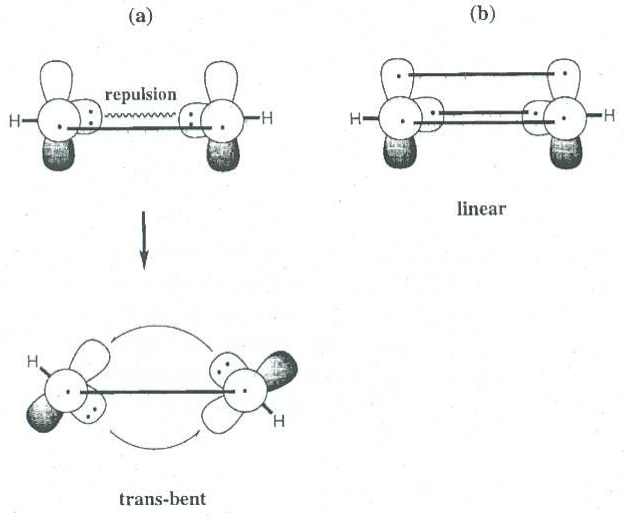

Figure 12: the preference of the trans-bent conformation

The stability of the trans-bent isomer in comparison to the linear one is the consequence, as abovementioned, of the different radial distribution between s and p orbitals and can be explained considering the MH fragment. In case of carbon, the doublet and quartet state are quite close in energy and therefore (b) bonding mode is affordable (Figure 12). In case of heavier group 14 elements, the gap is considerably larger and therefore the (a) bonding mode is occurring, forcing the trans-bent configuration because of the repulsion between the lone pairs. Therefore the bonding is better described as one π bond with two dative bonds. In spite of its simplicity, this model is not giving a satisfactory description of the bonding mode when the trans-bending angle get close to 90° as it is the case in Ar*PbPbAr*. Indeed the present model would result in a single π bond instead of a σ bond, which is more realistic. The binding mode here is not obvious and several models were reported [**81**].

4.2.2 Ar'CrCrAr' (Ar'=terphenyl)

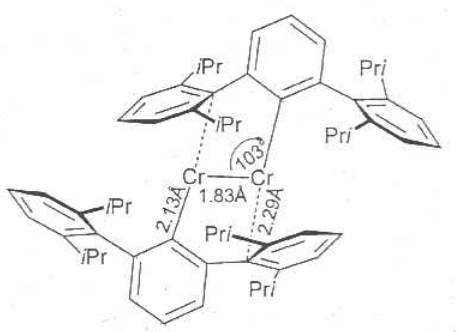

Figure 13: Ar'CrCrAr'

The Ar'CrCrAr' [**10**] is featuring a Cr-Cr and a Cr-C bond distance of 1.835 Å and 2.131 Å, respectively, a Cr-Cr-C angle of 102.8° and a secondary Cr-C (2.294 Å) interaction involving an ipso-carbon of one of the flanking aryl. Its architecture allows the isolation of the bimetallic unit in solution in its Cr_2^{2+} form and is able to protect the core unit against external interactions. As for main group elements, Ar'MMAr' (M=Cr,Fe,Co) compounds involving d-block transition metal are also featuring a trans-bent geometry. Landis and co-workers showed, studying simpler model such as bimetallic hydrides [**89**] that such conformation is preferred because it allows the formation of a strong σ bond arising from sd_{z^2} hybridization.

Moreover, the trans-bent configuration is also featuring two δ bonds arising from the interaction between two pure $3d_\delta$ orbitals and between two orbitals featuring sd^4 hybridization. CASPT2 calculations performed on a smaller model, namely PhCrCrPh (Ph=phenyl) [**90**], showed that the difference in energy between the linear structure and the trans-bent one is very small, about 1 kcalmol^{-1}.

Since the terphenyl ligand was successful in stabilizing main group elements with low coordination number, its ability in doing as well for transition metals was tested for Fe and Co [**91**]. As expected, it was able to protect the bimetallic unit keeping it in a low oxidation state. Although the protective property of this bulky ligand is well known and was widely studied, the arene-metal interactions shouldn't be undervalued as they can weaken the bonding between the two metal centres. For this purpose, the stability of the multiple bond was investigated by studying secondary metal-arene interactions performing calculations on different model compounds, using CASPT2 and DFT level of theory [**92**]. It has been reported that Co and Fe were featuring arene-metal η^6 interactions and therefore the removal of such interactions using smaller ligand, such as methyl and phenyl, was resulting in significant variations of the M-M bond length. Interestingly, Cr is not exhibiting such interactions as demonstrated by the feeble changes in the dichromium bond length. Wolf and co-workers investigated the effects of different terphenyl ligand substituents [**93**] and showed that modifying the external part of the ligand has no impact on the bimetallic unit.

4.2.3 Compounds featuring nitrogen-metal coordination

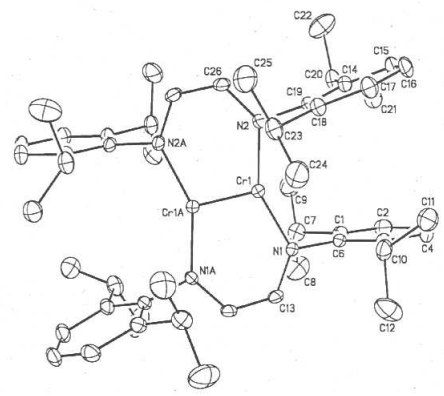

Figure 14

Since the synthesis of Ar'CrCrAr', a lot of compounds have been synthesized using nitrogen as coordinating atom to the transition metal center instead of carbon. The synthesis of dichromium diazadiene by Kreisel and co-workers [**11**] was the first step in this direction and for the first time allowed to overcome the world record Cr-Cr bond distance, which was previously in the hand of Cotton's Tetrakis compound (1978). Nitrogen-containing compounds such as azadienes have been widely studied because of their involvement in biological processes [**94**] and have been used in the present case to isolate and stabilize the Cr_2 unit which was reported to be a formal quintuple bond. Chromium diazadiene is characterized by a Cr-Cr, Cr-N_1 and Cr-N_2 bond distance of 1.803 Å, 1.913 Å and 1.914 Å, respectively. The metal in the Cr_2N_4 core unit exhibits a trigonal planar geometry and is coordinated to two different diazadiene ligands. According to the performed DFT calculations, the electronic configuration is a singlet closed shell and the bond order was reported to be 4.3. The years 2008 and 2009 have been fruitfull and witnessed the isolation of several species such as amidinates, lantern amidinates, aminopyridinates and guadinidates.

Amidinate ligands are commonly used to form complex with main group elements, transition metals and f-block elements and their field of application has been reported in several reviews [**95-97**]. The history of amidinates started with the synthesis of PhC(=$NSiMe_3$)-[$N(SiMe_3)_2$] in 1973 [**98**]. These anions present some steric and electronic properties which can be easily modified changing the substituents on either the carbon or nitrogen elements and for this reason they are synthetically very useful. Therefore their reactivity with the transition metal bimetallic unit and their ability to accommodate very short Cr-Cr bond distance were investigated experimentally and theoretically. Having isolated such kind of compound before [**99**], Tsai and co-workers decided to apply such kind of architecture to chromium and synthesized several compounds of the type $Cr_2(\mu\text{-}\eta^2\text{-}ArNC(R)NAr)_2$ (Figure 15)[**100**], which are featuring Cr-Cr bond distances close to 1.74 Å.

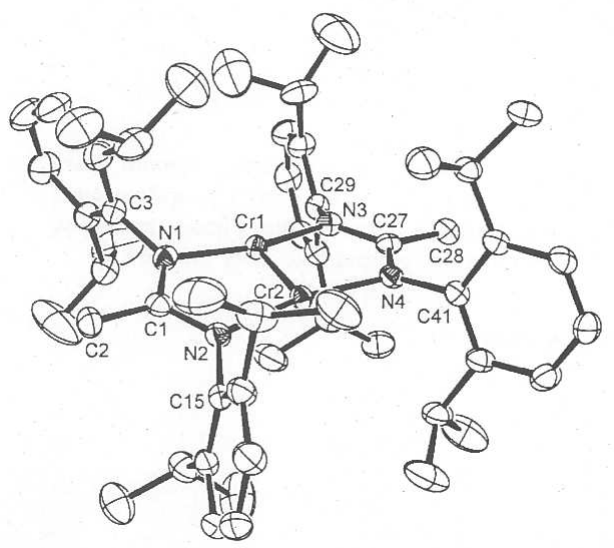

Figure 15: $Cr_2(\mu\text{-}\eta^2\text{-ArNC(R)NAr})_2$

As mentioned in the previous section dedicated to quadruply bounded compounds, amidinate ligands have been used within the paddlewheel structure without any breaktrough in the Cr-Cr bond length. Tsai and co-workers [**101**] did better using *lantern amidinate* architecture. Here, the paddlewheel structure is made of three $Ar^{Xyl}NC(H)NAr^{Xyl}$ (Ar^{Xyl}=2,6-C_6H_3-$(CH_3)_2$) ligands stabilizing the mixed-valent Cr_2^{3+} complex and the corresponding reduced species (Figure 16). The neutral and reduced forms are featuring a Cr-Cr bond length of 1.817 Å and 1.740 Å, respectively.

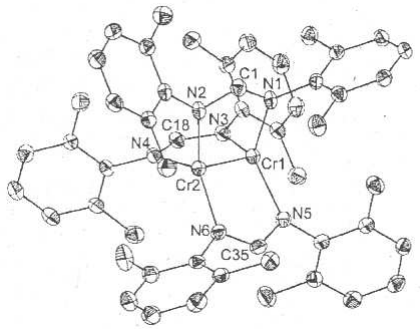

Figure 16: $Cr_2(Ar^{Xyl}NC(H)NAr^{Xyl})_3$

Aminopyridinates are another type of ligands which are similar to amidinates although they are bearing two different donor functionalities, the pyridine and the amido function, which are lacking in the former compounds. This ligand can accommodate two resonance forms (Figure 17):

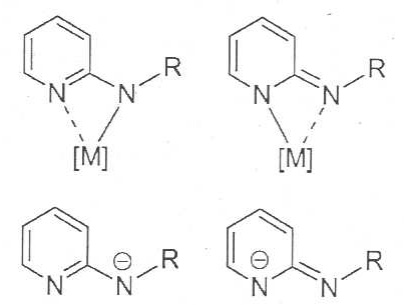

Figure 17: amidopyridine aminopyridinato

Aminopyridinates can be involved in strained η^2-N_{amido}-$N_{pyridine}$ coordination as well as in the bridging binding mode. The latter is characteristic of transition metal complexes and the former is more a feature of early transition metals and lanthanides [**102, 103**]. In the present case, Noor and co-workers [**104**] used aminopyridinates to isolate the dichromium unit and they reported a Cr-Cr, Cr-N_{amido} and a Cr-$N_{pyridine}$ bond distances of 1.749, 1.998 and 2.028 Å, respectively. The lately isolated dichromium species are involing guanidinates, which up to now allowed to synthesize the shortest Cr-Cr bond of 1.729 Å (Figure 18) [**105**].

Figure 18

4.2.4 The effect of the ligand on the bimetallic unit

Beside the bare Cr_2 molecule, all the compounds discussed in the introduction and reported later in the text have been isolated in solution. Therefore, one of the crucial task of the ligand is to protect the core bimetallic unit against any interactions with the surrounding. Such requirement is fulfilled by the bulky terphenyl ligand. However, shielding effect is only one of the functionalities that ligands can exhibit. Bridging ligands containing nitrogen atom as coordinating atom to the metal center, such as those enumerated above, can go further since they can exert structural pressure on the bimetallic unit. Such effect is at the origin of the increasing shortness of the Cr-Cr bond. Although bridging ligands can act as pincer forcing the two metals to get closer, their efficiency highly depends on the shape of the outer part of the ligand.

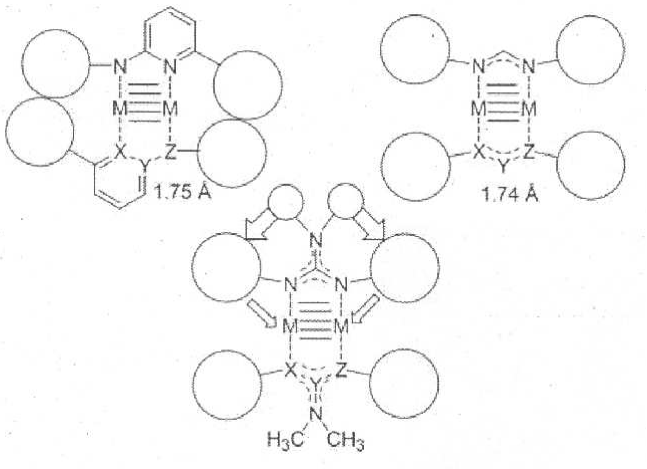

Figure 19: aminopyridinate (top left), amidinate (top right) and guanidinate (bottom)

As one can guess looking at figure 19, the first aim in using bulky residues relies in their capacity to keep the Cr-N distance enough far away, since the shortening of the Cr-Cr bond distance is tightly correlated to the lengthening of the Cr-N. The second function of the outer residues is to enhance the bending of the NC(R)N fragment. Guanidinates are particularly suitable for such task since the NC(N)N fragment is planar. Therefore, any increase in size of the functions connected to the nitrogen will efficiently increase the angle of the pincer and

consequenty make the Cr-Cr distance shorter.

4.3 The sextuple bond

Before the discovery of Ar'CrCrAr' in 2005, the only evidence of bond orders higher than four was the isolation of unstable transition metal dimers like Cr_2 [**106-109**]. Although group 6 dimers exhibit the highest bond multiplicity that transition metals can achieve, their lifetime is extremely short and make their isolation quite complicate. In spite of their instability, they are worth to be studied since the knowledge of their electronic configuration is essential for understanding the electronic configuration of more complicated structures involving the bimetallic unit. Since most of the newly synthesized molecules are based on chromium, the main attention will be addressed to the Cr_2 unit.

4.3.1 Cr_2: The centerpiece of the dichromium chemistry

In the sixties, the first studies on dichromium were dissociation energy measurements through Knudsen effusion mass spectrometry [**110**]. In 1974, Efremov examined the spectrum of $Cr(CO)_6$ by pulsed photolysis and observed a rotationally resolved band at 4600 Å and concluded that the observed spectrum was due to Cr_2 [**111**]. In 1975, Kündig [**112**] and co-workers arrived to the same conclusion performing matrix isolation experiment. Nowadays, the most accurate experimental values for bond length and dissociation energy are 1.68 Å [**113, 114**] and 1.53 eV [**115, 116**], respectively.

One of the features of Cr_2 is its complicated electronic configuration arising from the different atomic radii [**117**] of the 4s orbital (<R4s>=1.94 Å) and the 3d orbital (<R3d>=0.72 Å), both contributing to the multiple bond. At the equilibrium bond distance one expects the 3d orbital to be the major contributor to the chemical bond whereas the 4s orbital, because of its wide radial distribution, has more a destabilizing effect. Increasing the Cr-Cr bond distance will result in a weaker bond arising from the 4s orbital interactions. Therefore the 3d molecular orbitals are not bonding any longer. At such distance, the 3d electrons are antiferromagnetically coupled because of the exchange interaction. Such behavior is shown

by the shape of the experimental and theoretical potential curves obtained at the CASPT2 level (Figure 20) [**118, 119**]:

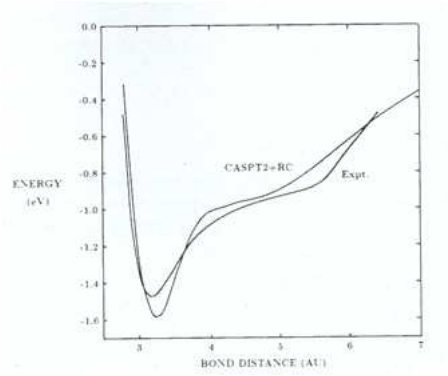

Figure 20

The plots clearly show, besides the minimum at the equilibrium bond distance, a plateau at a distance of about 2.5 Å arising from the long range 4s-4s orbital interaction. Such pattern was already reported by calculation of Goodgame and Goddard in 1982 for Mo_2 [**120**] although they weren't able to show the inner and outer well for Cr_2.

4.3.2 Cr_2: A challenge for Computational Chemistry

From the computational point of view, an accurate understanding of compounds containing a transition metal diatomic unit requires at a first stage a good understanding of the diatomic unit itself which is the centerpiece of the previously reported molecules. Among the d-block transition di-metals, Cr_2 is one of the most challenging because of its complex electronic configuration. Therefore this molecule was often used as a benchmark to test the ability of a method to describe accurately transition metal chemistry. Nowadays, the most recent experimental data predict a equilibrium bond distance of 1.68 Å [**113**] and a dissociation energy of 1.53 eV [**115**]. Both values will be considered as references for the following discussion.

The first theoretical description of the multiple bond in the dichromium unit, performed in the seventies, was based on the Extended Hückel (EH) and the SCF-Xα-SW molecular orbital techniques [**121**]. About 10 years ago, new semi-empirical studies [**122-124**] were performed to investigate the electronic configuration of Cr_2. However they were reporting open-shell singlet with antiferromagnetically coupled electron on each metal center at the equilibrium bond distance.

The single determinant Hartree-Fock (HF) method is predicting shorter bond length than experiment (1.454 Å) and is unable to reproduce the dissociation energy since the molecule was reported to be about 20 eV higher in energy than two separated chromium atoms [**125, 126**]. The method (HF) is quite good in describing the electronic configuration in the d-d bonding area but fails to describe the antiferromagnetically coupled region. This failure of HF is caused by the inability of the HF wave function to describe the system at large distances and instead of having two singly occupied orbitals, HF forces both electrons to be in one orbital. The solution is to use either the unrestricted HF (UHF) or the generalized valence bond (GVB) method [**127, 128**]. The latter was used by Goodgame and co-workers in 1982. They improve the description of the far region of the potential energy curve but they lost accuracy in describing the chemical bond. The reported dissociation energy and equilibrium bond distance are 0.3 eV and 3 Å [**120, 129**], respectively. Better results were obtained later using modified generalized valence bond (MGVB) method, leading to a De and Re values of 1.86 eV and 1.61 Å, respectively [**130**].

It clearly appears that a correct description of the electronic configuration of complex systems such as those involving chromium requires going beyond the HF method and using different approaches to recover the missing electron correlation. Several alternatives were proposed with more or less accurate results:

For example, internally contracted multireference configuration interaction (IC-MRCI) calculations were performed in the late eighties and predicted a negative binding energy of -0.03 eV [**131**]. Takahara and co-workers applied the approximately projected unrestricted Møller-Plesset perturbation theory (APUMP) on the top of an unrestricted Hartree-Fock wave function and they correctly described the dissociation of Cr_2 in two ground state atoms

although a longer Re of 2.8 Å and a De of 0.61 eV was reported [**132**]. In the nineties coupled-cluster calculations were performed on the dichromium unit. It appears that this method is giving good results although its application for investigating bigger systems is more difficult because of the computational cost. CCSD [**133**] and CCSD(T) [**134**] calculations were predicting equilibrium bond lengths which were, respectively, 0.117 and 0.075 Å shorter than experimental values. Such results indicate that higher than connected triple excitations are needed to recover the electron correlation. In both cases, the basis set for chromium included f functions which were shown to be required for accurate dissociation energy and equilibrium bond length [**125**]. In 1994, Bauschlicher and Partridge performed UCCSD(T) (unrestricted coupled cluster with single and double excitations and a perturbative correction for triples) obtaining a very large bond distance of 2.54 Å [**135**].

Other appealing post-HF models are CASSCF/CASPT2. Both are widely used and have been reported to give accurate results. In 1983, CASSCF was applied for the first time to describe Cr_2. The potential energy curve computed at that time was not able to reproduce any well near the experimental minimum but only a shoulder [**136**], precluding the existence of any bound dichromium molecule. The failure of CASSCF relies in the fact that the dynamical electron correlation effects were not properly described at this level of theory. Such results can be improved performing CASPT2 calculations, which were giving an equilibrium bond length, an harmonic vibrational frequency and a dissociation energy of Re=1.71 Å, ωe=625 cm^{-1} and Do=1.55 eV, respectively [**137**]. The potential energy curve (PEC) resulting from calculations performed using ANO basis set of the size 8s7p6d4f, including 3s3p correlation effects and relativistic corrections is in good agreement with experiment (Figure 21, left). The improvements going from CASSCF to CASPT2 is clearly shown in the PEC reported in Figure 21 (right). The method was applied as well to investigate dichromium excited states [**138**]. One of the main issues in previous studies [**137, 138**] was the apparition of intruder states in multiconfigurational second-order perturbation theory. Such problems were solved using a level shift technique leading to more accurate results [**139**]. The values for equilibrium bond distance, harmonic frequency and dissociation energy were respectively 1.69 Å, 535 cm^{-1} and 1.54 eV. In 2003, Roos performed new series of calculations using improved basis set [**118**].

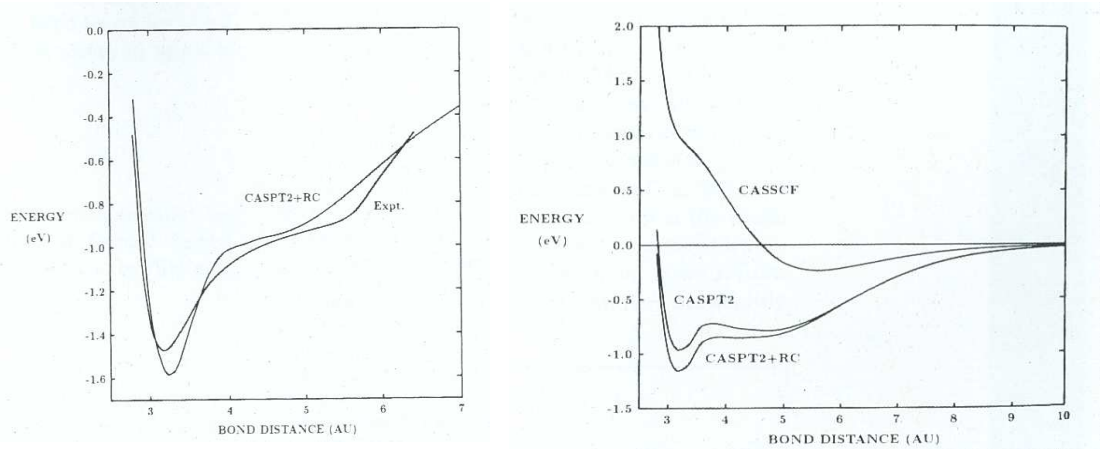

Figure 21

DFT is another alternative to the post Hartree-Fock methods and is based on the electron density. Because of its complexity, Cr_2 is a suitable candidate to test the ability of DFT in describing transition metals. One of the main concerns is to determine if such method is able to reproduce the double welled potential energy curve and other experimental data such as bond length, vibrational frequencies or dissociation energy. In 1995, Edgecombe and Becke [**140**] performed broken-symmetry spin-unrestricted DFT calculations using the BLYP and B3P86 exchange functional with and without spin-projection, using Noodleman model[**141**] to correct spin contamination. They reported that BLYP is giving a minima which agrees with experiment although the dissociation energy is 0.5 eV larger. The inclusion of spin-projection is worsening the results when BLYP is used. The trend is totally different for B3P86 since the spin-projection inclusion in this case leads to Re and De values in good agreements with experiments and allows to reproduce the double welled potential energy curve.

4.4 The sextuple bond: the line not to cross?

Nowadays the existence of the sextuple bond is not called into question any longer [**30, 142**]. The issue now is the following one: shall we stop here or shall we try to push back the limit, by considering the sextuple bond not as an ending point but as a new milestone in the achievement of higher bond order. Taking into account only the p- and d-block elements as the framework of the multiple bond chemistry would be underestimating the potential of other class of elements of the periodic table such as lanthanides and actinides. Among the two periods, the latter will be the centre of the attention here as the former cannot achieve high order multiple bond, given that the 4f orbitals are more contracted than the 5d and 6s orbitals, and therefore do not contribute to the chemical bond. We will focus here on actinides, especially on the uranium element. Handling such atoms is quite difficult and therefore not a lot of data about their diatomic chemistry is available. For example, regarding the uranium element, direct U-U interactions were reported only for the bare U_2 molecule, detected in the gas phase [**143**], H_2UUH_2 [**144**] and OUUO [**143**]. Although studying such heavy elements is still a challenge, their investigation from the computational point of view is nowadays affordable [**145, 146**].

Evaluating the bond order of actinides only considering the number of valence electrons is hazardous as other important factors are coming into play, making the achievement of bond order greater than six not an easy task. The electronic configuration of the uranium atom, whose ground state is $(5f)^3(6d)^1(7s)^2$, is a good example for understanding the complexity of the chemical bond when such elements are investigated. Since unpairing the 7s electrons by forming hybrids with 6d and 7p orbitals is affordable, the sextuple bond could be achieved. However the situation is more complex than it appears. First of all, about 16 orbitals, namely the 5f, 6d, 7s and 7p, are enough close in energy to be taken into account, making any prediction about the bond order uncertain. Moreover they are featuring different radial distribution and therefore their overlap at the equilibrium bond distance will not be the same.

All the aforementioned factors make the evaluation of the bond order not so obvious. For example, U_2 is better described as a formal quintuple bond than a sextuple bond, as reported

in a previous computational study [**146**]. The bond multiplicity in this diatomic has been shown to arise from three strong, doubly occupied bond, two one-electron bonds, two weak one-electron bonds and finally two non-bonded, localized electrons.

Because of its stability and its ability to form high order multiple bond, the U_2 molecule put himself as the centrepiece of a new kind of chemistry based on the diuranium unit. This hypothesis was verified investigating different compounds such as chlorides and carboxylates including the U_2 unit, which was reported to be stable and featuring multiple bond character [**147**]. Calculation performed on ${U_2}^{2+}$ [**148**] showed that U(I)-U(I) is featuring a $\sigma^2\pi^4\delta_g^1\delta_u^1\varphi_g^1\varphi_u^1$ electronic configuration, counting for a formal triple bond. Intuitively it is expected that such electronic configuration might occur for more complex compounds, like RU(I)-U(I)R, where the uranium diunit is surrounded by a ligand. However such mapping is not so straightforward. Indeed, [PhUUPh] for example is featuring a $\sigma^2\sigma^2\pi^4\delta^2$ electronic configuration, corresponding to a formal quintuple bond instead of the triple bond reported for ${U_2}^{2+}$. Such difference mainly arises from the molecular environment which is decreasing the Coulomb repulsion between the two uranium centers.

5. Transition metal chemistry: Introduction to the computational methods

5.1 Introduction to Density Functional Theory

5.1.1 The Equations:

Density Functional Theory (DFT) is based on the electron density ρ. Its formulation relies on the Hohenberg-Kohn theorems (1964)[**149**], which show that the knowledge of ground state ρ determines the external potential and all properties for the ground state. Moreover, they provide the energy variational principle: $E_0 \leqslant E_v[\tilde{\rho}]$, for a trial density $\tilde{\rho}(\vec{r})$ chosen in such way that $\tilde{\rho}(\vec{r}) \geqslant 0$ and $\int \tilde{\rho}(\vec{r}) \mathrm{d}\vec{r} = \mathrm{N}$.

The electron density $\rho(\vec{r}) = \int \psi^*(\vec{r}_1, \vec{r}_2, \ldots \vec{r}_N)\psi(\vec{r}_1, \vec{r}_2, \ldots \vec{r}_N) d\vec{r}_2, d\vec{r}_3, ..., d\vec{r}_N$ is described by only 3 coordinates independently of the number of electrons, whereas the wave function describing N-electron system depends on 3N coordinates. Therefore ρ is less complex than ψ and thus allows to describe bigger systems with a good accuracy/cost compromise. The energy is a function of the electron density as shown in the following equation:

$$E[\rho] = T[\rho] + E_{ne}[\rho] + E_{ee}[\rho]$$

Where the different terms stand for:

$T[\rho]$: kinetic energy

$E_{ne}[\rho]$: attraction between nuclei and electrons

$E_{ee}[\rho]$: electron-electron repulsion

Classical expression:

$$E_{ne}[\rho] = \sum_a \int \frac{Z_a \rho(r)}{|R_a - r|} dr$$

$$J[\rho] = \frac{1}{2} \int \int \frac{\rho(r)\rho(r')}{|r - r'|} dr dr'$$

The main concern in DFT consists in designing the "right" functional for the kinetic and exchange energies. One of the first attempts in defining both functionals was made by considering a non-interacting uniform electron gas, known as the Thomas-Fermi-Dirac (TDF) model. However such description was not satisfactory. In 1965, Kohn and Sham [**150**] developed a new strategy based on the study of a fictitious system of non-interacting particles, which is described by a wave function in the form of a single Slater determinant constructed from the set of orbitals that are solution of the Kohn-Sham equations. These orbitals are used for the definition of the kinetic energy $T_s[\rho]$:

$$T_s[\rho] = -\frac{1}{2} \sum_{j=1}^{N} \langle \chi_j | \nabla_j^2 | \chi_j \rangle \qquad \rho_s(\overrightarrow{r}) = \sum_{j=1}^{N} |\chi_j|^2$$

This description of the kinetic energy appears in the definition of the total energy, which also contains a new functional, $E_{xc}[\rho]$, which includes the correction to the kinetic energy and all non-classical corrections to the electron-electron repulsion energy:

$$E[\rho] = T_s[\rho] + J[\rho] + E_{en} + E_{nn} + E_{xc}[\rho]$$

$$E_{xc}[\rho] = T[\rho] - T_s[\rho] + E_{ee}[\rho] - J[\rho]$$

For a system of non-interacting electrons, the energy can be expressed using the Kohn-Sham orbitals:

$$E[\rho] = -\frac{1}{2} \sum_{j=1}^{N} \langle \chi_j | \nabla_j^2 | \chi_j \rangle + \frac{1}{2} \sum_{j=1}^{N} \sum_{i=1}^{N} \int \int \langle \chi_j \chi_i | \frac{1}{r_{12}} | \chi_j \chi_i \rangle - \sum_{a=1}^{M} \sum_{j=1}^{N} Z_a \langle \chi_j | \frac{1}{r_{12}} | \chi_j \rangle$$

$$+ \sum_{a=1}^{M} \sum_{b=1}^{M} \frac{Z_a Z_b}{r_{ab}} + E_{xc}[\rho]$$

The Kohn-Sham orbitals reported in the expression of the total energy are the solutions of the following eigenvalue equation:

$$\left\{-\frac{1}{2}\nabla_1^2 - \sum_{a=1}^{M} \frac{Z_a}{r_{aj}} + V_{KS}(r_1)\right\} \chi_j = \varepsilon_j \chi_j$$

$$V_{KS}(\overrightarrow{r_1}) = \int \frac{\rho(\overrightarrow{r_2})}{r_{12}} d\overrightarrow{r_2} + V_{xc}(\overrightarrow{r_1})$$

$$V_{xc}(r) = \frac{\delta E_{xc}[\rho]}{\delta \rho(r)}$$

V_{KS} is adjusted in such way that the same density is obtained for the hypothetical system with non-interacting electrons and the real system. The main issue consists in defining properly the exchange-correlation term. Nowadays different models are available:

1. Local Density Methods:

The density locally can be treated as a uniform electron gas. Here one makes the assumption that the density is a slowly varying function.

2. Gradient Corrected Methods:

Considering a uniform electron gas is a simplification of the reality. The exchange and correlation energy depend not only on the electron density but also on its derivative. These methods are known as Gradient Corrected or Generalized Gradient Approximation (GGA) methods.

3. Hybrid Methods:

A percentage of HF exchange is added. Since the systematic errors of HF and DFT are in opposite directions (e.g. barrier heights to chemical reactions), there is an error cancellation

that improves the results. One of the famous examples is the B3LYP functional:

$$E_{xc}^{B3LYP} = (1-a)E_x^{LSDA} + aE_x^{HF} + b\triangle E_x^B + cE_c^{LYP} + (1-c)E_c^{LSDA}$$

The constants a, b and c are 0.2, 0.72 and 0.81, respectively. They are obtained from data fitting from a reference set of atoms and compounds.

5.1.2 DFT and M_2 transition metals

Although chromium is a good test candidate, several studies investigated the performance of different kinds of functional using a wide choice of transition metal dimers [**151, 152, 153**]. Such investigation was performed in 2000 by Barden and co-workers for 3d homonuclear transition metals (Sc to Cu). They concluded that the accuracy is dependent on the choice of the functional and it appears that pure DFT such as BLYP and BP86 is giving better results than hybrid HF/DFT methods. Among the investigated parameters, the computed equilibrium bond lengths are close to the experimental values even if slightly underestimated. In the other side, DFT is less accurate for the description of the vibrational frequency and particularly the dissociation energy as discussed in Barden's paper and reported in Table 1.

	Average absolute error					
	B3LYP	B3P86	BHLYP	BLYP	BP86	LSDA
R_e(Å)	0.053 (2.4%)	0.051 (2.4%)	0.077 (4.1%)	0.024 (1.3%)	0.020 (1.1%)	0.056 (3.0%)
$\omega_e(cm^{-1})$	122 (31.1%)	122 (31.3%)	208 (49.3%)	98 (24.5%)	104 (25.6%)	158 (37.9%)
Do (eV)	7.61 (517.1%)	0.93 (64.7%)	1.29 (83.0%)	3.59 (238.1%)	0.83 (56.8%)	1.03 (70.9%)

Table 1

5.2 The CASSCF method

The only way to recover all the energy correlation consists in performing a full CI calculation, which is unaffordable. Therefore the solution would be either to do an arbitrary truncation of the CI expansion or to use the CASSCF method [**154**], which is more elegant than the former approximation. The power of CASSCF relies on the fact that the orbitals involved in the wave function expansion are chosen according to chemical criteria. Therefore it requires a basic knowledge about the electronic structure of the studied system. The method is based on the partitioning of the occupied molecular orbitals into different subsets:

1. Inactive orbitals: Always kept doubly occupied in all the configurations that are used to build the CASSCF wave function.
2. Active orbitals: They have an occupation number between 0 and 2.
3. External orbitals: They span the rest of the orbital space and are kept empty.

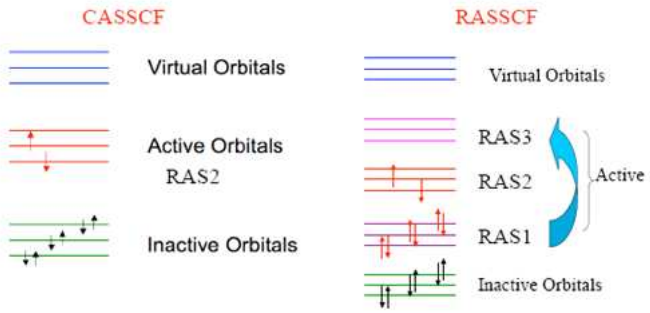

More constraints can be added in the splitting of the orbital space. Indeed, the active orbitals can be distributed into three restricted active spaces (RAS), RAS1, RAS2 and RAS3. In RAS1 a specific number of holes may be created. The RAS2 space has the same properties as the active orbital space in the CAS wave function. The RAS3 space is allowed to be occupied with up to a specific number of electrons.

The CASSCF wave function takes into account the non-dynamical correlation effects but the dynamic electron correlation is still missing. One solution is to perform either a multi-reference configuration calculation or to apply second order perturbation theory on top of the CASSCF wave function. The latter will be the subject of the next section.

5.3 The CASPT2 method

Before applying perturbation theory on the top of the complicate CASSCF wave function, it is worth to say few words about MP2 [**155**] which deals with the Hartree-Fock single determinant wave function. In this approach the total Hamiltonian of the system is divided into two parts: a zeroth-order part, H_0 whose eigenfunctions and eigenvalues are both known, and a perturbation V. Therefore the eigenvalue problem becomes:

$$\hat{H}\left|\Phi_i\right\rangle = (\hat{H}_0 + \hat{V})\left|\Phi_i\right\rangle = \varepsilon_i\left|\Phi_i\right\rangle$$

Eigenfunctions and eigenvalues of $\hat{H}_0$ are known:

$$\hat{H}_0\left|\psi_i^{(0)}\right\rangle = E_i^{(0)}\left|\psi_i^{(0)}\right\rangle$$

If the perturbation $\hat{V}$ is small we expect $|\Phi_i\rangle$ and ε_i to be close to $\left|\psi_i^{(0)}\right\rangle$ and $E_i^{(0)}$, respectively. The main target consists in improving $|\Phi_i\rangle$ and ε_i in such way they become closer to the eigenfunctions and eigenvalues of the total Hamiltonian. Such purpose is achieved by expanding $|\Phi_i\rangle$ and ε_i in a Taylor series. An ordering parameter λ is introduced and will be later set equal to unity:

$$\hat{H} = \hat{H}_0 + \lambda\hat{V}$$

$$\varepsilon_i = E_i^{(0)} + \lambda E_i^{(1)} + \lambda^2 E_i^{(2)} + \ldots$$

$$\left|\Phi_i\right\rangle = \left|\psi_i^{(0)}\right\rangle + \lambda\left|\psi_i^{(1)}\right\rangle + \lambda^2\left|\psi_i^{(2)}\right\rangle + \ldots$$

Where $E_i^{(n)}$ are the nth-order energy. Considering the eigenfunctions of $\hat{H}_0$ as normalized and choosing the normalization of $|\Phi_i\rangle$ such that $\left\langle \psi_i^{(0)} \right| \Phi_i \rangle = 1$, one can substitute the expressions for ε_i and $|\Phi_i\rangle$ in the eigenvalue equation and then equating coefficients of λ^n to get the following equations:

$$\hat{H}_0 \left|\psi_i^{(0)}\right\rangle = E_i^{(0)} \left|\psi_i^{(0)}\right\rangle n = 0$$

$$\hat{H}_0 \left|\psi_i^{(1)}\right\rangle + \hat{V} \left|\psi_i^{(0)}\right\rangle = E_i^{(0)} \left|\psi_i^{(1)}\right\rangle + E_i^{(1)} \left|\psi_i^{(0)}\right\rangle n = 1$$

$$\hat{H}_0 \left|\psi_i^{(2)}\right\rangle + \hat{V} \left|\psi_i^{(1)}\right\rangle = E_i^{(0)} \left|\psi_i^{(2)}\right\rangle + E_i^{(1)} \left|\psi_i^{(1)}\right\rangle + E_i^{(2)} \left|\psi_i^{(0)}\right\rangle n = 2$$

$$\hat{H}_0 \left|\psi_i^{(3)}\right\rangle + \hat{V} \left|\psi_i^{(2)}\right\rangle = E_i^{(0)} \left|\psi_i^{(3)}\right\rangle + E_i^{(1)} \left|\psi_i^{(2)}\right\rangle + E_i^{(2)} \left|\psi_i^{(1)}\right\rangle + E_i^{(3)} \left|\psi_i^{(0)}\right\rangle n = 3$$

Multiplying each of these equations by $\left\langle \psi_i^{(0)} \right|$ we obtain the expression of the nth-order energies:

$$E_i^{(0)} = \left\langle \psi_i^{(0)} \right| \hat{H}_0 \left|\psi_i^{(0)}\right\rangle$$

$$E_i^{(1)} = \left\langle \psi_i^{(0)} \right| \hat{V} \left|\psi_i^{(0)}\right\rangle$$

$$E_i^{(2)} = \left\langle \psi_i^{(0)} \right| \hat{V} \left|\psi_i^{(1)}\right\rangle$$

$$E_i^{(3)} = \left\langle \psi_i^{(0)} \right| \hat{V} \left|\psi_i^{(2)}\right\rangle$$

In most cases the truncation is made after the 2th-order energy and therefore $E_i^{(3)}$ is not required.

Going from the HF single determinant to the CASSCF wave function as reference wave function for the perturbation treatment adds a new layer of difficulty and therefore, before going further in the description of CASPT2 [**156, 157**], it is worth to make a clear description of the employed terminology:

1. $|\psi_0\rangle$ is the zeroth-order wave function which is generated from a CASSCF calculation.

2. The configuration space in which the wave function is expanded is divided in four subspaces:

- V_0: one-dimensional space spanned by $|\psi_0\rangle$
- V_K: space spanned by the orthogonal complement to $|\psi_0\rangle$
- V_{SD}: space spanned by all single and double replacement states generated from V_0 and not included in the two former spaces.
- $V_{TQ...}$: space containing all the higher order excitations not included in the previously abovementioned spaces.

The zeroth-order Hamiltonian:

$$\hat{H}_0 = \hat{P}_0\hat{F}\hat{P}_0 + \hat{P}_K\hat{F}\hat{P}_K + \hat{P}_{SD}\hat{F}\hat{P}_{SD} + \hat{P}_{TQ...}\hat{F}\hat{P}_{TQ...}$$

$\hat{P}_0 = |\psi_0\rangle\langle\psi_0|$: Projector onto V_0, $\hat{P}_K$ is the projector onto V_K,$\hat{P}_{SD}$ is the projector onto V_{SD}, $\hat{P}_{TQ...}$ is the projector onto $V_{TQ...}$

$\hat{F}$: One-particle; Its definition is arbitrary although it is preferably chosen in such way that $\hat{H}_0$ is equivalent to the Møller-Plesset Hamiltonian in case of closed shell single determinant reference state.

$$\hat{F} = \sum_{p,q} f_{pq} \hat{E}_{p,q}$$

$$\text{Where } f_{pq} = h_{pq} + \sum_{r,s} D_{rs} \left[(pq|rs) - \tfrac{1}{2} (pr|qs) \right]$$

Since the CASSCF wave function is invariant against rotation among the inactive orbitals, the active orbitals and the external orbitals, there is the possibility to subdivide $\hat{F}$ in three subsets for which the matrix can be diagonalized:

$$\hat{F} = \sum_i \varepsilon_i \hat{E}_{ii} + \sum_t \varepsilon_t \hat{E}_{tt} + \sum_a \varepsilon_a \hat{E}_{aa} + \sum_{i,t} f_{ti} \left[\hat{E}_{it} + \hat{E}_{ti} \right] + \sum_{i,a} f_{ai} \left[\hat{E}_{ia} + \hat{E}_{ai} \right] + \sum_{t,a} f_{at} \left[\hat{E}_{ta} + \hat{E}_{at} \right]$$

i,t and a are respectively the inactive, active and external orbitals.

NB: In case of optimized CASSCF wave function the one-electron operator can be simplified since in this specific case all f_{ai} are zero.

Similarly to MP2, one has to define the first order wave function ψ_1 in such way to get E_2. Only the configurations interacting directly with the CAS reference function have to be included into ψ_1. They all belong to the SD space:

$$|\psi_1\rangle = \sum_{p,q,r,s} C_{pqrs} |pqrs\rangle$$

$$|pqrs\rangle = \hat{E}_{pq} \hat{E}_{rs} |\psi_0\rangle$$

It is important to keep in mind that each $|pqrs\rangle$ consists in many configuration state functions (CSF).

Bibliography

[1] Xie, X., Li, Y., Liu, Z.-Q., Haruta, M. and Shen, W. 2009, *Nature* 458, p. 746.

[2] Theopold, K.H. 1990, *Acc. Chem. Res.* 23, p. 263.

[3] Brückner, A., Jabor, J.K., Mc Connell, A.E.C. and Webb, P.B. 2008, *Organometallics* 27, p. 3849.

[4] Klemps, C., Payet, E., Magna, L., Saussine, L., Le Goff, X.F. and Le Floch, P. 2009, *Chem. Eur. J.* 15, p. 8259.

[5] Zhang, J., Li, A. and Hor, T.S.A. 2009, *Organometallics* 28, p. 2935.

[6] Hurtado, J., Carey, D.M.-L., Munoz-Castro, A., Arriata-Pérez, R., Quijada, R., Wu, G., Rojas, R. and Valderrama, M. 2009, *J. Organomet. Chem.* 694, p. 2636.

[7] Bhaduri, S., Mukhopadhyay, S. and Kulkarni, S.A. 2009, *J. Organomet. Chem.* 694, p. 1297.

[8] Chirik, P.J. 2009, *J. Am. Chem. Soc.* 131, p. 3788.

[9] Cotton, F.A., Murillo, C.A. and Walton, R.A. Multiple bond between metal atoms 3rd ed. Berlin : Springer, 2005.

[10] Nguyen, T., Sutton, A. D., Brynda, M., Fettinger, J.C., Long, G. J., Power, P. P. 2005, *Science* 310, p. 844.

[11] Kreisel, K. A., Yap, G. P. A., Dmitrenko, O., Landis, C. R., Theopold, K. H. 2007, *J. Am. Chem. Soc.* 129, p. 14162.

[12] Chisholm, M.H. 2007, *PNAS* 104, p. 2563.

[13] Noor, A., Glatz, G., Müller, R., Kaupp, M., Demeshko, S. and Kempe, R. 2009, *Nature Chem.* 1, p. 322.

[14] Thompson, J.J. 1897, *Philosophical Magazine* 44, p. 293.

[15] Geiger, H., Marsden, E. 1909, *Proc. R. Soc. Lond.* A 82, p. 495.

[16] Bohr, N. 1913, *Philosophical Magazine* 26, p. 1.

[17] Bohr, N. 1913, *Philosophical Magazine* 26, p. 476.

[18] Bohr, N. 1913, *Philosophical Magazine* 26, p. 857.

[19] Lewis, G.N. 1916, *J. Am. Chem. Soc.* 38, p. 762.

[20] Einstein, A. 1905, *Annalen der Physik* 322, p. 132.

[21] de Broglie, L. 1925, *Ann. Phys.* 3, p. 22.

[22] Heisenberg, W. 1927, *Zeitschrift für Physik* 43, p. 172.

[23] Schrödinger, E. 1926, *Phys. Rev.* 28(6) , p. 1049.

[24] Heitler W., London, F. 1927, *Zeitschrift für Physik* 44, p. 455.

[25] Pauling, L. The nature of the chemical bond. Ithaca, NY : Cornell University Press, 1960.

[26] Frenking, G. 2005, *Science* 310, p. 796.
[27] Radius, U. and Breher, F. 2006, *Angew. Chem. Int. Ed.* 45, p. 3006.
[28] Weinhold, F. and Landis, C.R. 2007, *Science* 316, p. 61.
[29] Herzberg, G. 1929, *Z. Phys.* 57, p. 601.
[30] Roos, B. O., Borin, A. C., Gagliardi, L. 2007, *Angew. Chem. Int. Ed.* 46, p. 1469.
[31] Reed, A.E., Curtiss, L.A. and Weinhold F. 1988, *Chem. Rev.* 88, p. 899.
[32] Pauling, L. and Wheland, G.W. 1933, *J. Chem. Phys.* 1, p. 362.
[33] Weinhold, F. and Landis, C.R. 2001, *Chemistry Education* 2, p. 91.
[34] Glendening, E.D. and Weinhold, F. 1998, *J. Comput. Chem.* 19, p. 593.
[35] Glendening, E.D. and Weinhold, F. 1998, *J. Comput. Chem.* 19, p. 610.
[36] Coulson, C.A. 1939, *Proc. Roy. Soc. Lond.* A 169, p. 413.
[37] Wiberg, K.B. 1968, *Tetrahedron* 24, p. 1083.
[38] Cotton, F.A. 1978, *Acc. Chem. Res.* 11, p. 225.
[39] Pauling, L. The nature of the chemical bond 3rd ed. Ithaca, N.Y. : Cornell University Press, 1960.
[40] Kauffman, G.B. 1973, *Coord. Chem. Rev.* 9, p. 339.
[41] Bauschlicher, C.W.J. 1986, *J. Chem. Phys.* 84, p. 872.
[42] Dahl, L.F., Ishishi, E., Rundle, R.E. 1957, *J. Chem. Phys.* 26, p. 1750.
[43] Peligot, E. 1844, *C.R. Hebd. Seances Acad. Sci.* 19, p. 609.
[44] Brosset, C. 1946, *Arkiv Kemi, Miner. Geol.* A20(7).
[45] Bertrand, J.A., Cotton, F.A., Dollase, W.A. 1963, *J. Am. Chem. Soc.* 85, p. 1349.
[46] Bertrand, J.A., Cotton, F.A., Dollase, W.A. 1963, *Inorg. Chem.* 2, p. 1166.
[47] Cotton, F. A., Curtis, N. F., Harris, C. B., Johnson, B. F. G., Lippard, S. J., Mague, J.T, Robinson, W.R. and Wood, J.S. 1964, *Science* 145, p. 1305.
[48] Cotton, F. A., Curtis, N. F., Johnson, B. F. G., Robinson, W. R. 1965, *Inorg. Chem.* 4 , p. 326.
[49] Cotton, F. A., Harris, C. B. 1965, *Inorg. Chem.* 4, p. 330.
[50] Cotton, F.A. 1965, *Inorg. Chem.* 4, p. 334.
[51] Kotel'nikova, A.S. and Tronev, V.G. 1958, *J. Inorg. Chem. USSR* (english trans.) 3, p. 1008.
[52] Kuznetzov, B.G. and Koz'min, P.A. 1963, *Zhur. Strukt. Chim.* 4, p. 55.
[53] Brencic, J. V., Cotton, F. A. 1969, *Inorg. Chem.* 8, p. 7.
[54] Cotton, F. A. and Bratton, W.K. 1965, *J. Am. Chem. Soc.* 87, p. 921.
[55] Trogler, W.C. and Gray, H.B. 1978, *Acc. Chem. Res.* 11, p. 232.
[56] Gagliardi, L. and Roos, B.O. 2003, *Inorg. Chem.* 42, p. 1599.
[57] Cotton, F.A., Rice, C.E. and Rice, G.W. 1977, *J. Am. Chem. Soc.* 99, p. 4704.
[58] Cotton, F.A., Extine, M.W. and Rice, G.W. 1978, *Inorg. Chem.* 17, p. 176.
[59] Cotton, F.A. and Thompson, J.L. 1981, *Inorg. Chem.* 20, p. 1292.
[60] Cotton, F.A., Daniels, L.M., Murillo, C.A., Pascual, I. and Zhou, H.-C. 1999, *J. Am. Chem. Soc.* 121, p. 6856.

[61] Ketkar, S.N. and Fink, M. 1985, *J. Am. Chem. Soc.* 107, p. 338.
[62] Cotton, F.A., Hillard, E.A., Murillo, C.A. and Zhou, H.-C. 2000, *J. Am. Chem. Soc.* 122, p. 416.
[63] Cotton, F. A., Koch, S. A., Millar, M. 1978, *Inorg. Chem.* 17, p. 2084.
[64] Cotton, F.A., Koch, S.A. and Millar, M. 1977, *J. Am. Chem. Soc.* 99, p. 7372.
[65] Cotton, F.A. and Millar, M. 1978, *Inorg. Chem.* 17, p. 2014.
[66] Cotton, F.A., Niswander, R.H. and Sekutowski, J.C. 1978, *Inorg. Chem.* 17, p. 3541.
[67] Bino, A., Cotton, F.A. and Kaim, W. 1979, *J. Am. Chem. Soc.* 101, p. 2506.
[68] Bino, A., Cotton, F.A. and Kaim, W. 1979, *Inorg. Chem.* 18, p. 3566.
[69] Cotton, F.A., Daniels, L.M., Huang, P. and Murillo, C.A. 2002, *Inorg. Chem.* 41, p. 317.
[70] Clyburne, J.A.C and Mc Mullen, N. 2000, *Coord. Chem. Rev.* 210, p. 73.
[71] Yoshifuji, M., Shima, I., Inamoto, N., Hirotsu, K. and Higuchi, T. 1981, *J. Am. Chem. Soc.* 103, p. 4587.
[72] Lappert, M.F., Bassindale, A.R. and Gaspar, P.G. 1991, *Frontiers of organosilicon chemistry*, Royal Society of Chemistry, London, p. 231.
[73] Waggoner, K.M., Ruhlandt-Senge, K., Wehmschulte R.J., He, X., Olmstead, M.M. and Power, P.P. 1993, *Inorg. Chem.* 32, p. 2557.
[74] Goto, K., Holler, M. and Okazaki, R. 1997, *J. Am. Chem. Soc.* 119, p. 1460.
[75] Schiemenz, B. and P.P. Power. 1996, *Angew. Chem. Int. Ed.* 35, p. 2150.
[76] Su, J., Li, X.-W., Crittendon, R.C. and Robinson, G.H. 1997, *J. Am. Chem. Soc.* 119, p. 5471.
[77] Cotton, F.A., Cowley, A.H. and Feng, X. 1998, *J. Am.Chem. Soc.* 120, p. 1795.
[78] Goldberg, D.E., Hitchcock, P.B., Lappert, M.F., Thomas, K.M., Thorne, A.J., Fjelberg, T., Haaland, A., Schilling, B.E.R. 1986, *J. Chem. Soc. Dalton Trans.* , p. 2387.
[79] Pu, L., Senge, M.O., Olmstead, M.M. and Power, P.P. 1998, *J. Am. Chem. Soc.* 120, p. 12682.
[80] Olmstead, M.M., Simons, R.S. and Power, P.P. 1997, *J. Am. Chem. Soc.* 119, p. 11705.
[81] Power, P. P. 2003, *Chem. Commun.*, p. 2091.
[82] Pu, L., Twamley, B., Power, P. P. 2000, *J. Am. Chem. Soc.* 122, p. 3524.
[83] Stender, M., Phillips, A. D., Wright, R. J., Power, P. P. 2002, *Angew. Chem. Int. Ed.* 41, p. 1785.
[84] Philips, A. D., Wright, J. R., Olmstead, M. M., Power, P. P. 2002, *J. Am. Chem. Soc.* 124, p. 5930.
[85] Grev, R.S. 1991, *Adv. Organomet. Chem.* 33, p. 125.
[86] Nagase, S., Kobayashi, K. and Takagi, N. 2000, *J. Organomet. Chem.* 611, p. 264.
[87] Kobayashi, K. and Nagase, S. 1997, *Organometallics* 16, p. 2489.
[88] Chen, Y. Hartmann, M., Diedenhofen, M. and Frenking, G. 2001, *Angew. Chem. Int. Ed.* 40, p. 2051.
[89] Landis, C. R., Weinhold, F. 2006, *J. Am. Chem. Soc.* 128, p. 7335.
[90] Brynda, M., Gagliardi, L., Widmark, P.-O., Power, P.P. and Roos, B.O. 2006, *Angew. Chem. Int. Ed.* 45, p. 3804.
[91] Nguyen, T., Merrill, W.A., Ni, C., Lei, H., Fettinger, J.C., Ellis, B.D., Long, G.J., Brynda, M. and Power, P.P. 2008, *Angew. Chem. Int. Ed.* 47, p. 9115.
[92] La Macchia, G., Gagliardi, L., Power, P. P., Brynda, M. 2008, *J. Am. Chem. Soc.* 130, p. 5104.

[93] Wolf, R., Ni, C., Nguyen, T., Brynda, M., Long, G. J., Sutton, A. D., Fischer, R.C., Fettinger, J.C., Hellman, M., Pu, L. and Power, P.P. 2007, *Inorg. Chem.* 46, p. 11277.

[94] Jayakumar, S., Ishar, M.P.S. and Mahajan, M.P. 2002, *Tetrahedron* 58, p. 379.

[95] Barker, J. and Kilner, M. 1994, *Coord. Chem. Rev.* 133, p. 219.

[96] Edelmann, F.T. 1994, *Coord. Chem. Rev.* 137, p. 403.

[97] Edelmann, F.T. 2009, *Chem. Soc. Rev.* 38, p. 2253.

[98] Sanger, A.R. 1973, *Inorg. Nucl. Chem. Lett.* 9, p. 351.

[99] Tsai, Y.-C., Lin, Y.-M, Yu, J.-S.K. and Hwang, J.-K. 2006, *J. Am. Chem. Soc.* 128, p. 13980.

[100] Hsu, C.-W., Yu, J.-S. K., Yen, C.-H., Lee, G.-H., Wang, Y., Tsai, Y.-C. 2008, *Angew. Chem. Int. Ed.* 47, p. 9933.

[101] Tsai Y.-C., Hsu, C.-W., Yu, J.-S. K., Lee, G.-H., Wang, Y. and Kuo, T.-S. 2008, *Angew. Chem. Int. Ed.* 47, p. 7250.

[102] Deeken, S., Motz., G. and Kempe, R. 2007, *Z. Anorg. Allg. Chem.* 633, p. 320.

[103] Kempe, R. 2003, *Eur. J. Inorg. Chem.*, p. 791.

[104] Noor, A., Wagner, F. R., Kempe, R. 2008, *Angew. Chem. Int. Ed.* 47, p. 7246.

[105] Noor, A., Glatz, G., Müller, R., Kaupp, M., Demeshko, S. and Kempe, R. 2009, *Z. Anorg. Allg. Chem.* 635, p. 1149.

[106] Ozin, G.A. and Mitchell S.A. 1983, *Angew. Int. Ed.* 22, p. 674.

[107] Shim, I. 1985, *Mat. Fys. Medd. K. Dan. Vidensk. Selsk.* 41, p. 147.

[108] Morse, M.D. 1986, *Chem. Rev.* 86, p. 1049.

[109] DiLella, D.P., Limm, W., Lipson, R.H., Moskovits, M. and Taylor K.V. 1982, *J. Chem. Phys.* 77 , p. 5263.

[110] Kant, A. and Strauss B. 1964, *J. Chem. Phys.* 41, p. 3806.

[111] Efremov, Y.M., Samoilova, A.N. and Gurvich, L.V. 1974, *Opt. Spectry.* 36, p. 381.

[112] Kündig, E. P., Moskovits, M., Ozin, G. A. 1975, *Nature* 254, p. 503.

[113] Bondebey, V. E., English, J. H. 1983, *Chem. Phys. Lett.* 94, p. 443.

[114] Michalopoulos, D.L. Geusic, M.E., Hansen, S.G., Powers, D.E. and Smalley, R.E. 1982, *J. Phys. Chem.* 86, p. 3914.

[115] Simard, B., Lebeault-Dorget, M.-A., Marijnissen, A., ter Meulen, J. J. 1998, *J. Chem. Phys.* 108, p. 9668.

[116] Hilpert, K. and Ruthardt, K. 1987, Ber. Bunsenges. *Physik. Chem.* 91, p. 724.

[117] Bauschlicher, C.W. Jr., Walsh, S.P. and Partridge, H. 1982, *J. Chem. Phys.* 76, p. 1033.

[118] Roos, B. O. 2003, *Collect. Czech. Chem. Commun.* 68, p. 265.

[119] Casey, S. M., Leopold, D. G. 1993, *J. Phys. Chem.* 97, p. 816.

[120] Goodgame, M.M. and Goddard III, W.A. 1982, *Phys. Rev. Letters* 48, p. 135.

[121] Klotzbuecher, W. and Ozin, G.A. 1977, *Inorg. Chem.* 16, p. 984.

[122] Boudreaux, E.A. and Baxter, E. 2004, *Int. J. Quant. Chem.* 100, p. 1170.

[123] Boudreaux, E.A., Baxter, E. 2005, *Int. J. Quant. Chem.* 102, p. 866.
[124] Boudreaux, E.A. and Baxter, E. 2001, *Int. J. Quant. Chem.* 85, p. 509.
[125] McLean, A.D. and Liu, B. 1983, *Chem. Phys. Lett.* 101, p. 144.
[126] Richman, K.W. and McCullough Jr., E.A. 1987, *J. Chem. Phys.* 87, p. 5050.
[127] Goddard III, W.A. and Ladner, R.C. 1971, *J. Am. Chem. Soc.* 93, p. 6750.
[128] Goddard III, W.A., Dunning Jr., T.H., Hunt, W.J. and Hay, P.J. 1973, *Acc. Chem. Res.* 6, p. 368.
[129] Goodgame, M. M., Goddard III, W. A. 1981, *J. Phys. Chem.* 85, p. 215.
[130] Goodgame, M.M. and Goddard III, W.A. 1985, *Phys. Rev. Lett.* 54, p. 661.
[131] Werner, H.-J. and Knowles, P.J. 1988, *J. Chem. Phys.* 89, p. 5803.
[132] Takahara, Y., Yamaguchi, K. and Fueno, T. 1989, *Chem. Phys. Lett.* 158, p. 95.
[133] Scuseria, G.E. and Schaefer III, H.F. 1990, *Chem. Phys. Lett.* 174, p. 501.
[134] Scuseria, G.E. 1991, *J. Chem. Phys.* 94, p. 442.
[135] Bauschlicher Jr., C.W. and Partridge H. 1994, *Chem. Phys. Lett.* 231, p. 277.
[136] Walch, S.P., Bauschlicher Jr, C.W., Roos, B.O. and Nelin, C.J. 1983, *Chem. Phys. Lett.* 103, p. 175.
[137] Andersson, K., Roos, B.O., Malmqvist, P.-A. and Widmark, P.-O. 1994, *Chem. Phys. Lett.* 230, p. 391.
[138] Andersson, K. 1995, *Chem. Phys. Lett.* 237, p. 212.
[139] Roos, B.O. and Andersson K. 1995, *Chem. Phys. Lett.* 245, p. 215.
[140] Edgecombe, K.E. and Becke, A.D. 1995, *Chem. Phys. Lett.* 244, p. 427.
[141] Noodleman, L. and Davidson, E.R. 1986, *Chem. Phys.* 109, p.131
[142] Frenking, G. and Tonner, R. 2007, *Nature* 446, p. 276
[143] Gorokhov, L.N., Emelyanov, A.M., Khodeev, Y.S. 1974, *Teplofiz. Vys. Temp.* 12, p. 1307
[144] Souter, P.F., Kushto, G.P., Andrews, L. and Neurock, M. 1997, *J. Am. Chem. Soc.* 119, p. 1682
[145] Roos, B.O., Malmqvist, P.-A. and Gagliardi, L. 2006. *J. Am. Chem. Soc.* 128, p. 17000
[146] Gagliardi, L. and Roos, B. O. 2005, *Nature* 433, p. 848
[147] Roos, B.O. and Gagliardi, L. 2006, *Inorg. Chem.* 45, p. 803
[148] Gagliardi, L., Pykkö, P. and Roos, B.O. 2005, Phys. Chem. Chem. Phys. 7, p. 2415
[149] Hohenberg, P. and Kohn, W. 1964, *Phys. Rev.* 136, p. B864.
[150] Kohn, W. and Sham, L.J. 1965, *Phys. Rev.* 140, p. A1133.
[151] Barden, C.J., Rienstra-Kiracofe, J.C. and Schaefer III, H.F. 2000, *J. Chem. Phys.* 113(2), p. 690.
[152] Yanagisawa, S., Tsuneda, T. and Hirao, K. 2000, *J. Chem. Phys.* 112, p. 545.
[153] Gutsev, G.L. and Bauschlicher Jr, C.W. 2003, *J. Phys. Chem. A* 107, p. 4755.
[154] Roos., B.O. [ed.] Chichester, England, chap. 69 K.P. Lawley (John Wiley & Sons Ltd. 1987, Advances in Chemical Physics; Ab Initio Methods in Quantum Chemistry-II, p. 399.
[155] Bartlett, R.J. 1981, *Ann. Rev. Phys. Chem.* 32, p. 359.
[156] Andersson, K., Malmqvist, P.-A., Roos, B.O., Sadlej, A.J. and Wolinski, K. 1990, *J. Phys. Chem.* 94, p. 5483.
[157] Andersson. K., Malmqvist, P.-A. and Roos, B.O. 1992, *J. Chem. Phys.* 96, p. 1218.

Part 3

Results and Discussions

Paper I: Large Differences in Secondary Metal-Arene Interactions in the Transition-Metal Dimers ArMMAr (Ar = Terphenyl; M = Cr, Fe, or Co): Implications for Cr—Cr Quintuple Bonding

Large Differences in Secondary Metal—Arene Interactions in the Transition-Metal Dimers ArMMAr (Ar = Terphenyl; M = Cr, Fe, or Co): Implications for Cr—Cr Quintuple Bonding

Giovanni La Macchia[1], Laura Gagliardi[1], Philip P. Power[2], and Marcin Brynda[2]

[1]*Department of Chemistry, University of Geneva, 30 quai E. Ansermet, Geneva 1211, Switzerland*

[2]*Department of Chemistry, University of California, Davis, One Shields Avenue, Davis, California 95616*

Published in Journal of the American Chemical Society, 2008 (130), p. 5104

Abstract

Quantum mechanical calculations, using both CASPT2 and DFT methods, for the model systems (MeMMMe, PhMMPh, (MeMMMe)(C_6H_6)$_2$, Ar§MMAr§, Ar$^{\#}$MMAr$^{\#}$; M = Cr, Fe, Co; Ar§= C_6H_4-2(C_6H_5), Ar$^{\#}$ = C_6H_3-2,6(C_6H_3-2,6-Me_2)$_2$) are described. These studies were undertaken to provide a multireference description of the metal—metal bond in the simple dimers MeMMMe and PhMMPh (M = Cr, Fe, Co) and to determine the extent of secondary metal—arene interaction involving the flanking aryl rings of the terphenyl ligands in quintuply bonded Ar′CrCrAr′ (Ar′ = C_6H_3-2,6(C_6H_3-2,6-Pr^i_2)$_2$). We show that in the Cr—Cr species the Cr—arene interaction is a feeble one that causes only a small weakening of the quintuple bond. In sharp contrast, in the analogous Fe and Co species strong η^6-arene interactions that preclude significant metal—metal bonding are predicted.

1. Introduction

The recent characterization of the quintuply bonded chromium species Ar´CrCrAr´ (Ar´ = C_6H_3-2,6(C_6H_3-2,6-Pr^i_2)$_2$) has raised new bonding questions and stimulated theoretical work on transition-metal species with potentially high metal−metal bond orders [**1-4**]. The Ar´CrCrAr´ compound featured a short Cr−Cr bond of 1.8351(4) Å as well as a trans-bent, planar C_{ipso}−Cr−Cr−C_{ipso} core structure, Cr−Cr−C = 102.78(1)°. There was also a relatively short (2.294(1) Å) secondary Cr−C interaction involving an ipso-carbon of one of the flanking aryl rings as illustrated in Scheme 1. Earlier calculations [**5**] by Weinhold and Landis on the simple group 6 model species HWWH predicted that its optimized geometry had indeed a trans-bent (C_{2h}) structure as well as a quintuple W−W bond. These, as well as their more recent studies on the model species MeMMMe (M = Cr, Mo or W), led to the conclusion that the trans-bent structure of the RMMR compounds was a result of s−d hybridization which strengthened the M-M bond [**6**].

Scheme 1. X-ray Crystal Structure of the Ar'CrCrAr' Species[a]

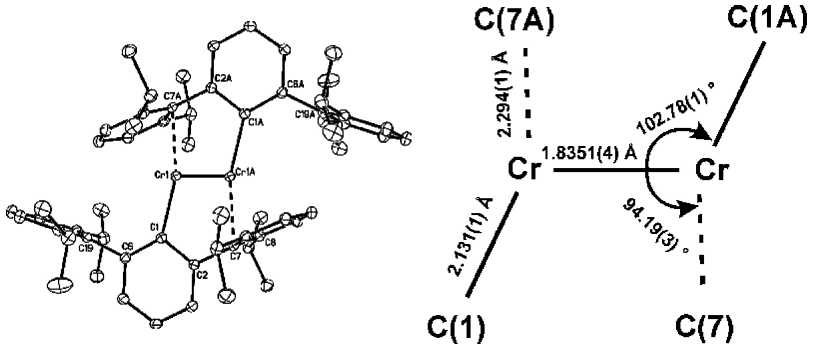

[a] *Hydrogens are omitted for clarity with schematic representation of the C_{ipso}-Cr-Cr-C_{ipso} core with relevant structural parameters including Cr-C distances in the secondary interactions with the flanking aryl of the terphenyl ligand.*

We also reported calculations performed with the high-level multiconfigurational CASPT2 method on model species PhCrCrPh. This study yielded structural parameters for the trans-bent configuration, Cr−Cr = 1.752 Å, Cr−Cr−C = 88.4°, that differed significantly from those experimentally observed for Ar´CrCrAr´ (a linear form of PhCrCrPh with Cr−Cr =

1.678 Å was calculated to be 1 kcal mol^{-1} more stable than the trans-bent form) [**7**]. In contrast, the bond length in the dimetal Cr_2 molecule calculated at the same level of theory [**8**] was found to be in almost exact agreement with the experimental value of 1.679 Å [**9**]. Thus, the following question arises: to what extent do any additional interactions found in the crystal structure, in particular those pertaining to the large size of the Ar´ substituent and the close secondary Cr-ligand approaches, affect the Cr−Cr bonding?

Since the use of large ligands containing flanking aryl moieties has become now a widely used strategy for the stabilization of dimeric, metal−metal bonded species among the main group and transition elements [**10-12**], we thought it important to address this topic by quantifying the impact of such weak interactions on the geometry of the CMMC core units for a selection of transition metal dimers, in this case derivatives of Cr, Fe, and Co. We provided a preliminary qualitative report of such interactions in a recent publication [**13**], but no quantitative analysis have yet been carried out by theoretical quantum chemistry methods. We restrict our study to the three transition metal dimers and exclude the manganese species since most of the theoretical methods are divided on this very challenging system [**14, 15**].

The paper is organized as follows: first, we present the theoretical methods used in this study and explain the choice of the model compounds for the metal dimers bearing bulky terphenyl ligands. We begin with the calculations of the energies for various spin multiplicities in the RMMR (R = Me, Ph) model species. Following this, we report the optimized structures of the model species in several spin states and introduce the most important structural features of the computed geometries, briefly discussing the results of torsional potential-energy surface scans that measure the strength of the metal−metal bond and characterize the flatness of the energy surfaces. The second part of the paper includes the results of the optimizations of monomeric ligand–metal/arene species Me−M−Bz, as well as its dimeric analogues, in which the simplest diorgano-dimetal complexes MeMMMe interact with benzene. Calculations on analogous models $Ar^{\S}MMAr^{\S}$ and $Ar^{\#}MMAr^{\#}$($Ar^{\S}$= C_6H_4-2(C_6H_5), $Ar^{\#}$ = C_6H_3-2,6(C_6H_3-2,6-Me_2)$_2$) are also reported, followed by the evaluation of the corresponding bond orders. We then discuss the energetics of the metal-arene interactions in our model species and close with some conclusions.

2. Computational Methods

Multiconfigurational quantum chemical calculations were performed using the complete active space-SCF (CASSCF) [**16**] method to generate wave functions for several electronic states of a given symmetry and spin multiplicity. Dynamic correlation was added using second-order perturbation theory, CASPT2 [**17**]. The CASSCF/CASPT2 calculations were performed using the MOLCAS 6.4 [**18**] program package. Scalar relativistic effects were included using the Douglas−Kroll−Hess Hamiltonian [**19, 20**] and the ANO-RCC basis set [**21**], where the primitive set 21s15p10d6f4g2h was contracted to 5s4p2d1f for the transition metals (M), the primitive set 14s9p4d3f2g was contracted to 3s2p1d for carbon, and the primitive set 8s4p3d was contracted to 2s1p for hydrogen. The active space was formed by 14 molecular orbitals (MOs). There are two bonding and two antibonding M−C MOs and five bonding and five antibonding M−M MOs, arising from a linear combination of the M 3d and 4s and the C(methyl/phenyl) radical orbitals. The number of active electrons included in the active space was 14 for the Cr compounds (six from each Cr, corresponding to the valence configuration $3d^5 4s^1$ and one from each C), 18 for the Fe compounds (eight from each Fe, corresponding to the valence configuration $3d^6 4s^2$ and one from each C) and 20 for the Co compounds (nine from each Co, corresponding to the valence configuration $3d^7 4s^2$ and one from each C). In the subsequent CASPT2 calculations the orbitals up to and including the 2p on the transition metals and 1s on C were kept frozen. Calculations on the ground-state of each system and several excited states were performed. Spin−orbit effects were not taken into account, but, according to the results of studies on similar compounds, they do not affect the structure of the ground state [**22**]. The effective bond order (EBO) [**4**] between the two M atoms was calculated as the sum of the occupation numbers of the bonding orbitals minus the sum of the occupation numbers of the antibonding orbitals, divided by two. DFT optimized geometries were used as starting points and subsequent CASPT2 geometry reoptimization of the most relevant parameters, like the M−M bond distance, M−C bond distance and MMC angle, was performed. Dissociation energies (De) have been calculated as energy differences between the energy of the full systems minus twice the energy of half-the systems (at their optimized DFT geometry) with the correction to basis set superposition error (BSSE) using the counterpoise correction. The method has proven to be successful in the study of similar

transition-metal compounds, for example, $Re_2Cl_8^{2-}$ [**23**] and $Re_2(CH_3)_8^{2-}$ [**24, 25**].

The investigation of the arene/transition metal interactions was performed with DFT, which is known to reproduce the transition metal–ligands geometries to satisfactory accuracy [**26-35**]. Since the theoretical analysis of the metal−metal bonds with multiple character (for which the DFT description is known to suffer from its intrinsic monodeterminental character) is not at the focus here, only the quantitative trends in both, M−M bond lengths and the geometries of the CMMC cores induced by the interactions with arene ligands are analyzed. The differences between the noninteracting geometries (MeMMMe) and the geometries of the (MeMMMe)$(C_6H_6)_2$ models are then mapped on the geometrical features obtained from the CASPT2 calculations and finally compared to the experimental geometries. This methodology proved to be successful in our recent description of the quintuple character of the Cr−Cr bond in Ar´CrCrAr´ [**7**]. The DFT calculations were performed at both scalar relativistic and nonrelativistic level of theory. The relativistic effects were included using the zero order relativistic approximation (ZORA) relativistic Hamiltonian [**36**], which treats the core−electrons explicitly, as implemented in ADF program [**37**]. In this case the ZORA Hamiltonian was combined with Kohn−Sham formalism using BLYP functional and Slater type of orbitals of triple-ζ quality with one polarization function (TZP). Throughout the text, this implementation is labeled as BLYP/ZORA/TZP. Optimizations of the model molecules with the $Ar^{\#}$ ligands ($Ar^{\#}$ = C_6H_3-2,6-(C_6H_3-2,6-Me_2)$_2$) were performed using BLYP/ZORA combined with TZP basis set for the metal centers and DZP basis set for C and H atoms. The nonrelativistic calculations were carried out using the Gaussian 03 program [**38**] with the Ahlrichs all electron basis set of double-ζ quality augmented with polarization functions [**39**] combined with B3LYP functional (this level of theory is hereafter reported as B3LYP/pVDZ). The binding energies form B3LYP/pVDZ calculations were corrected for basis set superposition error (BSSE) using the counterpoise method of Boys and Bernardi [**40**]. The graphical representations of the optimized structures were generated with GOpenMol software.

Model. The complexity of the terphenyl ligands makes the use of multireference methods for the study of the complete Ar´MMAr´ (Ar´ = C_6H_3-2,6(C_6H_3-2,6-$Pr^i{}_2$)$_2$) dimers difficult. Even with use of the monodeterminental DFT methods, it is not trivial to deal

with the weak interactions in molecules of such size at a satisfactory theoretical level. The difficulty in describing the secondary intramolecular interactions [**41**] occurring between covalently bonded fragments lies in the fact that, in order to quantify the fragment−fragment interaction based on the calculated energies, one has to "divide" the molecule into separate subunits, so that the bonding energies between different fragments can be easily computed. To overcome these difficulties, we decided to conduct our theoretical studies on simplified species: benzene-MeMMMe-benzene hereafter abbreviated (MeMMMe)$(C_6H_6)_2$. In these models, the MeMMMe fragment mimics the metal−metal core (C_{ipso}−M−M−C_{ipso}) found in the Ar´MMAr´ dimers, whereas the nearby two flanking aryl of the ligand are modeled by two surrounding benzene molecules. The geometry of the two benzenes was kept frozen during the geometry optimization of the central MeMMMe fragment, and the C_6H_6−C_6H_6 separation (centroid−centroid distance and mutual orientation) was based on the analogous flanking aryl−flanking aryl distance from the X-ray crystallographic files [**42**]. For the MeMMMe models two possible geometries are involved because of the methyl C_3 symmetry axis: C_{2h} where the distance between the two methyl protons in the symmetry plane remain minimal, and $C_{2h'}$ where this distance is maximized. The (MeMMMe)$(C_6H_6)_2$ molecules were also optimized within C_{2h} and $C_{2h'}$ symmetries (the MeMMMe fragment is constrained into the symmetry plane containing the two opposite carbon atoms of each benzene molecule). The differences between the optimized structures in both symmetries are very small, and we focus mainly on the $C_{2h'}$ symmetry, since this minimizes the steric constraints between the benzenic protons and the proton of the MeMMMe methyl groups in our (MeMMMe)$(C_6H_6)_2$ molecules; in addition, it reflects the situation found in the ArMMAr molecules the most closely. We are of course aware of the fact that this is a rather important simplification and some of its weaknesses are discussed later in the paper. However, it offers the advantage of dealing with a model system containing well-defined fragments. Our initial attempts to use a similar model system containing two benzene molecules, in which the C−M−M−C_{ipso} core was represented by the phenyl−M−M−phenyl (PhMMPh) core remained unsuccessful due to unrealistic sterical constraints between the two benzene molecules and the phenyl groups. For comparison, we also present analogous results on two models mimicking simplified bulky aryls ligands: $Ar^{\S}MMAr^{\S}$ ($Ar^{\S}$ = C_6H_4-2(C_6H_5) and $Ar^{\#}MMAr^{\#}$ ($Ar^{\#}$ = C_6H_3-2,6(C_6H_3-2,6-Me_2)$_2$).

3. Results

Geometries of the RMMR Models (R = Me, Ph; M = Cr, Fe, Co) Obtained from CASSCF/CASPT2 and DFT Calculations. The CASSCF/CASPT2 calculations performed on the MeMMMe and PhMMPh models in their ground-state yielded the structural parameters reported in Table 1. Additional calculations were also performed on some excited states. We shall report here only some of these results. In the MeFeFeMe case, for example, a ^5B_g state lies 9.3 kcal mol^{-1} higher in energy than the ^7A_u ground state. Two other quintet states, ^5A_u, ^5A_g, lie 19.3 and 21 kcal mol^{-1} higher than the septet. Energetically distant septet states were found to be 28.7 kcal mol^{-1} higher in energy than the ground state. In the MeCoCoMe case, the first excited state, a ^5A_g state, lies 4.8 kcal mol^{-1} higher than the ^5B_u ground state and the next quintet state lies 11.2 kcal mol^{-1} higher than the ground state. We will not discuss the excited states further, but instead, focus on the ground state of each system. Inspection of Table 1 shows that the M−M bond distance is about 1.75−1.85 Å in the M = Cr compounds, while it is ca. 0.1−0.2 Å longer (1.94–1.99 Å) in all the M = Fe and M = Co compounds. For all the MeMMMe systems, the energy as a function of the C−M−M−C dihedral angle was determined in order to test if the structure with a nonplanar C−M−M−C moiety had a lower energy. The results indicate that the energy increases upon closure of the dihedral angle and the planar trans-bent structure exhibits the lowest energy. For MeCoCoMe the possible existence of lower energy minima at a longer Co−Co bond distance (2.80 Å) was also investigated, but the present calculations indicate that there is no such double minimum. The Cr−Cr distance is shorter in the Ph compound than in the Me compound. The other difference between the two species is the CCrCr angle, which is smaller in the Me case rather than in the Ph case. In the Me case a diamond-like structure, in which the two Me are bridging between the two Cr atoms, is the one energetically preferred. This explains why the Cr−Cr bond is longer in the Me compound. The Ph compound, on the other hand, has a more trans-bent-like structure with the PhCrCr angle closer to 90°, and this explains why the Cr−Cr bond is shorter in this case.

Table 1. CASPT2 M−M, C−M Bond Distances (Å), C−M−M and C−M−M−C angles (deg), Dissociation Energies (kcal mol^{-1}), and M−M effective bond orders (EBO) for RMMR species (R = Me, Ph; M = Cr, Fe, Co)

model species	M-M (Å)	C-M (Å)	C-M-M (deg)	C-M-M-C (deg)	EBO	De (kcalmol^{-1})
MeCrCrMe, ^1A_g	1.849	2.100	82.2	180.0	2.96	48
PhCrCrPh **[7]**, ^1A_g	1.752	2.018	88.4	180.0	3.52	76
Ar'CrCrAr' **[1]**, ^1A	1.836[a]	2.132[a]	102.8[a]	180.0[a]	3.43	-
MeFeFeMe, ^7A_u	1.989	1.955	129.6	180.0	-	30
PhFeFePh, ^7A_u	1.970	2.017	79.2	180.0	1.47	36
Ar'FeFeAr', ^7A	2.519[a]	2.016[a]	100.4[a]	159.6[a]	-	-
MeCoCoMe, ^5B_u	1.948	1.844	124.3	180.0	-	42
PhCoCoPh, ^5B_g	1.940	1.926	76.4	180.0	1.38	61
Ar'CoCoAr', ^5A	2.801[a]	2.019[a]	94.1[a]	163.5[a]	0	-

[a] *The coordinates and the corresponding bond lengths and bond angles of the Ar´CrCrAr´, Ar´CoCoAr´, and Ar´FeFeAr´ structures (Ar´ = C_6H_3-2,6(C_6H_3-2,6-$Pr^i{}_2$)$_2$) are taken from experimental X-ray crystallographic data* [**42**]

The nature of the metal−metal interaction has been analyzed along the Me and Ph series in terms of the metal−metal effective bond order (EBO) [**4**]. The EBOs are reported together with the M−M and C−M bond distances and the dissociation energies in Table 1. For MeCrCrMe, with a Cr−Cr bond distance of 1.849 Å, the following occupation numbers for the natural orbitals involved in the Cr−Cr bond were obtained: $\sigma_g(1.55), \sigma_u(0.45), \pi_u(3.04), \pi_g(0.96), \delta_g(3.36), \delta_u(0.63)$. These values yield an EBO of 2.96. A similar study on PhCrCrPh [**7**] predicted a ^1A_g ground state, with a Cr−Cr bond distance of 1.752 Å for the trans-bent structure. The EBO between the two Cr atoms in that case was calculated to be equal to 3.52. The Cr−Cr bond is significantly longer and weaker in MeCrCrMe than it is in PhCrCrPh, probably because of a stronger interaction between Cr and Me than that between Cr and Ph. Inspection of the molecular orbitals involved in the Cr−Cr bond in the two systems shows that they are more delocalized toward the Cr−C fragment in case of the Me ligand, in comparison to the Ph ligand.

Single point CASPT2 energy calculations were also performed on the Ar´CrCrAr´ coordinates extracted from the X-ray crystallographic structure corresponding to a Cr−Cr bond distance of 1.836 Å. The following occupation numbers for the natural orbitals involved in the Cr−Cr bond were obtained: $\sigma_g(1.64), \sigma_u(0.35), \pi_u(3.26), \pi_g(0.73), \delta_g(3.52), \delta_u(0.48)$. These values yield to an EBO of 3.43. In other words, the Cr−Cr EBO and bond distance are similar in the Ar´CrCrAr´ system and PhCrCrPh model compound and little changes occur with respect to the other model compound, MeCrCrMe.

The bonding is vastly different in the Co−Co case. The Co−Co bond distances are 1.95 and 1.94 Å for MeCoCoMe and PhCoCoPh, respectively, which are ca. 0.2 Å longer than the metal−metal distance for the corresponding Cr species despite the smaller size of Co. It was not possible to calculate the EBO value between the two Co atoms in the case of MeCoCoMe, because the orbitals involved in the bonds are highly delocalized over the system. In PhCoCoPh the molecular orbitals are more localized and they yield a much lower EBO of 1.38 for the Co−Co bond. In the Ar´CoCoAr´ case, the Co−Co bond distance greatly increased to 2.80 Å, almost 1 Å longer than it is in the methyl- or phenyl-substituted compounds. Analysis of the molecular orbitals shows that the two Co atoms interact exclusively with the flanking arenes and not with each other. The EBO between the two Co is zero in this case. The bonding for the Fe molecules resembles that of their Co counterparts rather than their Cr analogues. For MeFeFeMe, as for MeCoCoMe, it was not possible to calculate the Fe−Fe EBO because of the strong delocalization. To summarize, the CASPT2 results clearly show that the metal−metal interaction is barely affected by the nature of the ligand in the Cr case. On the other hand, it is seriously affected in the Fe and Co case.

For simplicity, only computational results obtained at the quasi-relativistic BLYP/ZORA/TZP level are discussed in the following sections, because the differences in computed geometries between B3LYP/ZORA/TZP and B3LYP/pVDZ are only of minor importance and both approaches exhibit exactly the same trends. However, the reader can find the analogous information from the nonrelativistic calculations in all the tables containing the relevant geometrical parameters. The DFT optimized geometries of the same MeMMMe models in the constrained $C_{2h'}$ symmetry are shown in Figure 1 and the important structural parameters are reported in Table 2. The MeCrCrMe was optimized in the singlet ground state; for the

MeFeFeMe and MeCoCoMe the septet and quintet ground states, as predicted by CASPT2, were used respectively in the calculations. First, the DFT calculated chromium−chromium distances for both C_{2h} and $C_{2h'}$ symmetries (1.697; 1.695 Å) lie in the range of the previously reported Cr−Cr distances that we have obtained probing various combinations of basis sets and functionals [**1**]. In the optimized MeCrCrMe models, the CrCrC angle is close to 100° (95.7; 99.1°). Not surprisingly, the optimized geometries are very different in the case of the analogous iron and cobalt species: For the Fe species, the optimized MeMMMe structure is characterized by longer metal−metal distances (2.092; 2.097 Å) and a wider FeFeC angle (115.9; 115.4°). The MeCoCoMe species have the longest metal−metal separation with the CoCo distances 2.101 and 2.099 Å, and also the most open CoCoC angle (120.2; 119.9°). The situation is similar for the PhMMPh species. The metal−metal separations are close to 1.7 Å for PhCrCrPh and exceed 2.1 and 2.0 Å in PhFeFePh and PhCoCoPh, respectively. It is worth noting, that none of the optimized planar trans-bent structures, except for the $C_{2h'}$ MeFeFeMe, is a minimum on the potential energy surface (PES). The optimized C_{2h} and $C_{2h'}$ MeCrCrMe models are characterized by one or two negative frequencies, respectively. All the optimized PhMMPh species exhibit two negative frequencies.

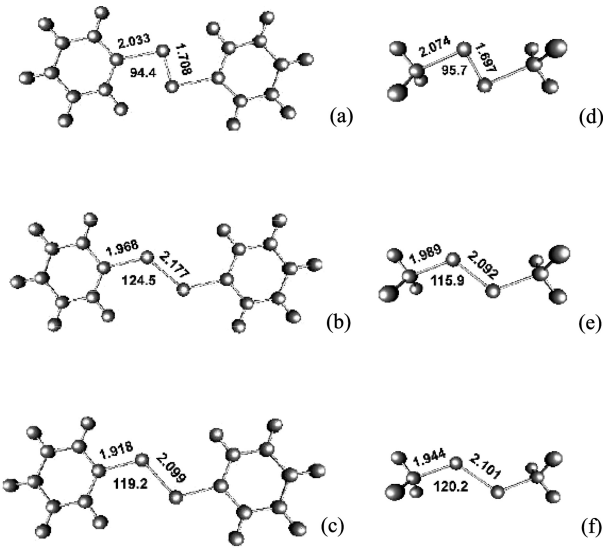

Figure 1. DFT optimized structures of the MeMMMe and PhMMPh species in their ground states obtained at BLYP/ZORA/TZP level. PhMMPh: (a) M =Cr, (b) M = Fe, (c) M = Co. MeMMMe: (d) M =Cr, (e) M = Fe, (f) M = Co.

Table 2. M−M Bond Distances (Å), C−M−M and C−M−M−C angles (deg) in the DFT-optimized Ground States Planar Trans-Bent Structures of MeMMMe and PhMMPh Species at BLYP/ZORA/TZP Level (M = Cr, Fe, Co)[a]

model species (multiplicity)	M-M (Å)	C-M (Å)	C-M-M (deg)
MeCrCrMe, C_{2h} (1)	1.697 (1.626)	2.074 (2.064)	95.7 (92.0)
MeCrCrMe, $C_{2h'}$ (1)	1.695 (1.626)	2.081 (2.078)	99.1 (95.6)
PhCrCrPh, C_{2h} (1)	1.708 (1.634)	2.033 (2.042)	94.4 (93.1)
MeFeFeMe, C_{2h} (7)	2.092 (2.077)	1.989 (1.977)	115.9 (119.5)
MeFeFeMe, $C_{2h'}$ (7)	2.097 (2.070)	1.986 (1.980)	115.4 (121.3)
PhFeFePh, C_{2h} (7)	2.177 (2.173)	1.968 (1.969)	124.5 (124.6)
MeCoCoMe, C_{2h} (5)	2.101 (2.237)	1.944 (1.951)	120.2 (127.4)
MeCoCoMe, $C_{2h'}$ (5)	2.099 (2.227)	1.953 (1.935)	119.9 (124.7)
PhCoCoPh, C_{2h} (5)	2.099 (2.137)	1.918 (1.916)	119.2 (118.1)

[a]Values in parentheses were obtained at B3LYP/pVDZ level.

As mentioned in the introduction, DFT yields inappropriate bond lengths for the RCrCrR dimer because of its intrinsic inability to properly treat its multiconfigurational character [**7**]. The same issue arises in the CoCo and FeFe species, although one would expect the errors to be smaller because of the lower extent of the multiconfigurational character and quantitatively smaller number of d electrons involved in the metal−metal bonding. It is clear however from the DFT optimized geometries that the computed bond lengths for CoCo and FeFe species are much longer (by ∼0.4 Å) than those in the chromium analogue. The effect of the substitution of the methyl group by an electron-rich π system such as a phenyl ligand on the metal−metal bonding, is only moderately embraced by DFT since differences in the optimized metal−metal bond lengths of model RMMR species bearing the two ligands are not very significant. These differences are slightly greater in the case of Fe, but are insignificant for Co. However, they remain small compared to the multireference CASPT2 results.

The relaxed potential-energy curves were generated by performing the C_2 constrained optimizations at discrete values of the CMMC torsion angle ϑ for the high spin configurations of MeFeFeMe and MeCoCoMe dimers (Figure 2) and the singlet spin state MeCrCrMe; analogous curves were obtained for the planar trans-bent geometries where the C−M−M angle φ was varied in the C_{2h} constrained geometry optimizations. The PES of the MeCrCrMe model proved particularly complex. The constrained C_2 optimizations were unsuccessful, since for all the geometries with $\vartheta < 120$, the optimizations led to linear D_{3d} structures, indicating a fairly flat PES in this region. As reported in our previous publications [**1, 7**], the planar trans-bent geometry scan, where φ is varied, indicates an important barrier (ca. 18 kcal mol^{-1}) around 130° between the trans-bent and the linear structure (similar value of 131° and 20 kcal mol^{-1} was found in our previous study of the PhCrCrPh dimer) [**7**]. The computed energy values for the MeFeFeMe and MeCoCoMe C_2 constrained optimizations exhibit monotonically decreasing behavior for the complete 180° rotation around the metal−metal bond with minimum energy for the linear species. In the case of the MeCoCoMe molecule however, the energy values for the torsional angles at 160, 170, and at 180° are almost identical. This part of the curve (torsion angle 160−180°) is very flat, and there is the possibility that a minimum occurs at ϑ value close to 160°. Nevertheless, a very small energy difference ($\Delta E = 0.2$ kcal mol^{-1}) between this geometry and the planar trans-bent configuration ($\vartheta = 180°$) makes it rather unlikely. Moreover, the CASPT2 results seem to indicate that the only minimum occurs for the linear species. Finally, the planar trans-bent geometry scans are characterized by minima occurring for the trans-bent MeMMMe species at 110° and 120°, for M = Co and M = Fe, respectively.

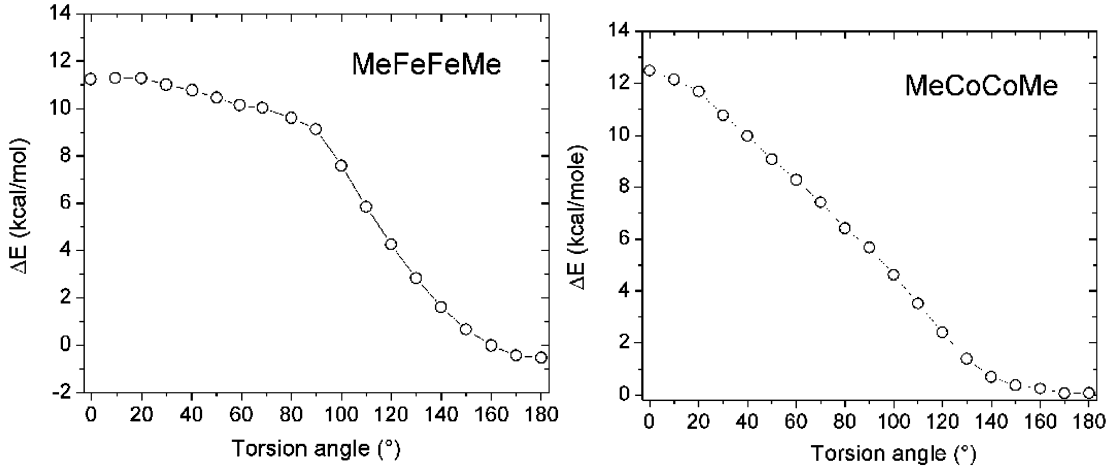

Figure 2. Relaxed torsional angle energy scans for MeMMMe species (M = Fe, Co) obtained at BLYP/ZORA/TZP level of theory.

Since the electronic structure of the MeCrCrMe was discussed in details elsewhere [**6, 43**], we present only the bonding picture arising from the analysis of the molecular Kohn–Sham orbitals for the planar trans-bent MeFeFeMe and MeCoCoMe species. Briefly, in contrast to the singlet MeCrCrMe analogue where all the five 3d orbitals participate in bonding combinations yielding two π, two σ, and one δ bond for CrCr, in the high-spin septet MeFeFeMe, metal−metal bond is composed of two π bonds that are formed by pairs of metal d_{xz} and d_{yz} orbitals and an additional σ bond, which arises from the combination of d_{z^2} orbitals. In the high spin quintet MeCoCoMe, the M−M bond is essentially composed of two d_{xz} orbitals that combine to yield a single π bond and two d_{z^2} orbitals, which form an additional σ bond.

DFT and CASPT2 Optimized Structures of the Monomeric MeM-C_6H_6 Species. In the first stage of the evaluation of the metal−arene interactions in ArMMAr species, we attempted to optimize the geometries of the monomeric MeM−C_6H_6 models. The optimizations were performed for different spin states in order to assess the tendency to spin pairing of the metal d orbitals that could be potentially induced by the vicinity of the aryl π system. The optimized structures are summarized in Figure 3 (see Table 3 for important geometrical parameters). It is clear that the high-spin states always exhibit the lowest energy for all the three benzene-transition metal monomers. The energy differences between the ground

and the next higher energy spin state of lower multiplicity are quite similar for Cr, Fe, and Co, and are ca. 20 kcal mole^{-1}. The most interesting features observed in the optimized structures are the differences in the way the MeM fragment interacts with the benzene ring in the case of the high-spin species. For both Fe and Co, the optimized structures have a η^6 coordination mode and retain the approximate D_{3d} symmetry (no constraints on symmetry were applied during optimizations) with the C_{Me}−M bond being perpendicular to the plane containing the benzene unit, and collinear with the C_6 symmetry axis of the ring. None of these structures however is a minimum on PES and attempts to locate such a minimum remained unsuccessful. In contrast, for chromium, the optimized geometry of the high-spin species, which is a minimum on PES, clearly shows a displacement of the MeM fragment toward a pseudo-η^2 coordination mode (Figure 3), where the C_{Me}−M bond lies on a normal to the ring plane and bisects one of the C−C bonds of the benzene. There are also noticeable differences in the M−C distances to the closest C carbon in benzene, between the Cr and Fe and Co species. These distances, which remain at 2.207 Å (M−centroid = 1.728 Å) and 2.256 Å (M−centroid = 1.807 Å) for Fe and Co, respectively, are much shorter than the corresponding distance for the chromium analogue, for which the distance to the closest two carbons is 2.455 Å (M−centroid = 2.726 Å).

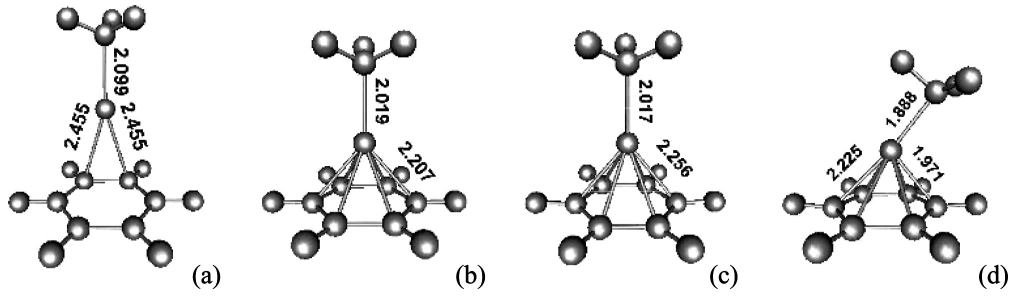

Figure 3. DFT-optimized structures of the MeM−C_6H_6 model species: (a) M =Cr, sextet; (b) M = Fe, quartet; (c) M = Co, triplet; (d) M = Co, singlet. Detailed geometrical parameters are reported in Table 3.

Table 3a. Important Structural Parameters for the DFT Optimized (BLYP/TZP/ZORA) MeM-C_6H_6 Species in Their Ground States (Bond Distances (Å)).

model	MeCr-C_6H_6	MeFe-C_6H_6	MeCo-C_6H_6
M-C_{Me}	2.099 (2.102)	2.019 (2.024)	2.017 (2.029)
$M - C_1^c$	2.455 (2.475)	2.207 (2.203)	2.256 (2.244)
$M - C_2^c$	2.455 (2.475)	2.207 (2.203)	2.256 (2.242)
$M - C_3^c$	3.074 (3.032)	2.207 (2.203)	2.256 (2.242)
$M - C_4^c$	3.597 (3.515)	2.208 (2.204)	2.256 (2.244)
$M - C_5^c$	3.599 (3.518)	2.208 (2.204)	2.257 (2.245)
$M - C_6^c$	3.079 (3.037)	2.208 (2.204)	2.257 (2.245)
M-centroid	2.726 (2.691)	1.728 (1.683)	1.807 (1.743)

[c]M−C_n distances defined such as n = 1 corresponds to the closest carbon and the subsequent numbering is done clockwise in the benzene ring.

Table 3b-1. Important Structural Parameters for the DFT Optimized (BLYP/TZP/ZORA) (MeMMMe)$(C_6H_6)_2$ Species in Their Ground States (Bond Distances (Å), Angles (deg)). C_{2h} symmetry constraint.

model	(MeCrCrMe)$(C_6H_6)_2$	(MeFeFeMe)$(C_6H_6)_2$	(MeCoCoMe)$(C_6H_6)_2$
M-M	1.726	2.740	3.116
M-C_{Me}	2.161	2.088	2.048
MMC	119.3	132.5	122.1
CMMC	180.0	180.0	180.0
$M - C_1^c$	2.235	2.400	2.188
$M - C_2^c$	2.445	2.406	2.229
$M - C_3^c$	2.820	2.418	2.310
$M - C_4^c$	2.990	2.424	2.350
$M - C_5^c$	2.820	2.418	2.310
$M - C_6^c$	2.445	2.406	2.229
M-centroid	2.240	1.968	1.791

[c]M−C_n distances defined such as n = 1 corresponds to the closest carbon and the subsequent numbering is done clockwise in the benzene ring.

Table 3b-2. Important Structural Parameters for the DFT Optimized (BLYP/TZP/ZORA) (MeMMMe)$(C_6H_6)_2$ Species in Their Ground States (Bond Distances (Å), Angles (deg)). $C_{2h'}$ symmetry constraint.

model	(MeCrCrMe)$(C_6H_6)_2$	(MeFeFeMe)$(C_6H_6)_2$	(MeCoCoMe)$(C_6H_6)_2$
M-M	1.733 (1.647)	2.663 (2.653)	3.006 (3.038)
M-C_{Me}	2.147 (2.117)	2.067 (2.076)	2.033 (2.032)
MMC	115.4 (115.7)	127.5 (128.2)	117.5 (115.6)
CMMC	180.0	180.0	180.0
$M-C_1^c$	2.233 (2.230)	2.347 (2.364)	2.219 (2.198)
$M-C_2^c$	2.443 (2.453)	2.367 (2.384)	2.242 (2.224)
$M-C_3^c$	2.817 (2.847)	2.407 (2.423)	2.286 (2.275)
$M-C_4^c$	2.986 (3.024)	2.427 (2.443)	2.308 (2.300)
$M-C_5^c$	2.817 (2.847)	2.407 (2.423)	2.286 (2.275)
$M-C_6^c$	2.443 (2.453)	2.367 (2.384)	2.241 (2.224)
M-centroid	2.237 (2.261)	1.937 (1.958)	1.783 (1.765)
$\triangle_{M-M}$	0.038	0.566	0.907
$\triangle_{C-M-M}$	16.3	12.1	-2.4

[c]M−C_n distances defined such as n = 1 corresponds to the closest carbon and the subsequent numbering is done clockwise in the benzene ring. Data in parentheses obtained at B3LYP/pVDZ level of theory.

Table 3c. Important Structural Parameters for the DFT Optimized (BLYP/TZP/ZORA) $Ar^{\S}MMAr^{\S}$ and $Ar^{\#}MMAr^{\#}$ Species in Their Ground States (Bond Distances (Å), Angles (deg)).

model	$Ar^{\S}CrCrAr^{\S}$	$Ar^{\S}FeFeAr^{\S}$	$Ar^{\S}CoCoAr^{\S}$	$Ar^{\#}CrCrAr^{\#}$	$Ar^{\#}FeFeAr^{\#}$	$Ar^{\#}CoCoAr^{\#}$
M-M	1.736	2.216	2.211	1.744	2.215	2.467
M-C_{Me}	2.071[d]	1.980[d]	1.972[d]	2.126[d]	2.020[d]	1.998[d]
MMC	99.3	97.0	96.8	102.9	101.9	102.2
CMMC	180.0	180.0	180.0	180.0	171.7	169.2
$M-C_1^c$	2.356	2.318	2.189	2.349	2.346	2.210
$M-C_2^c$	2.556	2.505	2.324	2.567	2.587	2.284
$M-C_3^c$	3.056	2.986	2.696	3.024	3.013	2.511
$M-C_4^c$	3.302	3.231	2.898	3.258	3.216	2.699
$M-C_5^c$	3.056	2.986	2.696	3.036	2.987	2.573
$M-C_6^c$	2.556	2.505	2.324	2.576	2.577	2.325
M-centroid	2.434	2.255	2.082	2.463	2.431	1.990
$\triangle_{M-M}$	0.028	0.124	0.112	0.041	0.126	0.369
$\triangle_{C-M-M}$	4.9	-17.2	-20.2	7.1	-11.0	-18.6

[c] $M-C_n$ distances defined such as n = 1 corresponds to the closest carbon and the subsequent numbering is done clockwise in the benzene ring.

[d] $M-C_{ipso}$ distance.

For the lower-spin states the situation is more complex. We encountered severe SCF convergence problems for the lowest spin (doublet) Cr and Fe species and were unable to perform complete optimization geometries of the corresponding molecules. The three small negative frequencies obtained on the partially optimized geometries relate to one rotational and two stretching modes of the methyl fragment. Spurious convergence problems with several transition metals are known, and we are aware of several reports of redundant problems with the geometry optimization problems for several transition metal complexes [**44-46**]. However, the partially optimized geometries are instructive enough for the purpose of our study. An

interesting change in geometry is associated with the spin-state change for MeCo−C_6H_6. The optimized singlet structure exhibits a "bent" geometry with Co-Me bond making an angle of 44.5° with the plane containing the benzene ring.

The distance between the M−Me fragment and the C_6H_6 ring and their relative positions were reoptimized using CASPT2. In agreement with DFT, CASPT2 predicts a shorter M−C_6H_6 bond distance in $MeFeC_6H_6$ and $MeCoC_6H_6$ than in the $MeCrC_6H_6$ case as well as different bonding mode between these species. For $MeCrC_6H_6$, the MMe fragment is aligned with one of the C−C bonds of the benzene ring, instead of being centered above C_6H_6.

DFT Optimized Structures of the MeMMMe Models in a Constrained Arene Environment. The optimized structures of the $(MeMMMe)(C_6H_6)_2$ species with the MeMMMe fragment constrained to $C_{2h'}$ symmetry are illustrated in Figure 4 and important geometrical parameters are cited in Table 3. The most striking difference between the CoCo and FeFe models and the corresponding Cr−Cr species is the retention of practically the same M-M distance by the chromium dimer in a constrained conformational space between the two benzene molecules. The optimized geometry (in comparison to the isolated MeCrCrMe species) exhibits only minor changes in the Cr−Cr bond length (Δl_{CrCr} = 0.038 Å) but is characterized by a significantly wider C−Cr−Cr angle ($\triangle\varphi_{CCrCr}$ = +16.3°). This is in contrast to the Fe and Co analogues in which the corresponding MM bond lengths are dramatically affected by the interaction with benzene. The corresponding M-M elongation is 0.566 Å for Fe and it is 0.907 Å for Co respectively. For all the three species the metal–carbon(methyl) bond is very slightly weakened, which is translated into the small elongation of the M-C bonds: Δl_{CCr} = 0.073, Δl_{CFe} = 0.078 and Δl_{CCo} = 0.123.

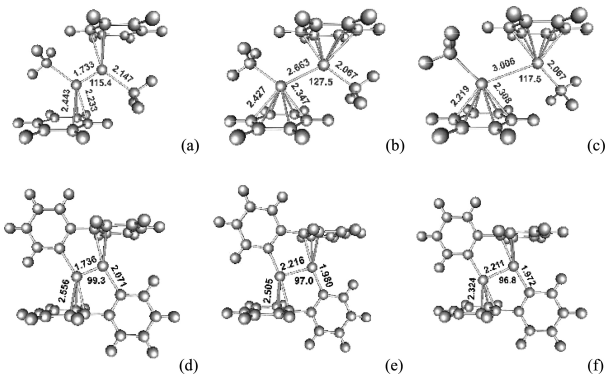

Figure 4. DFT optimized structures of the (MeMMMe)$(C_6H_6)_2$ (a) M =Cr, singlet; (b) M = Fe, septet; (c) M = Co, quintet and A$r^{\S}$MMA$r^{\S}$ (Ar§ = C_6H_4-2(C_6H_5)) (d) M =Cr, singlet; (e) M = Fe, septet; (f) M = Co, quintet; model species. Detailed geometrical parameters in Table 3.

The change in the CMM angle for Fe is slightly smaller than that found for MeCrCrMe ($\Delta A_{FeFeC} = 12.1°$) but for the MeCoCoMe dimer the angle decreases to an optimized value of 117.5° ($\Delta A_{CCoCo} = -2.4°$). Inspection of the metal-benzene carbon distances in the optimized structures is instructive and shows clearly that for both (MeFeFeMe)$(C_6H_6)_2$ and (MeCoCoMe)$(C_6H_6)_2$, an η^6 coordination mode is adopted. The six M-C (benzene) distances display only a small variation in MeFeFeMe and MeCoCoMe, whereas for the MeCrCrMe species, major asymmetry is apparent and the Cr-benzene coordination can be described as between η^1 and η^3 (depending on how the "coordinating" C-M distance is defined). In the process of optimizing the (MeMMMe)$(C_6H_6)_2$ structures, we have also attempted to lift the C_{2h} symmetry constraint relating the planar MeMMMe fragments to the frozen geometry of the benzene rings. Although these attempts did not afford fully optimized structures due to an oscillatory behavior of the geometry optimization cycle, it was however interesting to find that in case of the chromium dimer, the planar MeCrCrMe fragments adopts a slightly "twisted" conformation out of the initial symmetry plane containing the CMMC core and 4 out of 12 carbon atoms of the nearby benzenes. In this particular geometry, the plane containing the CCrCrC core of the MeCrCrMe, almost exactly bisects the C−C bond of each of the benzene molecule. This configuration is very similar to the conformation of the MeCr fragment in the optimized structure of the monomeric MeCr-C_6H_6.

DFT Optimized Structures of the Ar§MMAr§ (Ar§ = C$_6$H$_4$-2(C$_6$H$_5$)) and Ar$^{\#}$MMAr$^{\#}$ (Ar$^{\#}$ = C$_6$H$_3$-2,6(C$_6$H$_3$-2,6-Me$_2$)$_2$) Model Species. The important geometrical features of the optimized Ar§MMAr§ and Ar$^{\#}$MMAr$^{\#}$ species are reported in Table 3. The M−M bond lengths in the Ar§CrCrAr§ and Ar$^{\#}$CrCrAr$^{\#}$ are very similar to the ones obtained in the planar trans-bent PhCrCrPh models optimized at the same level of theory. We have previously attributed the small elongation (ΔL_{CrCr} = 0.041 Å) between PhCrCrPh and Ar$^{\#}$CrCrAr$^{\#}$ to the interaction of the Cr atoms with the nearby flanking aryl, and apparently it is also responsible for the small discrepancy between the CASPT2 calculated Cr−Cr distance in PhCrCrPh and the experimental Cr−Cr separation found in the X-ray crystal structure of the Ar´CrCrAr´ [**7**]. The optimized C_{2h} geometries of the Ar§FeFeAr§ and Ar§CoCoAr§ are, as expected, very similar to the Ar$^{\#}$FeFeAr$^{\#}$ and Ar$^{\#}$CoCoAr$^{\#}$ species. However these latter exhibit two important features: first, the C_{ipso}−M−M−C_{ipso} core is not completely planar as in the case of the Ar$^{\#}$CrCrAr$^{\#}$ (171.7 and 169.2°). In addition, all the three geometries are characterized by much narrower C_{ipso}−M−M angles: 102.9, 101.9, and 102.2° for Cr, Fe, and Co, respectively (note that the C_{ipso}−Cr−Cr angle in the experimental structure is 102.8°). The M−M elongations in Ar§MMAr§ and Ar$^{\#}$MMAr$^{\#}$ versus the optimized PhMMPh species for iron and cobalt are smaller than the analogous elongation computed for the MeMMMe/(MeMMMe)(C$_6$H$_6$)$_2$ congeners. They remain however significantly longer than in the corresponding ArCrCrAr species (0.028 vs 0.039 and 0.112 Å for Fe and Co, respectively, in Ar§MMAr§) and 0.041 vs 0.126 and 0.369 Å for Fe and Co species, respectively, in Ar$^{\#}$MMAr$^{\#}$.

DFT Calculated Wiberg Bond Orders (WBO). The calculated Wiberg bond orders are compiled in Table 4. First, we report the calculations on the model Ar´MMAr´ (Ar´ = C$_6$H$_3$-2,6(C$_6$H$_3$-2,6-Pr$^i_2$)$_2$) molecules on coordinates obtained from the single crystal X-ray analysis. As previously highlighted, the DFT calculation on a singlet chromium dimer results in a Wiberg bond order of 4.11 and is, as expected, less than a value corresponding to a formally quintuple bond. The metal−metal WBOs for Fe and Co are 0.44 and 0.10, respectively, and correspond, at least in case of Co, to an essential absence of bonding between metal centers.

Table 4. DFT Calculated Wiberg Bond Orders (WBO) on the Optimized Structures of MeM−C_6H_6, (MeMMMe)$(C_6H_6)_2$ model species, and Ar´MMAr´ experimental species[a]

	Cr	Fe	Co
MeMMe			
M-M	4.94	1.63	1.23
M-C	0.87	0.91	0.97
[b]*MeMMMe* (LS)*	(HS)		
M-M	0.54	3.49	2.29
M-C	0.78	1.08	1.10
PhMMPh			
M-M	4.77	1.28	1.26
M-C_{ipso}	0.81	0.98	0.99
(MeMMMe)$(C_6H_6)_2$			
M-M	4.22	0.50	0.17
M-C	0.89	0.87	0.88
M-C_6H_6	0.95	1.50	1.96
MeM-C_6H_6			
M-C_{Me}	0.93	0.91	0.95
M-C_6H_6	0.53	2.47	2.04
ArMMAr			
M-M	4.11	0.44	0.10
M-C_{ipso}	0.98	0.73	0.89
M-Ar	0.17	1.23; 1.57	1.90

[a](a) M = Cr, singlet; (b) M = Fe, septet; (c) M = Co, quintet.

[b]Computed for comparison in high spin Cr (S = 5) and low spin Fe (S = 0) and Co (S = 0) species.

The WBOs calculated for the Cr−Cr dimer in the MeMMMe and PhMMPh models are in agreement with those found in the Ar´CrCrAr´ species. The higher Cr−Cr bond orders (4.94, 4.77) in comparison to the Ar´CrCrAr´ molecules are due to the absence of multiple

atomic centers in the surrounding ligands and consequently to a simpler spatial extent of the molecular orbital overlaps. The WBOs for the analogous FeFe and CoCo species are relatively low (1.63, 1.28, and 1.23, 1.26), but this is expected for the high-spin septet and quintet metal−metal interactions.

The bond orders calculated for the arene−metal interactions are also of considerable interest. First, in the "monomeric" MeM−C_6H_6 models, where no metal−metal interaction is present, the calculated bond orders are quite different for Cr, Fe, and Co. The Cr−benzene interaction has a WBO of only 0.53 [**47**], whereas the corresponding bond orders for benzene−Fe and benzene−Co exceed two (2.47 for Fe and 2.05 for Co). This is indicative of strong covalent interaction between the Me−metal fragment and the π system of benzene. Another important observation is the trend in the WBOs calculated in the constrained arene geometry for the (MeMMMe)$(C_6H_6)_2$ species. The metal−metal bond order for Cr−Cr is moderately diminished (4.22 vs 4.94) but the bond order remains higher than four. In contrast, the already low M−M bond orders for Fe and Co are lowered further: from 1.63 to 0.50 for Fe and from 1.23 to 0.17 for Co. This trend is accompanied by a substantial increase in the metal−benzene BO: 1.50 and 1.96 for FeFe and CoCo, respectively. Finally, the methyl carbon−metal bond orders remain almost unaffected and are essentially independent of the presence (or absence) of the secondary arene−metal interaction.

Interaction Energies. The metal−metal bond energies obtained from the CASPT2 calculations are in agreement with the intuitive trend expected for these metal dimers: 75 kcal mole^{-1} for quintuply bonded PhCrCrPh, followed by 61 kcal mole^{-1} for PhCoCoPh and 36 kcal mole^{-1} for PhFeFePh (Table 1). The interaction energies in the (MeMMMe)$(C_6H_6)_2$ species based on the fragment oriented approach were calculated on the previously optimized structures and are reported in Tables 5 and 6. Note that within the hybrid B3LYP approximation to the exchange-correlation functional, the energy difference corresponding to the bonding energy between the two MeCr fragments in MeCrCrMe remains positive (ΔE = +57 kcal mole^{-1}). The energy values computed at the BLYP/ZORA/TZP level show a very small and positive interaction energy between MeCr and benzene (ΔE = +2.5 kcal mole^{-1}), but this value lies within the limit of the DFT accuracy, and consequently the sign of the energy has to be taken with caution. Nevertheless, it is clear that the calculated

MeM−benzene interaction energies are higher for the Fe and Co species (−8.1 and −22.8 kcal mole^{-1}, respectively), in comparison to MeCr−C_6H_6. An approximate estimate of the stabilization energy provided by the secondary interaction with benzene can be obtained from the energy difference between the optimized (MeMMMe)$(C_6H_6)_2$ dimer and the similar structure in which the optimization was performed with constraints on the MeMMMe fragment (kept as optimized on the isolated MeMMMe molecule). This energy is similar for Cr and Co species (15.6 and 12.9 kcal mol^{-1}, respectively) and slightly higher for Fe species (−20.5 kcal mol^{-1}).

Table 5. The Interaction Energies (kcal mol^{-1}) Calculated at the BLYP/ZORA/TZP Level of Theory Using Fragment-Oriented DFT Approach in the Optimized Structures of (MeMMMe)$(C_6H_6)_2$ Model Species (Values in Parentheses Obtained at B3LYP/pVDZ Level)

	M-M	M'-M'	$\triangle E_{stab}$[a]	MeM-C_6H_6
(MeCrCrMe)$(C_6H_6)_2$	-28.2 (+47.1)	-16.5 (+57.0)	-15.6 (-11.4)	+2.5 (+1.8)
(MeFeFeMe)$(C_6H_6)_2$	-44.6 (-29.1)	-25.1 (-8.6)	-20.5 (17.0)	-8.1 (-3.1)
(MecoCoMe)$(C_6H_6)_2$	-40.7 (-49.2)	-26.9 (-35.9)	-12.9 (-9.8)	-22.8 (-21.5)

[a]As calculated from difference between the energy of the optimized (MeMMMe)$(C_6H_6)_2$ and the similar optimized structure, where the MeMMMe fragment was restrained to the geometry obtained for the isolated MeMMMe.

Table 6. The Interaction Energies (kcal mol^{-1}) Calculated at BLYP/ZORA/TZP Level of Theory Using Fragment-Oriented DFT Approach in the Optimized Structures of MeM−C_6H_6 Model Monomeric Species (Values in Parentheses Obtained at B3LYP/pVDZ Level)

	MeM-C_6H_6
MeCr-C_6H_6	-9.6 (-4.9)
MeFe-C_6H_6	-22.9 (-17.1)
MeCo-C_6H_6	-22.1 (-27.7)

The interaction energies were also calculated for the optimized monomeric species where the mutual arrangement of the two fragments (MeM vs benzene) is different (Me-M bond

perpendicular to the plane of the benzenic ring). Although the computed energies exhibit higher absolute values (note that for MeCr-C_6H_6 the energy is now negative), the overall trend is identical. For the η^2 coordinated MeCr in MeCr-C_6H_6, small interaction energy of -9.6 kcal mole^{-1} is found, while for the η^6 coordinated MeFe-C_6H_6 and MeCo-C_6H_6 the values are almost identical, but much higher: -22.9 and -22.1 kcal mole^{-1} for Fe and Co analogues, respectively.

4. Discussion

The optimized geometries of the MeMMMe and PhMMPh models calculated with the CASPT2 method show that for M = Cr the metal−metal interaction is significantly affected by the nature of the ligand (Me vs Ph), in particular the CrCr bond length is shortened by ca. 0.097 Å. The corresponding effective M−M bond order (EBO) increases from 2.96 in MeCrCrMe to 3.52 in PhCrCrPh. The latter value is very close to that calculated for the entire Ar´CrCrAr´ molecule (3.43). The CASPT2 calculations show that the nature of the metal−metal bond (although not the metal−metal distances) in the RFeFeR and RCoCoR species is modified by replacement of Me with Ph. For example for the cobalt dimers, although there is only a minor shortening of the Co−Co bond by ca. 0.008 Å, it is accompanied by the reduction of the EBO from 2.72 in MeCoCoMe to 1.38 in PhCoCoPh. Moreover, the analogous calculation performed on Ar´CoCoAr´ results in an EBO of zero. Similar behavior is also observed for the iron species: the FeFe bond is shortened by 0.019 Å, but the EBO is reduced from 2.31 in MeFeFeMe to 1.47 in PhFeFePh.

The DFT calculations performed on the same model species show a slightly different picture. The Wiberg bond orders (WBO) calculated for the optimized MeMMMe and PhMMPh species remain almost unaffected, and the nature of the ligand does not seem to induce any significant change in the computed WBO within the DFT framework. This is an interesting observation, since it not only confirms the known issues intrinsic to the limited ability of DFT to properly describe the metal−metal bonding in these transition metal dimers, but also raises the question of the correctness of the WBOs calculated within the DFT frame for these truly multiconfigurational species.

At this point, it is interesting to recall the electronic structure of the Cr, Fe, and Co dimers. The main difference between the monovalent first series transition metal RMMR species and the analogous M_2 dimers lies in the fact that in the former, a pair of 4s electrons is used to form the M−C bond with the ligand. However, with this exception only, the overall electronic configuration should remain the same. As discussed in our previous paper on the PhCrCrPh, its CrCr $3d\sigma_g^2 3d\pi_u^4 3d\delta_g^4$ + CrC $4s\sigma_g^2$ singlet ground configuration (with all the spin-paired electrons) corresponds to the analogous configuration obtained for Cr_2: $3d\sigma_g^2 3d\pi_u^4 3d\delta_g^4 4s\sigma_g^2$ where the two 4s electrons participate in the metal−metal bonding. A similar situation occurs in RCoCoR and RFeFeR. For RCoCoR, CASPT2 yields the quintet ground state (^5B_u in the MeCoCoMe case, and ^5B_g in the PhCoCoPh case) which has its homologue in the quintet ground-state configuration of Co_2 obtained by DFT calculations [**48**]: $[3d\sigma_g^1 3d\pi_u^2 3d\delta_g^2 4s\sigma_g^1 3d\sigma_u^{*1} 3d\pi_g^{*2} 3d\delta_u^{*2}]\uparrow[3d\sigma_g^1 3d\pi_u^2 3d\delta_g^2 4s\sigma_g^1 3d\delta_u^{*1}]\downarrow$. In the case of RFeFeR (R = Me and Ph) with the ^7A_u septet, the corresponding ground state for Fe_2 is expressed as $[3d\sigma_g^1 3d\pi_u^2 3d\delta_g^2 4s\sigma_g^1 3d\sigma_u^{*1} 3d\pi_g^{*2} 3d\delta_u^{*2}]\uparrow[3d\sigma_g^1 3d\pi_u^2 3d\delta_g^1 4s\sigma_g^1]\downarrow$.

With these data in hand, it is worthwhile to examine the factors involved in the rather dramatic differences between (a) the chromium dimer, where the secondary ligand interactions have only a minor effect on the geometry of the CMMC core as well as the quintuple character of the Cr−Cr bond and (b) the Co and Fe species, where analogous interactions result in an almost complete disruption of the bonding between the metal centers in the computed ArMMAr and $(MeMMMe)(C_6H_6)_2$ structures. The first point of concern is the interaction of the monomeric MeM fragment with benzene. From the results obtained on the monomeric MeM-C_6H_6 species it is obvious that the interaction of the MeCr fragment is very much weaker than those observed for MeFe and MeCo. In the chromium case, the preferred geometry (see Figure 3) is an approximately η^2 bonding mode, while an η^6 coordination mode is observed for Fe and Co. The differences are also confirmed by the inspection of the corresponding bonding energies. The interaction energy between the MeCr fragment and C_6H_6 is relatively small (or even positive when the MeCr fragment is "bent" toward C_6H_6), while the analogous bonding interactions for Fe and Co exceed 20 kcal/mol). The large difference between the strength of the interaction of benzene with the MeCr moiety and its interaction with the MeFe and MeCo fragments is perhaps the most striking feature of the computational results. What are the reasons for such different complexation behavior?

The origins of the different interaction energies are not straightforward. Simple electronic considerations suggest that the Cr−benzene interactions should be the strongest, since the valence electron count of MeCr (7) is lower than MeFe (9) and MeCo (10), and hence it should bind more strongly to the benzene π-electrons. This is not the case, however, and other factors are apparently of greater importance. One possible contributing factor to the weakness of the MeCr−benzene interaction is the d^5-electron configuration of the MeCr moiety. The d^5 configuration has a favorable exchange energy which is lost if there is a strong η^6-π-interaction with an aryl ring. Our calculations clearly show that the high-spin d^5 configuration is preserved in the weak MeCr(η^2-C_6H_6) complex, and the average energy of the d^5 levels increases slightly. In addition, the HOMO e_1 levels of the benzene are only slightly stabilized upon complexation. In contrast, both the metal d-electrons and the benzene π-levels in the iron and cobalt complexes become stabilized, consistent with the formation of a stronger complex with the C_6H_6 ring. Another possible factor relates to the ionic size of the metal centers. Chromium is the largest of the three metals and in purely electrostatic terms is expected to have the weakest interaction with π-electrons of the aryl ring. Although these reasons seem plausible, they have not been quantified to date. Perhaps the most surprising aspect of these results is the fact that the weakness of the interaction between an arene and a monohapto ligated d^5 metal fragment had not been anticipated. This is especially so in light of the extremely large volume of experimental and theoretical work in the metal−arene area. The very similar Cr−C_6H_6 bonding energies found in the monomeric MeCr−C_6H_6 and dimeric (MeMMMe)$(C_6H_6)_2$ species strongly suggests that the inability of a high-spin monodentate RCr(I) fragment to strongly complex an arene partner is an inherent property of this high-spin moiety.

Additional conclusions can also be drawn from the analysis of the Wiberg bond orders for the (MeMMMe)$(C_6H_6)_2$ species, which reflect the ability of the secondary metal−arene interaction to disrupt the metal−metal bonding. It is noteworthy that instead of relatively short CoCo and FeFe bonds predicted by both DFT and CASPT2 calculations for MeMMMe and PhMMPh, an almost complete absence of M−M bonding has been observed experimentally in Ar´MMAr´ (M = Fe or Co) [**42**] which display strong η^6-metal−arene interactions to the flanking aryl rings. This is in agreement with the computations for the model (MeMMMe)$(C_6H_6)_2$ species. The decrease of WBOs for the M−M bond from 1.63

in MeFeFeMe (1.28 in PhFeFePh) to 0.53 in (PhFeFePh)$(C_6H_6)_2$ or even to 0.44 in the experimental ArFeFeAr, does not leave any doubt that there are two formally unbound metal fragments that are in effect "half-sandwich" moieties. The same situation occurs in case of Co, where the similar decrease in WBO is even more striking: from 1.23 in MeCoCoMe to 0.18 in (MeCoCoMe)$(C_6H_6)_2$ and 0.10 in ArCoCoAr. These results are reinforced by the CASPT2 calculations. The EBO calculated for ArCoCoAr is formally zero.

Before summarizing our final conclusions, it is important to restate some issues that are intrinsic to the model used in this study. First, since the terphenyl ligands are characterized by a large flexibility, one can legitimately argue that the metal−metal separation could only be dictated by the metal−metal interaction itself and that the secondary interaction with the flanking aryl is just a *post factum* occurrence, due to the specific spatial extent of the ligand. However, proving this computationally is not a simple matter as we have seen. Thus, the choice of the C_6H_6−C_6H_6 separation in our (MeMMMe)$(C_6H_6)_2$ models (distances taken from the experimental structures) may seem a little arbitrary. However, in order to obtain insight into the energetics of the M−C_6H_6 interactions and related structural changes, one has to proceed with the fragmentation (i.e., "division" into separate halves) of the molecular system under investigation. Such fragmentation automatically induces a certain lack of control of the interacting fragments, and this is the main reason for the choice of the frozen constrained benzene environment imposed in our model, which is, of course, based on the actual experimental findings. This begs the question of how different would the interaction of the metal center with flanking aryl be in comparison to the M−C_6H_6 interaction in our simplified model? Even if such interactions were different (there are no good reasons to expect large differences), it is difficult to model the flanking aryl−metal interaction without disconnecting it from the central ligand ring bearing the metal center. It is noteworthy that the results obtained with the optimized geometries of the "connected" ligands, modeled using $Ar^{\S}MMAr^{\S}$ or even more crowded $Ar^{\#}MMAr^{\#}$ species, show exactly the same trend as in the (MeMMMe)$(C_6H_6)_2$, even though there are large size and flexibility differences between the ligands present in both these model species.

5. Conclusions

Calculations performed on a simple molecular model to probe the extent of feeble arene-metal interactions that occur in the transition metal dimers bearing the terphenyl ligands suggest that at least two factors contribute to the structural differences observed between the quintuply bonded chromium dimer and its cobalt and iron congeners. First, the robustness of the Cr−Cr quintuple bond is related to the character of the RCr(I) species, whose electronic (d^5) structure precludes strong interactions with the nearby arenes, such as benzene or phenyl fragments. This apparent reluctance to interact more strongly with the surrounding π system of the ligand is an important factor that contributes to the stability of the quintuple Cr−Cr bond. The most important attribute of the CrCr bond is the presence of a high number (10) of valence electrons that exactly match the number of bonding molecular orbitals. It is noteworthy that the recently synthesized monomeric, univalent chromium(I) compounds 3,5-Pr^i_2Ar*CrL (3,5-Pr^i_2Ar* = C_6H-2,6(C_6H_2-2,4,6-Pr^i_3)$_2$-3,5-Pr^i_2, L = THF or PMe_3) whose crystal structures reveal either a THF or a PMe_3 molecule coordinated to two coordinate chromium, decompose when reacted with toluene or benzene [**49**]. In contrast, the analogous Fe or Co derivatives form stable η^6 complexes with arenes to the exclusion of metal−metal bonding [**50**]. Further design and tuning of the ligand should allow unwanted, "spurious" metal–ligand interactions to be excluded. In addition, the significant differences in the occupations of the bonding and antibonding parts of the frontier orbitals observed in the CASPT2 calculations for Me and Ph ligands (which in case of Fe and Co result in a quite different metal−metal bond orders), suggests that in contrast to the Cr dimer, new ligands with strong electron acceptor or electron donor groups could be designed to influence the nature of the metal−metal interaction in these low-valent transition metal dimers.

Acknowledgement. We acknowledge the National Science Foundation for partial financial support. G.L.M. and L.G. thank the Swiss National Science Foundation Grant No. 20021-111645/1. M.B. acknowledges the use of the computational resources at the University of Geneva.

Bibliography

[1] Nguyen, T.; Sutton, A. D.; Brynda, M.; Fettinger, J. C.; Long, G. J.; Power, P. P. *Science* 2005, 310, 844–847.

[2] Frenking, G. *Science* 2005, 310, 796.

[3] Radius, U.; Breher, F. *Angew. Chem., Int. Ed.* 2006, 45, 3006–3010.

[4] Roos, B. O.; Borin, A. C.; Gagliardi, L. *Angew. Chem., Int. Ed.* 2007, 46, 1469–1472.

[5] Weinhold, F.; Landis, C. R. *Chem. Educ.: Res. Pract. Eur.* 2001, 2, 91–104.

[6] Landis, C. R.; Weinhold, F. *J. Am. Chem. Soc.* 2006, 128, 7335– 7345.

[7] Brynda, M.; Gagliardi, L.; Widmark, P.-O.; Power, P. P.; Roos, B. O. *Angew. Chem., Int. Ed.* 2006, 45, 3804–3807.

[8] Roos, B. O. *Collect. Czech. Chem. Commun.* 2003, 68, 265.

[9] Bondybey, V. E.; English, J. H. *Chem. Phys. Lett.* 1983, 94, 443– 447.

[10] (a) Clyburne, J. A. C.; McMullen, N. *Coord. Chem. Rev.* 2000, 210, 73–99. (b) Twamley, B.; Haubrich, S. T.; Power, P. P. *Adv. Organomet. Chem.* 1999, 44, 1–65.

[11] Power, P. P. *Organometallics* 2007, 26, 4362–4372.

[12] Robinson, G. H. *Organometallics* 2007, 26, 2–11.

[13] Nguyen, T.; Panda, A.; Olmstead, M. M.; Richards, A. F.; Stender, M.; Brynda, M.; Power, P. P. *J. Am. Chem. Soc.* 2005, 127, 8545– 8552.

[14] Valiev, M.; Bylaska, E. J.; Weare, J. H. *J. Chem. Phys.* 2003, 119, 5955–5964.

[15] Yanagisawa, S.; Tsuneda, T.; Hirao, K. *J. Chem. Phys.* 2000, 112, 545–553.

[16] Roos, B. O. In *Advances in Chemical Physics: Ab Initio Methods in Quantum Chemistry*-II; Lawley, K. P., Ed.; John Wiley & Sons Ltd.: Chichester, England, 1987; p 399.

[17] Andersson, K.; Malmqvist, P. A.; Roos, B. O.; Sadlej, A. J.; Wolinski, K. *J. Phys. Chem.* 1990, 94, 5483–5488.

[18] Karlströem, G.; Lindh, R.; Malmqvist, P.-A.; Roos, B. O.; Ryde, U.; Veryazov, V.; Widmark, P.-O.; Cossi, M.; Schimmelpfennig, B.; Neogrady, P.; Seijo, L. *Comput. Mater. Sci.* 2003, 28, 222–239.

[19] Kroll, N. M. *Phys. Rev. A* 1974, 82, 89–155.

[20] Hess, B. A. *Phys. Rev. A* 1986, 33, 3742–3748.

[21] Roos, B. O.; Lindh, R.; Malmqvist, P.-A.; Veryazov, V.; Widmark, P.-O. *J. Phys. Chem. A* 2005, 109, 6575–6579.

[22] La Macchia, G.; Brynda, M.; Gagliardi, L. *Angew. Chem., Int. Ed.* 2006, 45, 6210–6213.

[23] Gagliardi, L.; Roos, B. O. *Inorg. Chem.* 2003, 42, 1599–1603.

[24] Ferrante, F.; Gagliardi, L.; Bursten, B. E.; Sattelberger, A. P. *Inorg. Chem.* 2005, 44, 8476–8480.

[25] Gagliardi, L. *Theor. Chem. Acc.* 2006, 116, 307–315.

[26] Frenking, G.; Sola, M.; Vyboishchikov, S. F. *J. Organomet. Chem.* 2005, 690, 6178–6204.

[27] Frenking, G.; Wichmann, K.; Frohlich, N.; Loschen, C.; Lein, M.; Frunzke, J.; Rayon, V. M. *Coord. Chem. Rev.* 2003, 238–239, 55– 82.

[28] Bencini, A.; Carbonera, C.; Dei, A.; Vaz, M. G. F. *Dalton Trans.* 2003, 1701–1706.

[29] Dietz, O.; Rayon, V. M.; Frenking, G. *Inorg. Chem.* 2003, 42, 4977– 4984.

[30] Atanasov, M.; Daul, C. A. *Chem. Phys. Lett.* 2003, 379, 209–215.

[31] Goh, S.-K.; Marynick, D. S. *J. Comput. Chem.* 2001, 22, 1881–1886.

[32] Frenking, G.; Froehlich, N. *Chem. Rev.* 2000, 100, 717–774.

[33] Frohlich, N.; Frenking, G. *Phys. Organomet. Chem.* 1999, 2, 173– 226.

[34] Creve, S.; Pierloot, K.; Nguyen, M. T. *Chem. Phys. Lett.* 1998, 285, 429–437.

[35] Abashkin, Y. G.; Burt, S. K.; Collins, J. R.; Cachau, R. E.; Russo, N.; Erickson, J. W. *NATO ASI Ser., Ser. C* 1996, 474, 1–22.

[36] van Lenthe, E.; Baerends, E. J.; Snijders, J. G. *J. Chem. Phys.* 1994, 101, 9783–9792.

[37] ADF ADF 2002. 03, SCM, Theoretical Chemistry, Vrije Universiteit, Amsterdam, The Netherlands, http://www.scm.com.

[38] Frisch, M. J.; et al. Gaussian 03, revision A.1; Gaussian, Inc.: Pittsburgh, PA, 2003.

[39] Schafer, A.; Horn, H.; Ahlrichs, R. *J. Chem. Phys.* 1992, 9, 2571-2577.

[40] Boys, S. F.; Bernardi, F. *Mol. Phys.* 1970, 19, 553.

[41] By a secondary interaction we mean an intramolecular interaction occurring between two (or more) fragments of the same molecule, in which the interacting fragment are covalently linked at a place other than the one where the secondary interaction occurs.

[42] The experimental crystallographic and magnetic data for the new ArFeFeAr and ArCoCoAr compounds will be published in a separate communication: Merill, A.; Nguyen, P.; Sutton, A.; Long, G. J.; Fettinger, J. C.; Power, P. P. Unpublished work, 2007. Some structural parameters for the experimental species are reported in the Supporting Information file.

[43] Merino, G.; Donald, K. J.; D'Acchioli, J. S.; Hoffmann, R. *J. Am. Chem. Soc.* 2007, 129, 15295–15302.

[44] Daniels, A. D.; Scuseria, G. E. *Phys. Chem. Chem. Phys.* 2000, 2, 2173–2176.

[45] Rabuck, A. D.; Scuseria, G. E. *J. Chem. Phys.* 1999, 110, 695–700.

[46] Wedderburn, K. M.; Bililign, S.; Levy, M.; Gdanitz, R. *J. Chem. Phys.* 2006, 326, 600–604.

[47] However, thermochemical and computational data show that η^6-C_6H_6- Cr bonding is in the range of ca. 35–40 kcal mol^{-1} in Cr(0) bisarene complexes. See: Skinner, H. A.; Coonor, J. A. *Pure Appl. Chem.* 1985, 1957, 1979.

[48] Gutsev, G. L.; Bauschlicher, C. W. *J. Phys. Chem. A* 2003, 107, 4755– 4767.

[49] Wolf, R.; Brynda, M.; Ni, C.; Long, G. J.; Power, P. P. *J. Am. Chem. Soc.* 2007, 129, 6076–6077.

[50] Ni, C.; Ellis, B. D.; Fettinger, J. C.; Long, G. J.; Power, P. P. *Chem. Commun.* 2008, 1014.

Paper II: Bond Length and Bond Order in One of the Shortest Cr−Cr Bonds

Bond Length and Bond Order in One of the Shortest Cr—Cr Bonds

Giovanni La Macchia[1], Francesco Aquilante[1], Valera Veryazov[2], Björn O. Roos[2] and Laura Gagliardi[1]

[1]*Department of Chemistry, University of Geneva, 30 quai E. Ansermet, Geneva 1211, Switzerland*

[2]*Department of Theoretical Chemistry, University of Lund, Chemical Center, P.O. Box 124, S-221 00 Lund, Sweden*

Published in Inorganic Chemistry, 2008 (47), p. 11455

Abstract

Multiconfigurational quantum chemical calculations on the R-diimines dichromium compound confirm that the Cr−Cr bond, 1.80 Å, is among the shortest $Cr^{I}-Cr^{I}$ bonds. However, the bond between the two Cr atoms is only a quadruple bond rather than a quintuple bond. The reason why the bond is so short has to be attributed to the strain in the NCCN ligand moieties.

1. Introduction

The Cr atom plays an important role in multiple bond chemistry [**1**]. Because of its electronic configuration, Cr, together with Mo and W, the other members of group 6, is one of the best candidates for the formation of the highest bond order involving d-block elements, namely, the sextuple bond [**2-5**]. The latter requires the involvement of the six valence electrons on each center, which are distributed into the nd and the (n + 1)s orbitals. Recent synthetic work by several groups has highlighted the existence of very short Cr−Cr bonds, corresponding to high-order multiple bonds and a low oxidation state of Cr. Nguyen et al. [**6**] have characterized the Ar´CrCrAr´ (Ar´ = C_6H_3-2,6(C_6H_3-2,6-Pr^i_2)$_2$) species, with a short Cr−Cr bond of 1.8351(4) Å as well as a trans-bent, planar C_{ipso}−Cr−Cr−C_{ipso} core structure, Cr−Cr−C = 102.78(3)°. This system also presents a relatively short [2.294(3) Å] secondary Cr−C interaction involving an ipso-carbon of one of the flanking aryl rings. We performed high-level multiconfigurational CASPT2 calculations [**7, 8**] on the MeMMMe, PhMMPh, (MeMMMe)(C_6H_6)$_2$, Ar§MMAr§, Ar$^{\#}$MMAr$^{\#}$ species, where M = Cr, Fe, Co, Ar§= C_6H_4-2(C_6H_5), and Ar$^{\#}$ = C_6H_3-2,6(C_6H_3-2,6-Me_2)$_2$, in order to determine the extent of secondary metal−arene interaction involving the flanking aryl rings of the terphenyl ligands in quintuply bonded Ar´CrCrAr´ (Ar´ = C_6H_3-2,6(C_6H_3-2,6-Pr^i_2)$_2$).

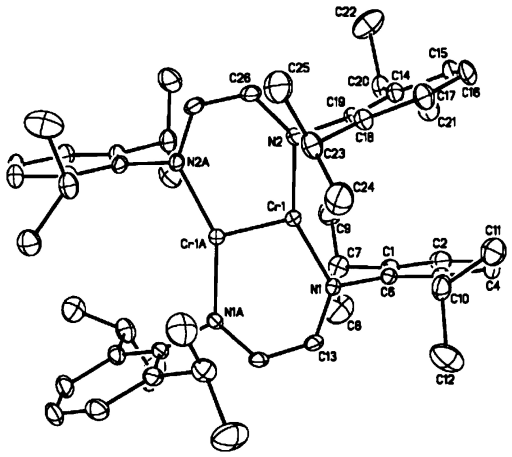

Figure 1. Structure of the R-diimine dichromium compound

More recently, Kreisel et al. [**9**] synthesized a dichromium compound (Figure 1) coordinated by diazadienes (or R-diimines). The geometry around each Cr atom is trigonal planar, with each metal being coordinated by two N atoms from two different diazadiene ligands as well as by the neighboring Cr atom. The interesting feature is the very short Cr−Cr distance of 1.8028(9) Å, making it one of the shortest metal−metal distances. It should be noticed that recently two papers [**10, 11**] have reported even shorter Cr−Cr distances. Complementary closed-shell density functional theory (DFT) calculations were performed at the BLYP/6-311g level using a model complex where the 2,6-diisopropylphenyl substituents were replaced by H atoms. Geometry optimizations on the model complex gave bond distances in good agreement with the experimental compound. Natural bond order (NBO) [**12**] and natural resonance theory analysis were performed, showing the formation of a quintuple bond between the two Cr atoms (bond order 4.3). Earlier studies [**8**] indicate that this result is partly an artifact due to the use of a closed-shell DFT wave function. We decided to study the above compound using the multiconfigurational quantum chemical approach CASSCF/CASPT2 in order to obtain a better understanding of the electronic structure of the system and the nature of the Cr−Cr bond. The method has been very successful in earlier studies of metal−metal bonding [**13-20**].

2. Computational Methods

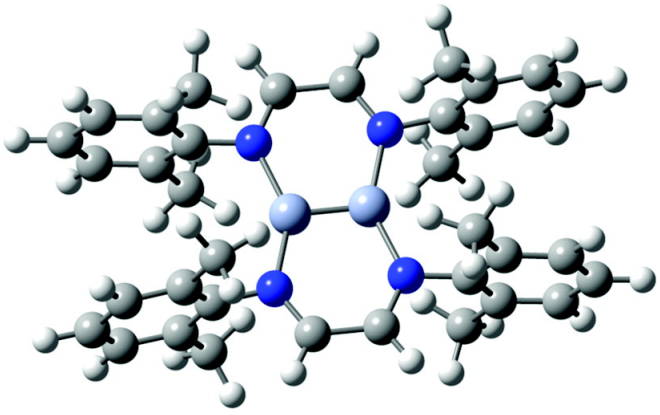

Figure 2. Structure of the model compound used in the calculation.

The size of the experimental compound was slightly reduced by replacing the isopropyl substituents by methyl groups (Figure 2). The whole geometry has been slightly modified to fulfill C_{2v} symmetry. Because the distortion of the real compound from C_{2v} is minimal, we do not think that this geometry constraint will affect the final result. Preliminary DFT calculations were performed using the B3LYP functional and DZP basis sets. A total of 2 degrees of freedom were investigated, namely, the Cr−Cr and Cr−N bond distances. For each point on the grid, corresponding to a given value of the Cr−Cr and Cr−N distances, the rest of the geometry was fully optimized at the DFT level of theory. Successive CASPT2 [**21**] geometry optimization of the Cr−Cr and Cr−N bonds was performed at each point of the grid.

The CASPT2 calculations were performed using the MOLCAS-7.1 package [**22**]. The ANO-RCC [**23**] VTZP basis set was used for chromium whereas the ANO-RCC [**23**] VDZP was used for the other atoms. The calculations were performed imposing C_{2v} symmetry. Scalar relativistic effects were included using the Douglas-Kroll-Hess hamiltonian [**24**]. The computational costs arising from the two-electron integrals were drastically reduced by employing the Cholesky decomposition (CD) technique in all CASSCF/CASPT2 calculations [**25, 26**] combined with the Local Exchange (LK) screening [**27**]. The decomposition threshold was chosen to be 10^{-4}, as this should correspond to an accuracy in total energies of the order of mHartree or higher [**25-28**]. A new approach [**29**] for the calculations of the dynamic electron correlation effects was used ("freeze-and-delete" FD-CASPT2). In this approach, an "active site" is identified as the collection of atoms where the active orbitals effectively extend. Accordingly, the inactive and secondary orbitals can be separately localized and partitioned between the active site and the remaining atoms (environment). Accurate relative energies and potential energy surfaces can be then obtained by performing CD-CASPT2 calculations in which the correlating orbitals are restricted to those assigned to the active site. For the system studied in the present communication, this corresponds to excluding a large number of inactive and virtual orbitals, namely all those localized on the phenyl and methyl groups. Only thanks to the corresponding savings in disk requirements and computational costs, it has been possible to perform a CASSCF/CASPT2 potential energy surface scan of reliable accuracy.

The active orbitals included in the CASSCF [**30**] wave function are linear combinations of the Cr 3d orbitals forming the quintuple bond. In addition some orbitals describing the interaction between the Cr ions and the nitrogen ligands need to be included. One would expect that the Cr-N interaction would involve the Cr 4s orbital and the nitrogen σ lone pairs. This bonding, however, turns out to be very ionic with nitrogen σ orbitals that do not interact strongly with the Cr ions. Instead there is a formation of covalent bonds between the Cr 3dδ orbitals and the π orbitals of the nitrogen ligands. This unusual bonding type seems to occur between transition metal ions and imido type nitrogens. A recent example is the Co-imido bond in the complex Co(III)(diiminato)(NPh) [**25**]. We thus selected two of the nitrogen π orbitals having the correct symmetry in order to interact with Cr 3dδ. Finally one more orbital, which is mainly Cr 4s, was also included, resulting in a total active space of twelve electrons in thirteen orbitals. The orbitals up to 1s for carbon, nitrogen and up to 2p for chromium were kept frozen in the subsequent CASPT2 calculations.

The presence of delocalized orbitals in the active space makes the evaluation of the EBO difficult. The problem was overcome by identifying a region "A", composed by the two Cr atoms, and a region "B", consisting of all the remaining atoms. A value of 0.3 for the gross Mulliken population of each localized orbitals have been used in order to assign the orbital to the Cr-Cr region. *Ad hoc* Cholesky decompositions [**28**] have been used to obtain Localized Molecular Orbital (LMOs). Although in this orbital basis the CASSCF density matrix is no longer diagonal, we can assume that the matrix is sparse in the cross-term sub-blocks mixing LMOs from region A and B. With this assumption, the density matrix can be approximated as composed by two *non-interacting sub-blocks*, corresponding to LMOs of region A and B, respectively. These sub-blocks can be diagonalized separately to produce orbitals that are by definition confined in one of these two regions, and also have an occupation number.

3. Results and Discussions

The Cr−Cr and Cr−N bond distances, optimized at the CASPT2 and closed-shell B3LYP levels of theory, are reported in Table 1, together with the corresponding experimental values. CASPT2 distances are in good agreement with the experiment, while closed-shell B3LYP slightly underestimates the Cr−Cr bond distance. The nature of this particularly short Cr−Cr bond has been analyzed in terms of the electronic configuration of the ground state of the compound and the molecular orbitals intervening in the bond.

Table1. Cr-Cr and Cr-N bond distance (in Å), computed at the CASPT2 and DFT levels of theory, together with the experimental values.

	Cr-Cr	Cr-N
CASPT2	1.799	1.909
B3LYP	1.726	1.911
BLYP [**9**]	1.764	1.904
Exp. [**9**]	1.803	1.914

Inspection of the wave function shows that the closed-shell configuration, (Cr-Cr)σ^2(Cr-Cr)π^4(Cr-Cr)δ^2(Cr-N)π^4, dominates with a weight of 0.6, while all other configurations (about 185000) contribute with weights lower than 0.05. The most important among them correspond to double excitations from the bonding orbitals to their antibonding counterparts. Their presence is responsible for the fractional occupation number of the orbitals and the multiconfigurational character of the wave function. A total of 10 molecular orbitals are almost completely localized on the Cr−Cr moiety, while the remaining 3 (orbitals 9 to 11) are more delocalized (Figure 3).

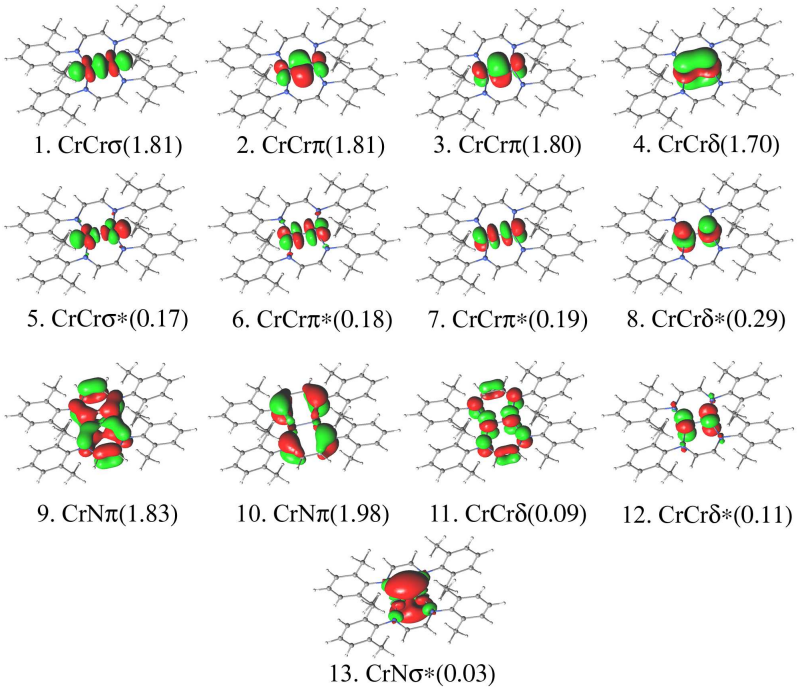

Figure 3. The active molecular orbitals and their occupation number.

The occupation numbers of the active orbitals can be used to determine the effective bond order (EBO) between the two Cr atoms, calculated as half the difference between the sum of the occupation numbers of the bonding orbitals minus the sum of the occupation numbers of the antibonding orbitals [**2**]. The presence of delocalized orbitals in the active space makes the evaluation of the EBO less straightforward because their contribution to the Cr−Cr bond cannot be univocally assigned.

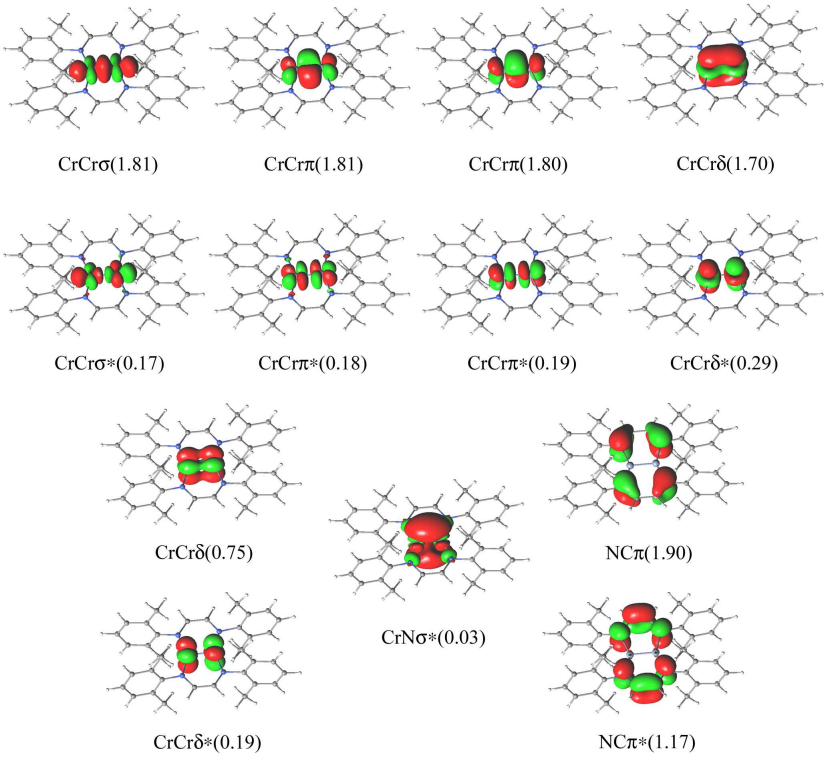

Figure 4. The localized active molecular orbitals and their occupation number.

The use of the localization procedure, described in the computational section, allowed to isolate the contribution of the delocalized orbitals to the Cr-Cr multiple bond. The comparison between the resulting Localized Natural Orbitals (LNOs) and those before localization shows that the shape and the occupation numbers has not changed for the orbitals which were already localized as MOs (Figure 3). The evaluation of the EBO for the Cr-Cr bond is very straightforward in terms of the LNOs of Figure 4, as there is no ambiguity in deciding which orbitals to include in the counting. Except for the orbitals denoted as CrN and NC, all other 10 orbitals are involved in the CrCr bond. With this approach, a value of 3.43 has been obtained for the EBO, which differs significantly from the bond order of 4.28 proposed by Kreisel et al. [**9**] but is consistent with the value of 3.5 that we obtained from NBO analysis based on LoProp [**31**] densities. We thus consider the present Cr-Cr bond as a quadruple bond rather than a quintuple bond because one of the 3dδ orbitals is mainly involved in the

π bonding with the nitrogen ligands. It should be pointed out at this point that it is a matter of semantics to describe a bond with a bond order of 3.5 as a quadruple bond or a quintuple bond where a couple of bonds are very weak. Both descriptions are possible, but what is important is that the quantitative measure of a bond order is given by its EBO.

The EBO of 3.43 obtained in this case is similar in value to the EBO of 3.52 obtained for the model compound PhCrCrPh or of 3.43 obtained for the Ar´CrCrAr´ species synthesized by Nguyen et al. [**6**]. In the above case, the Cr-Cr bond distance, 1.84 Å, is longer than that in the present R-diimines Cr-Cr compound, 1.80 Å.

Such a situation naturally raises the question, why is the Cr-Cr bond shorter here than in the earlier cases even if the bond order is smaller? One should, of course, realize that there is no simple linear relationship between the bond order and the bond length. Many other factors determine a bond length, and here we believe that the strain in the NCCN ligand moieties is the key factor that holds the two Cr atoms in place and limits the variations in the bond distance. So, it is the specific ligands used here that make the Cr-Cr bond so short. This effect is even more obvious in the two recently synthesized systems [**10, 11**].

The formal oxidation state of Cr is not straightforward. Kreisel et al. [**9**] point to the fact that the oxidation state could be 2+, 1+, or 0 because of the redox ambiguity of diimine and other imine-containing ligands. On the basis of geometrical arguments, they concluded that the most likely oxidation state is between 1+ and 2+. This conclusion is well supported by the present study. The Cr atoms lose the 4s electrons, which go to the ligands. In addition, π bonds are formed between Cr and N, half a bond per Cr-N pair. This gives an oxidation number of 1.5+. The Cr-Cr bond is then essentially a quadruple bond with a small extra contribution from the delocalized CrN π bonding orbitals. This is quite different from the Cr-Cr bond of Ar´CrCrAr´, where all five Cr 3d orbitals are involved in the bond. Still the bond order is about the same because the δ orbitals in Ar´CrCrAr´ form only quite weak bonds.

4. Conclusions

In conclusion, we have performed multiconfigurational quantum chemical calculations on the R-diimines dichromium compound recently synthesized by Kreisel et al. [**9**]. Our calculations confirm that the Cr-Cr bond, 1.80 Å, is among the shortest Cr^I-Cr^I bonds to date. However, inspection of the wave function and the relevant molecular orbitals shows that the bond between the two Cr atoms has an EBO of 3.43 and not of 4.28 as proposed by Kreisel et al. [**9**]. The analysis of the electronic structure shows that the electronic structure is best described with a formal oxidation state of 1.5+ for each of the Cr atoms. This leads to a bond that comprises between four and five 3d electrons per atom. Taking into account the weakness of the δ bond, this is consistent with the computed bond order. We are currently investigating similar species in order to try to understand how one could influence the length and strength of a metal-metal multiple bond by using different central metals and different ligands.

Acknowledgment. This work was supported by the Swiss National Science Foundation (Grants 200021-111645/1 and 200020-120007) and the Swedish Research Council (VR) through the Linnaeus Center of Excellence on Organizing Molecular Matter (OMM).

Bibliography

[1] Cotton, F. A.; Curtis, N. F.; Harris, C. B.; Johnson, B. F. G.; Lippard, S. J.; Mague, J. T.; Robinson, W. R.; Wood, J. S. *Science* 1964, 145, 1305.

[2] Roos, B. O.; Borin, A. C.; Gagliardi, L. *Angew. Chem., Int. Ed.* 2007, 46, 1469.

[3] Frenking, G.; Tonner, R. *Nature* 2007, 446, 276.

[4] Weinhold, F.; Landis, C. R. *Science* 2007, 316, 61.

[5] Landis, C. R.; Weinhold, F. *J. Am. Chem. Soc.* 2006, 128, 7335.

[6] Nguyen, T.; Sutton, A. D.; Brynda, M.; Fettinger, J. C.; Long, G. J.; Power, P. P. *Science* 2005, 310, 844.

[7] La Macchia, G.; Gagliardi, L.; Power, P. P.; Brynda, M. *J. Am. Chem. Soc.* 2008, 130, 5104.

[8] Brynda, M.; Gagliardi, L.; Widmark, P. O.; Power, P. P.; Roos, B. O. *Angew. Chem., Int. Ed.* 2006, 45, 3804.

[9] Kreisel, K. A.; Yap, G. P. A.; Dmitrenko, O.; Landis, C. R.; Theopold, K. H. *J. Am. Chem. Soc.* 2007, 129, 14162.

[10] Noor, A.; Wagner, F. R.; Kempe, R. *Angew. Chem., Int. Ed.* 2008, 47, 7246.

[11] Tsai, Y.-C.; Hsu, C.-W.; Yu, J.-S. K.; Lee, G.-H.; Wang, Y.; Kuo, T.-S. *Angew. Chem., Int. Ed.* 2008, 47, 7250.

[12] Reed, A. E.; Curtiss, L. A.; Weinhold, F. *Chem. Rev.* 1988, 88, 899.

[13] Roos, B. O.; Gagliardi, L. *Inorg. Chem.* 2006, 45, 803.

[14] La Macchia, G.; Brynda, M.; Gagliardi, L. *Angew. Chem., Int. Ed.* 2006, 45, 6210.

[15] Hagberg, D.; Karlstrom, G.; Roos, B. O.; Gagliardi, L. *J. Am. Chem. Soc.* 2005, 127, 14250.

[16] Gagliardi, L.; Roos, B. O. *Nature* 2005, 433, 848.

[17] Gagliardi, L.; Roos, B. O. *Inorg. Chem.* 2003, 42, 1599.

[18] Gagliardi, L.; Heaven, M. C.; Krogh, J. W.; Roos, B. O. *J. Am. Chem. Soc.* 2005, 127, 86.

[19] Gagliardi, L.; Pyykko, P.; Roos, B. O. *Phys. Chem. Chem. Phys.* 2005, 7, 2415.

[20] Gagliardi, L. *Theor. Chem. Acc.* 2006, 116, 307.

[21] Andersson, K.; Malmqvist, P.-Å.; Roos, B. O. *J. Chem. Phys.* 1992, 96, 1218.

[22] Karlström, G.; Lindh, R.; Malmqvist, P.-Å.; Roos, B. O.; Ryde, U.; Veryazov, V.; Widmark, P.-O.; Cossi, M.; Schimmelpfennig, B.; Neogrady, P.; Seijo, L. *Comput. Mat. Sci.* 2003, 287, 222.

[23] Roos, B. O.; Lindh, R.; Malmqvist, P. Å.; Veryazov, V.; Widmark, P. O. *J. Phys. Chem. A* 2005, 109, 6575.

[24] Hess, B. A. *Physical Review A* 1986, 33, 3742.

[25] Aquilante, F.; Malmqvist, P.-A.; Pedersen, T. B.; Ghosh, A.; Roos, B.O. *J. Chem. Theory Comp.* 2008, 4, 694.

[26] Aquilante, F.; Lindh, R.; Pedersen, T. B. *J. Chem. Phys.* 2007, 127, 114107.

[27] Aquilante, F.; Pedersen, T. B.; Lindh, R. *J. Chem. Phys.* 2007, 126, 194106.

[28] Aquilante, F.; Pedersen, T. B.; Sanchez de Meras, A.; Koch, H. *J. Chem. Phys.* 2006, 125, 174101.

[29] Aquilante, F.; Gagliardi, L.; Roos, B. O. to be published 2009.

[30] Roos, B. O.; Taylor, P. R.; Siegbahn, P. E. M. *Chemical Physics* 1980, 48, 157.

[31] Gagliardi, L.; Lindh, R.; Karlstrom, G. *J. Chem. Phys.* 2004, 121, 4494.

Paper III: Correlation between the effective bond order (EBO) and a Cr-Cr bond distance in different classes of compounds

Correlation between the effective bond order (EBO) and a Cr-Cr bond distance in different classes of compounds

G. La Macchia, G. Li Manni, T. K. Todorova, M. Brynda, F. Aquilante, B. O. Roos and L. Gagliardi

Department of Chemistry, University of Geneva, 30 quai E. Ansermet, Geneva 1211, Switzerland

submission stage

Abstract

Since the discovery of a formal quintuple bond in Ar'CrCrAr' (CrCr=1.8351 Å) by Power and co-workers in 2005, a lot of efforts have been dedicated to isolate dichromium species featuring quintuple bond character. In the present study we investigate the electronic configuration of several, recently synthesized dichromium species with ligands containing nitrogen to coordinate the metal centers. We show that the correlation between the CrCr bond length and the effective bond order (EBO) is strongly affected by the nature of the ligand, as well as by the steric hindrance due to the ligand architecture (e.g. the nature of the coordinating nitrogen). As a result, the CrCr species based on the amidinate, aminoprydinate and guanidinate ligands have bond pattern similar to the Ar'CrCrAr' compound. Unlike these latter species, the dichromium diazadiene complex is characterized by a different bonding pattern involving Cr-Nπ interactions featuring a lower bond order associated with a short metal-metal bond distance. In this case the short CrCr distance is most probably the result of the constraints imposed by the diazadiene ligand implying a Cr_2N_4 core with a closer CrCr interaction.

1. Introduction

The nature of the interactions governing chemical bonds has always fascinated chemists. For quite a long time, the transition metal chemistry was ruled by the ideas developed at the end of the 19th century by Alfred Werner [**1**]. Werner's theory was able to explain, at least partially, the coordination chemistry of these elements, although the metal ion was considered as an isolated unit surrounded by ligands, precluding any direct metal-metal bonding. At best, only indirect transition metal interactions through shared ligands were taken into account. The ability of d-block elements to be involved in direct metal-metal interaction was revealed half a century ago by Cotton and co-workers, giving birth to a new research field of inorganic chemistry: the chemistry of metal-metal multiple-bonded species. In 1963, the first achievement in this area consisted in the isolation of the $[Re_3Cl_{12}]^{3-}$ molecule containing the $Re(III)_3{}^{9+}$ core unit made of three double bonds [**2, 3**]. The second one came in 1964, with the quadruply bonded Re(III)-Re(III) unit in the $K_2[Re_2Cl_8]\bullet 2H_2O$ complex [**4-7**] featuring a Re-Re distance of 2.24 Å, shorter than the one found in the metallic rhenium (2.75Å). The overcome of the triple bond limit ruled by the p-block elements gave rise to a new challenge: the quest for the multiple bonds with highest achievable order. Since then, a lot of efforts have been dedicated to isolate compounds featuring high order metal-metal multiple bonds. About one thousand of such compounds have been synthesized and characterized since [**8**].

After Cotton's milestone discovery in 1964, no real breakthrough was performed in this area until the synthesis of the Ar'CrCrAr' (CrCr=1.8351 Å) by Power and co-workers in 2005 [**9**], bringing to light the first compound featuring a formal quintuple bond. Such achievement was possible by making the right choice of the transition metal, as well as providing a ligand assuring sufficient kinetic stabilization of the metal-metal bond. In this perspective, the group 6 elements, such as chromium, are *par excellence* the best candidates for the quintuple metal-metal interaction. Five out of their six valence electrons can be used to form the quintuple bond, leaving one electron free to share a bond with the surrounding ligand. The choice of the ligand is the crucial parameter that allows keeping the transition metal in the lowest oxidation state possible, at the same time maximizing the number of valence electrons available for the formation of the multiple bond.

The synthesis of the Ar'CrCrAr' gave a new momentum to the chemistry of multiple-bonded metal-metal species and became a new impetus for the isolation of increasingly shorter metal-metal interactions. In this paper we will discuss several of these compounds (see the numbering in Table 1 and 2). The very short Cr-Cr bond of 1.828 Å measured in solid Tetrakis(2-methoxy-5-methylphenyl)dichromium [**10**], was challenged in 2007 by Kreisel and co-workers who isolated the dichromium diazadiene complex (**1**) [**11**] featuring a Cr-Cr bond distance of 1.803 Å and a Cr-N distances of 1.913 and 1.914 Å. The work of Kreisel highlighted the possibility of using a new class of ligands relying on nitrogen, that were subsequently used to isolate species featuring short metal-metal bonds [**12-15**]. Recently, several such molecules were reported. In 2008, Hsu and co-workers [**12**] used amidinate ligands to form closely related compounds of the type $[Cr_2(\mu\text{-}\eta^2\text{-}ArNC(R)NAr)_2]$ ($\mathbf{2}_{a-d}$). Their Cr-Cr equilibrium bond distances are close to 1.74 Å (the exact values are reported in Table 2). During the same year, Tsai and co-workers [**13**] showed that amidinate ligands of the type $Ar^{Xyl}NC(H)NAr^{Xyl}$ (Ar^{Xyl}=2,6-C_6H_3-$(CH_3)_2$) can be used to achieve very short Cr-Cr bond length within the paddlewheel architecture (**3**). They investigated the paramagnetic neutral species, $[Cr_2\text{-}(Ar^{Xyl}NC(H)NAr^{Xyl})_3]$, as well as its reduced form, $[Cr_2\text{-}(Ar^{Xyl}NC(H)NAr^{Xyl})_3]^-$. Both are featuring short bimetallic distances of 1.817 and 1.740 Å, for the neutral and reduced species, respectively. Noor and co-workers [**14**] investigated a Cr_2 compound based on the aminopyridinate ligand (**4**). This species, unlike compounds **2** and **3**, is composed of a ligand with two non equivalent coordinated nitrogens, N_{amido} and $N_{pyridine}$. The relevant structural parameters of this structure are the Cr-Cr bond of 1.749 Å, and the Cr-N_{amido} and Cr-$N_{pyridine}$ bond distances of 1.998 and 2.028 Å, respectively. In 2009, the gap between the bare Cr_2 featuring a bond distance of 1.68 Å and the Cr(I)-Cr(I) unit was bridged by Noor and co-workers [**15**]. They were able to isolate a Cr-Cr bond length of 1.729 Å, the shortest metal-metal bond observed to date. It was obtained using guanidinate ligands (**5**), which were shown in a previous study to ensure a very short Cr(II)-Cr(II) distance of 1.773 Å in $\{(Me_3Si)_2NC(Ncy)_2CrMe\}_2$ [**16**].

The aforementioned compounds, based on amidinates, aminopyridinates and lately on guanidinates, have almost the same $Cr_2(RNC(R)NR)_2$ core unit but differ considerably in the outer architecture. The guanidinates are the newest generation of ligands, which seem to be the most suitable candidates to achieve even shorter Cr-Cr bond lengths. The most

interesting feature of these ligands is their possible modification by attaching different groups to the nitrogen not involved in the bonding with the metal. Such fine-tuning of the ligand allows the N-C-N fragment to behave as a pincer, forcing the two transition metals to approach each other to different extent.

As for now, the main target in the dichromium chemistry is the synthesis of the compounds with the Cr-Cr interactions closest to the limit imposed by the Cr_2 molecule. However, the connection between the Cr-Cr bond length and the order of the chemical bond is anything but obvious. Although the nature of the chemical bond can be accurately described using modern quantum chemistry, its quantification in term of bond order is still challenging as it doesn't refer to any physical observable. Among different methods available to quantify the bond multiplicity, the Effective Bond Order (EBO) is one of the most accurate, reflecting the multiconfigurational character of the electronic configuration of the bond. It is calculated as half the difference between the sum of the occupation numbers of the bonding orbitals minus the sum of the occupation numbers of the antibonding orbitals. In the past, we have applied highly accurate ab initio method such as CASPT2 for the study of several dichromium compounds [**17-19**]. In this work, we propose to investigate the recently synthesized structures featuring new ligands with the main goal of establishing the correlation between the EBO and the chromium-chromium bond length in dichromium compounds bearing different classes of stabilizing ligands.

Table 1. Structure of the investigated compounds and their numbering.

Labelling of the discussed compounds:				
1	**2**	**3**	**4**	**5**
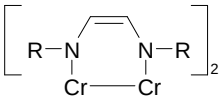	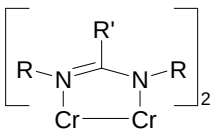	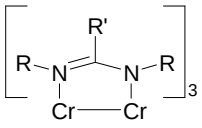	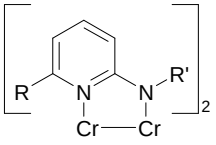	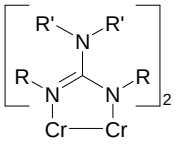
diazadiene	amidinate	lantern amidinate	aminopyridinate	guanidinate

The nature of the fragments R and R' is specified in the text.

Table 2. The different variants of species **2**

Species 2:							
a		b		c		d	
R	R'	R	R'	R	R'	R	R'
2,4,6-$Me_3C_6H_2$	H	2,6-$Et_2C_6H_3$	H	2,6-iPr$_2C_6H_3$	H	2,6-iPr$_2C_6H_3$	Me
1.7404(8) Å		1.7454(1) Å		1.7472(10) Å		1.7395(7) Å	

*Only the variant b of species **2** has been investigated in the present work. No relevant changes are expected to occur for the other variants.*

2. Computational Method

The dichromium compounds discussed in this work were studied using the following scheme based on combined DFT and CASPT2 approach. The CASSCF/CASPT2 multi-configurational quantum chemical method was used to treat the Cr-Cr as well as the Cr-N bonds. For the lantern species (**3**) only the bimetallic unit was treated at the CASPT2 level. For a fixed point on the grid, corresponding to a given value of the Cr-Cr and Cr-N distances, the rest of the geometry was optimized at the DFT level. The DFT calculations employed DZP basis sets and the B3LYP functional using the TURBOMOLE software [**20**]. Due to the size of this molecule, geometry optimization of the Cr_2-guanidinate (**5**) complex employed the triple-zeta valence plus polarization (def-TZVP) basis sets on all atoms along with the PBE functional and resolution of the identity. Analysis of the electronic structure was performed on the DFT/CASPT2 optimized models.

The CASPT2 calculations were performed using the MOLCAS-7.3 package [**21**]. The ANO-RCC basis set with triple-zeta quality (ANO-RCC-VTZP) [**22**] was used for chromium, whereas double-zeta basis set quality (ANO-RCC-VDZP) [**23, 24**] was used for the other atoms. Only for the Cr_2-guanidinate complex, triple-zeta quality basis sets were employed for Cr and N, double-zeta quality on C and minimal basis set (ANO-RCC-MB) on H [**24**]. C_2 symmetry was imposed for the lantern and the Cr_2-guanidinate species, whereas C_i and C_{2h} symmetry was imposed for aminopyridinate and $Cr_2(\mu\text{-}\eta^2\text{-ArNC(R)NAr})_2$, respectively. Scalar relativistic effects were included using the Douglas-Kroll-Hess Hamiltonian [**25**]. The

computational costs arising from the two-electron integrals were drastically reduced by employing the Cholesky decomposition (CD) technique in all CASSCF/CASPT2 calculations [**26, 27**] combined with the Local Exchange (LK) screening [**28**]. The decomposition threshold was chosen to be 10^{-4}, as this should correspond to an accuracy in total energies of the order of mHartree or higher. The Frozen Natural Orbital approach with 70% of the virtual orbitals taken into account was applied to CASPT2 (FNO-CASPT2) for saving disk requirements and reducing computational costs [**29**]. For all the investigated species, orbitals up to and including the 1s for carbon and nitrogen and 2p for chromium were kept frozen.

For species **2**, **4** and **5**, the complete active space (CAS) contains twelve electrons distributed in twelve orbitals (12, 12). This space comprises all the 3d orbitals forming the Cr-Cr multiple bond as well as one bonding and one antibonding orbital describing the Cr-N interactions. The Cr-N bonding and antibonding orbitals are lying lower and higher in energy, respectively, and therefore their occupation numbers are either 2 or 0. For species **3**, only the orbitals describing the Cr-Cr multiple bond were included resulting in 10 and 9 electrons distributed in 10 orbitals, for the reduced and neutral compound, respectively. Species **1** has been investigated in a previous study [**19**].

3. Results

3.1 Cr_2 and amidinate ligands

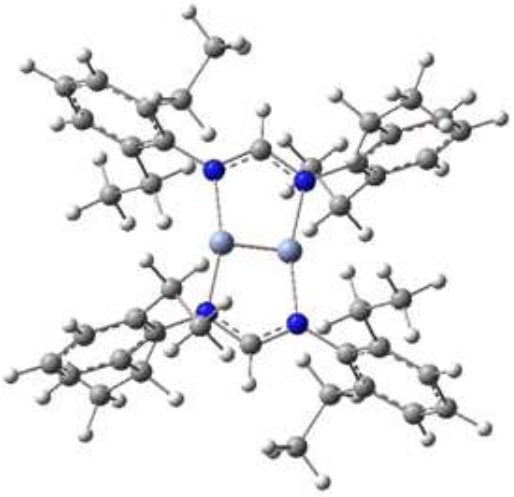

Figure 1. *The Cr_2-amidinate complex* (**2**). Cr is depicted in light blue, N in dark blue, C and H in gray and white, respectively.

Following the successful synthesis of dimolybdenum complex with each metal center coordinated to two nitrogen donors [**30**], Tsai and coworkers extended the same concept to the dichromium species using sterically cumbersome amidinates. In the present study we have investigated the bonding situation in $Cr_2(\mu\text{-}\eta^2\text{-ArNC(R)NAr})_2$ (R=H, Ar=2,6-$Et_2C_6H_3$) at the CASPT2 level of theory. The Cr-Cr and the Cr-N bond lengths optimized at CASPT2 level of theory gave 1.764 and 1.991 Å, respectively, in good agreement with the experimental values of 1.746 and 2.014 Å.

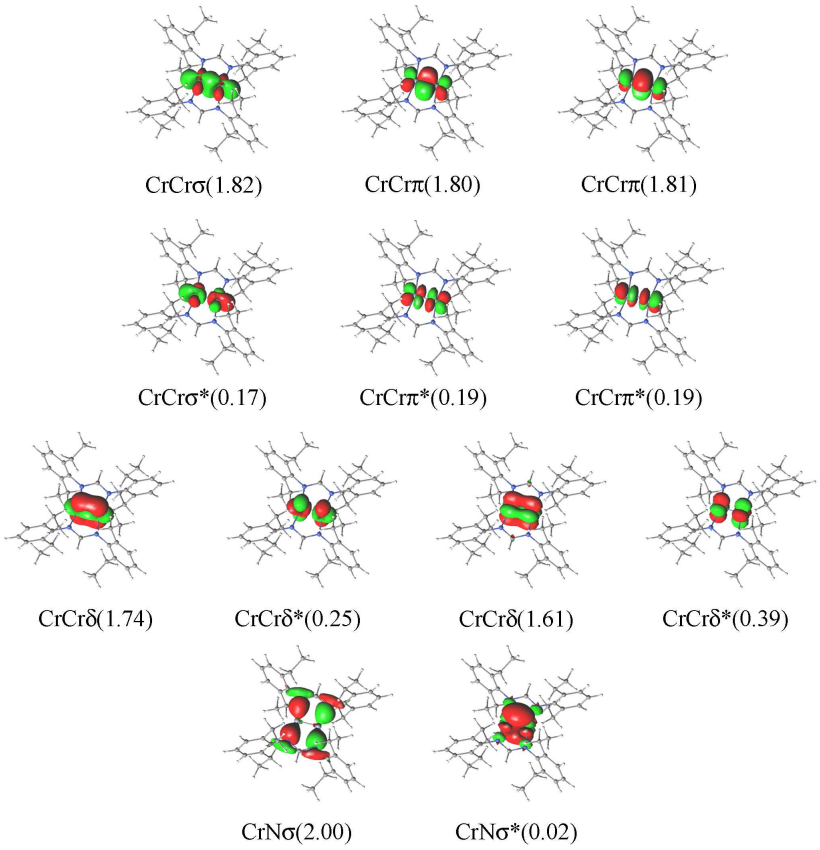

Figure 2. *Cr_2-amidinate species.* Molecular orbitals of the active space and their occupation numbers.

The associated EBO of 3.80 is obtained using the natural orbital occupations numbers (Figure 2). The charge distribution within this compound can be depicted as a combination of two negatively charged ligands stabilizing the central dichromium unit with a formal charge of +2. Although the CrCr core unit is interacting with four equivalent nitrogens (in contrast to the two equivalent carbon atoms in PhCrCrPh), both structure have similar bonding pattern leading to the formation of a formal quintuple bond. An interesting feature characterizing the bonding is the total absence of the Cr-Nπ interaction, which is present in compound **1**. This situation can be explained based on the charge distribution within each ligand. The electron is delocalized over the $N_1C(R)N_2$ fragment and therefore N_1 can be

the N_{amido} nitrogen involved in the bonding with the CrCr, whereas N_2 can be the N_{imino} involved in the π bond with the central carbon atom. Two resonance forms can be drawn, shown as A_2 and B_2 in Figure 2.

The coordination pattern differs in case of species **1**, for which one of the resonance form is of diamido type (B_1 in Figure 3). However, the oxidation state attribution is not so obvious in this case and can be considered in the range from +1 and +2, as reported in a previous work [**19**]. In order to understand how the bond multiplicity is affected by the type of the nitrogen featured by the ligands, it is interesting to look at two closely related ligands, namely RNSi(Me_2)NR and RNC(R')NR, used to stabilize the Mo-Mo unit [**30, 31**]. The difference, eventhough small, is sufficient enough to result in a decrease of the bond order, going from a quintuple to a quadruple bond.

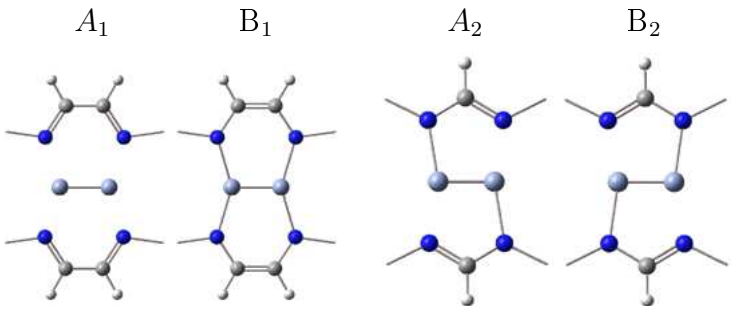

Figure 3. Resonance forms for species **1** (left) and **2** (right).

3.2 Cr_2 and lantern amidinate ligands

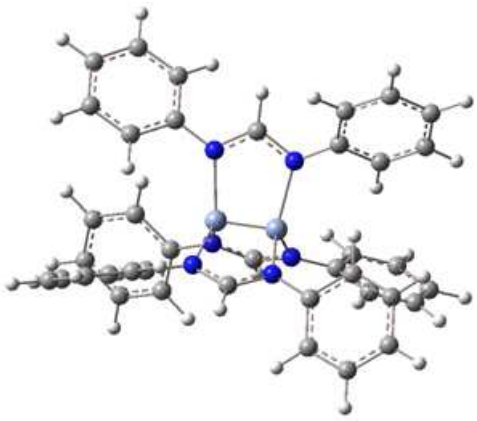

Figure 4. The lantern *Cr_2-amidinate complex (**3**)*. See figure 1 for color coding.

Amidinate molecules proved to be efficient stabilizing ligands for dichromium species resulting in a paddle-wheel type architecture with the dichromium unit residing inside the cage created by $[Ar^{Xyl}NC(H)NAr^{Xyl}]_3$ (Ar^{Xyl}=2,6-C_6H_3-$(CH_3)_2$). In the model used for the present study, the 2,6-C_6H_3 methyl groups were replaced by hydrogens. The most important structural parameters obtained from the DFT/CASPT2 optimizations are the Cr-Cr and the Cr-N bond lengths, which are 1.738 (1.740) and 2.017 (2.092) Å for the reduced species (**3**) and 1.777 (1.817) and 1.982 (2.044) Å for the neutral paramagnetic one (**3**). The experimental bond lengths are reported in brackets. Both theory and experiment confirm a shortening of the Cr-Cr bond when going from the neutral to the reduced species. Such trend arises from the change of the number of electrons involved in the chemical bond. In case of the neutral paramagnetic species, the Cr_2^{3+} unit has a $\sigma^2\pi^4\delta^3$ electronic configuration, whereas the Cr_2^{2+} in the reduced compound has a $\sigma^2\pi^4\delta^4$ electronic configuration, featuring an extra electron. The lack of one electron in the δ bonding orbital in the former case lowers the corresponding bond order.

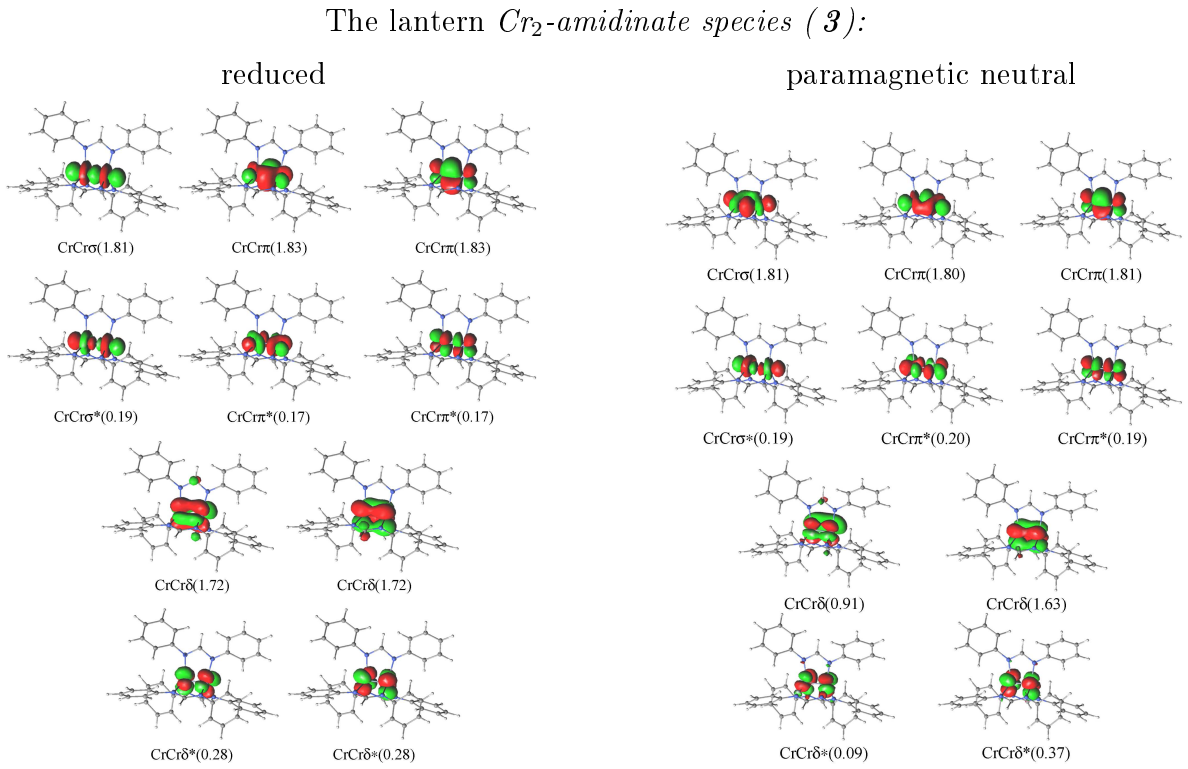

Figure 5. The lantern *Cr_2-amidinate complex (3)*. Molecular orbitals of the active space and their occupation numbers.

The EBO values calculated for these compounds are 3.91 and 3.46 for the reduced and neutral species, respectively. The nature of the chemical bond for the neutral species **3** can be viewed as an intermediate situation between species **1** and **2**, as one of the 3dδ molecular orbital is neither empty (**1**) nor doubly occupied (**2**). The resulting difference in the EBO values caused by the single occupation of the 3dδ orbital is interesting as it shows the important role played by these orbitals in the Cr-Cr bond, eventhough they are characterized by smaller overlap compared to the remaining metal-metal orbitals. Such changes can be only attributed to the occupation number of the δ bonding orbital (Figure 5) as there are no changes to the EBO contribution from the σ and π bonds (Table 3).

3.3 Cr_2 and aminopyridinate ligands

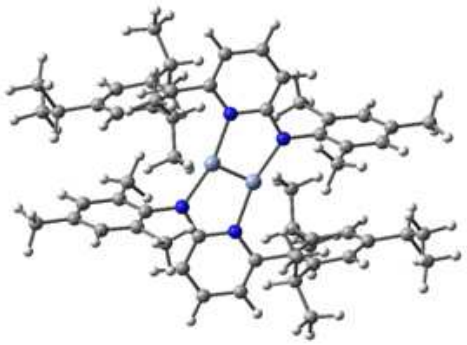

Figure 6. The *Cr_2-aminopyridinate complex (**4**)*. See figure 1 for color coding.

The calculations were performed on a simplified model where the cumbersome (TIP) 2,4,6-triisopropylphenyl and (Mes) 2,4,6-trimethylphenyl flanking aryls were replaced by phenyl groups (**4**). The compound has two types of nitrogen atoms, namely the N_{amido} and $N_{pyridine}$. Species **4** can be described by two resonance forms where the electron can be localized either on the N_{amido} (resonance form 1) or on the $N_{pyridine}$ (resonance form 2). Both nitrogens are involved with the same weight in the interaction with the CrCr core, as indicated by the shape of the Cr-N molecular orbitals (Figure 7) as well as their charge obtained from the Mulliken Population Analysis ($N_{pyridine}$:-0.6294 N_{amido}:-0.7156). As a consequence, the two resonance forms exhibit a single Cr-Nσ interaction which involves either the N_{amido} or the $N_{pyridine}$ atom. The most relevant parameters obtained from the DFT/CASPT2 optimizations are the Cr-Cr, the Cr-N_{amido} and Cr-$N_{pyridine}$ bond distances which are respectively 1.806 (1.749), 1.990 (1.998) and 2.010 (2.028) Å. The experimental bond lengths are reported in bracket. The difference of about 0.06 Å between the experiment and the theory in case of the Cr_2 bond distance might be due to the less pronounced steric hindrance when replacing TIP and Mes groups by the smaller phenyl groups. The effective bond order exhibits a value of 3.65 at the computed equilibrium bond distance.

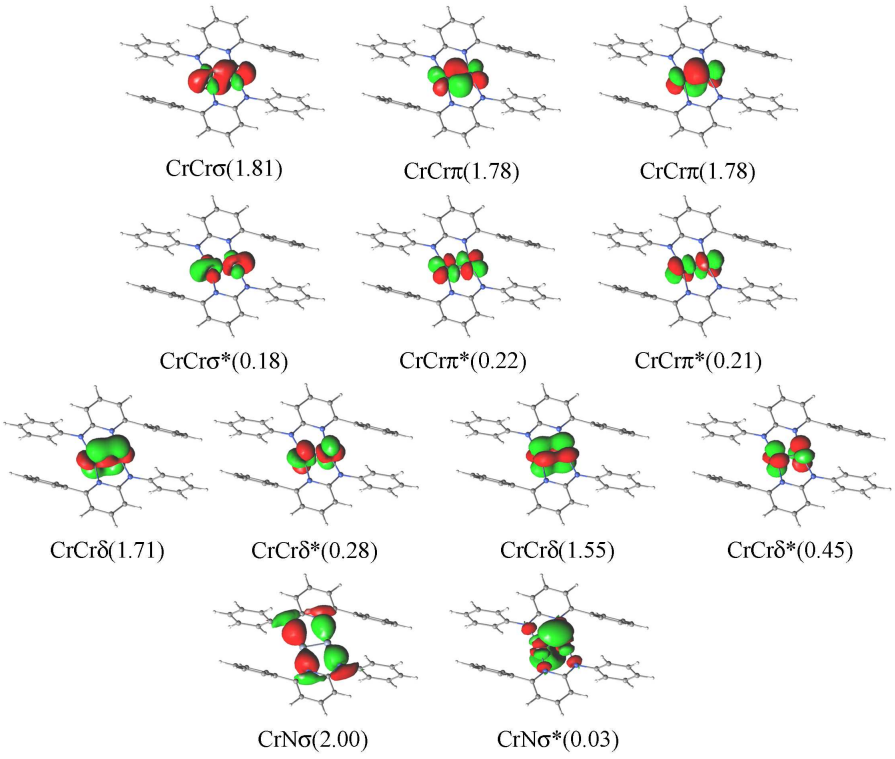

Figure 7. *Cr_2-aminopyridinate species.* Molecular orbitals of the active space and their occupation numbers.

3.4 Cr_2 and guanidinate ligands

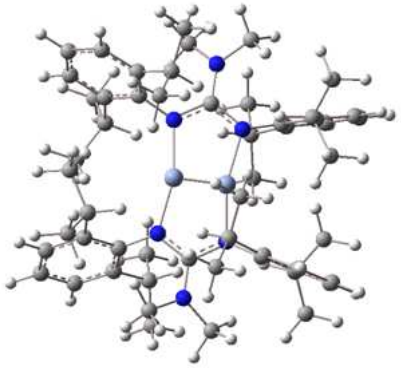

Figure 8. The *Cr_2-guanidinate complex (**5**).* See figure 1 for color coding.

The potential of guanidinates to stabilize short metal-metal distances was shown by Gambarotta and co-workers [**16**]. Very recently Kempe and co-workers succeeded in synthesizing a new homobimetallic chromium complex with guanidinate ligands [**15**], which is visualized in Figure 8. The Cr-Cr bond length is 1.729 Å and is the shortest metal-metal distance reported for a stable compound. A specific feature of this structure is the planar arrangement of the three nitrogen atoms and their residues which are frozen between two bulky 2,6-isopropyl phenyls. Such ligand architecture excludes any out of plane arrangement of the methyl groups attached to the non-coordinating nitrogen atom. These methyl groups push the two 2,6-isopropylphenyl groups further down resulting in a shortening of the metal-metal bond. We have performed two sets of calculations: one on the experimentally synthesized complex (**5**) and one on a model structure, in which the isopropyl substituents were replaced by methyl groups. The Cr-Cr and Cr-N bond lengths optimized at CASPT2 level of theory are 1.752 and 1.990 Å, respectively, in good agreement with the experimental values of 1.729 and 2.022/2.013 Å. In the simplified model, the corresponding optimized bond lengths are 1.772 and 2.002 Å. Thus, having less bulky substituents (and consequently a weaker steric hindrance) affects significantly the Cr-Cr bond length, which increases by about 0.02 Å. This is compatible with the N-C-N fragment acting as a pincer and therefore forcing the two metals to approach each other. The formal charge of each Cr atom is +1. The bonding scheme in the Cr_2-guanidinate complex (**5**) is virtually the same as that in the Cr_2-amidinate (**2**) (Figure 9).

The values for the computed effective bond order for structure **5** and its simplified model are 3.79 and 3.72, respectively. The result show that they are identical in terms of its electronic structure, which supports the assumption that the observed bond lengths are primarily determined by the structural pressure of the ligands rather that changes in the electronic structure.

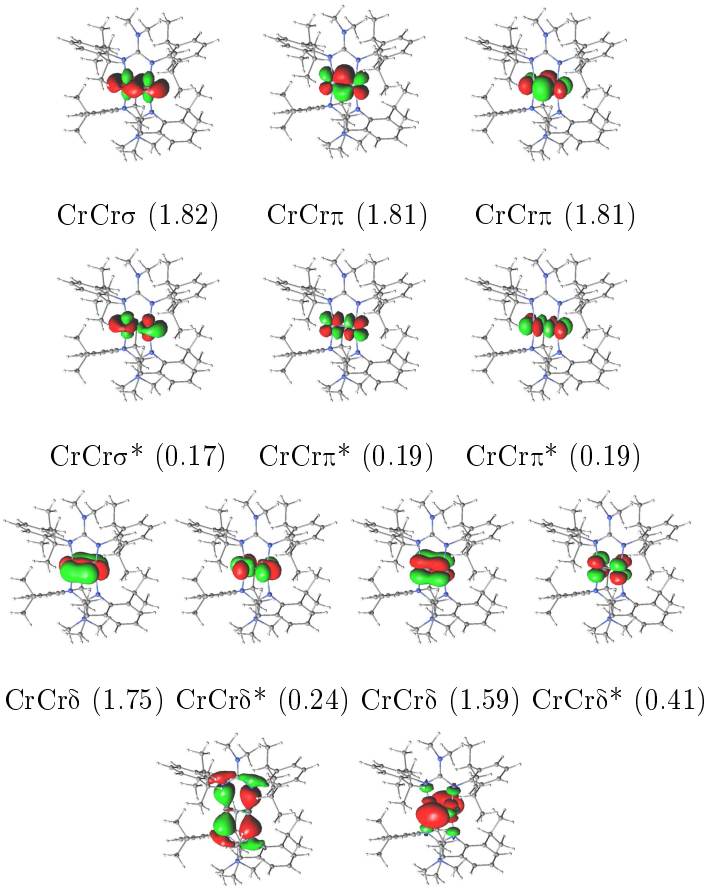

Figure 9. *Cr_2-guanidinate species.* Molecular orbitals of the active space and their occupation numbers.

Table 3. The different contributions to the EBO

Species 2-5: EBO in termo of σ, π and δ contribution											
2			**3**			**4**			**5**		
σ	π	δ	σ	π	δ	σ	π	δ	σ	π	δ
0.83	1.62	1.36	0.81*(0.81)*	1.66*(1.61)*	1.44*(1.04)*	0.82	1.57	1.23	0.83	1.62	1.35
*Total EBO for species **2-5**:*											
3.80			3.91 (3.46)			3.65			3.79		

The total EBO's were calculated using the natural orbital occupation numbers reported in figures 2,5,7 and 9. For species **3**, the values reported in bracket refer to the paramagnetic neutral compound.

4. Discussion

With the most relevant parameters for the different species containing the dichromium unit in hand, we can now attempt to rationalize the results, by establishing a trend between the effective bond order and the Cr-Cr bond length. A quick glance at table 4 doesn't allow drawing any immediate conclusions, since bond length and EBO do not seem to be correlated. However, a more detailed analysis of the plot (Figure 10) of the EBO versus CrCr bond distance, allows to find a linear correlation within the same group of ligands. At this point, one has to recall that the EBO value is a function of the orbital's overlap, which is tightly correlated to their shape and to the effect of the ligands. Therefore, in order to correlate the EBO's with the observable CrCr bond lengths, the analysed compounds have to be divided into subgroups according to the class of the ligand.

Table 4. Cr-Cr, Cr-Ligand bond distance (Å) computed at the CASPT2 level for different species containing the dichromium unit and their EBO value. Ar'CrCrAr' structure was taken from experimental X-ray crystallographic data.

LCrCrL	d(Cr-Cr) Å	d(Cr-L) Å	EBO
Cr_2	1.66	-	4.46
Lantern reduced (**3**)	1.738	2.017	3.91
PhCrCrPh	1.752	2.018	3.52
Cr_2-amidinate (**2**)	1.764	1.991	3.80
Lantern neutral (**3**)	1.777	1.982	3.46
Cr_2-diazadiene (**1**)	1.799	1.909	3.43
Cr_2-aminopyridinate (**4**)	1.806	1.990/2.010	3.65
Cr_2-guanidinate (**5**)	1.752	1.990	3.79
ArCr'Cr'Ar	1.836	2.132	3.43

Figure 10. Correlation between bond order and bond distance.

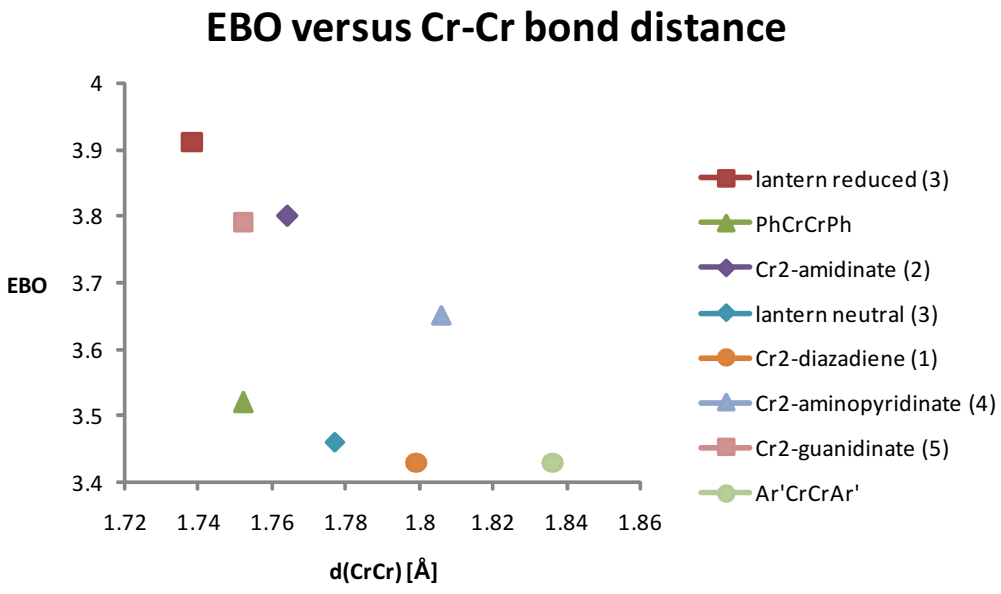

Based on the nature of the ligands two groups can be defined. The first one refers to Ar'CrCrAr' and PhCrCrPh, in which the element coordinating the metal center is a carbon atom. In addition, two carbons, which are interacting with the bimetallic unit do not belong to the same ligand. The second group encompasses species **1** to **5**, in which nitrogen is the element coordinating the metal center. In contrast to the first group, these are bridging ligands and therefore the two nitrogens of a single ligand are able to interact with Cr_2. Such differences have important effects on the dichromium bond distance. Indeed, in the Ar'CrCrAr' species, the role of the ligand seems to be more protective: it acts as a shield against interactions of Cr with the surrounding rather than a pincer meant to allow the two Cr atoms to approach each other. In our previous work [**18**], we have shown that the bulky terphenyl ligand has only very small effect on the chromium-chromium interaction since replacing it by a phenyl group does not affect significantly the optimized CrCr bond length. In addition to their ability to protect the Cr_2 unit, bridging ligands such as amidinates, aminopyridinates and guanidinates can have a direct effect on the Cr-Cr bond length by tuning the size of the residues localized in the outer part of the bulky ligands. Another function of the use of bulky ligands is to keep the nitrogen atom at the correct distance since the shortening of the Cr-N bond length is tightly connected to the dichromium bond distance. The importance of both, forcing the two transition metals to get closer and keeping the nitrogen at the appropriate distance, is suggested also by the calculations performed on the modified aminopyridinate compound. Indeed, replacing the bulky TIP and Mes residues by smaller groups such as phenyl results in a CrCr bond length longer than the experimental one. Such lengthening can be explained by the increase of about one degree of the angle described by the $N_{pyridine}CN_{amido}$ fragment and by a very small change in the Cr-N bond distance.

Closer inspection of Figure 10 shows that two of the studied molecules, species **1** and the neutral form of species **3**, are not in agreement with the general trend observed for the remaining species. The case of complex **1** has been discussed before and its unusual behaviour is the consequence of the CrNπ interaction, which is not present in the other compounds. The neutral form of species **3** is also an exception, connected with its electronic configuration, characterized by a singly occupied δ orbital. Indeed, the reduction of this compound leads to the reduced lantern species, which behaviour is in agreement with the expected linear

correlation trend.

5. Conclusions

The present work allowed us to clearly demonstrate that a linear correlation between the Cr-Cr bond length and the effective bond order exists, if one compares the dichromium compounds belonging to the same class of supporting ligands. The shortening of the Cr-Cr bond length is the result of the stabilization of the bimetallic unit as well as the structural constraint exercised by the ligand on the CrCr core. The latter point is clearly demonstrated by species **1**, which is featuring a short CrCr bond distance associated to a small EBO value. However, one of the most interesting characteristics of the chemical bond is its stability. It can be expressed in terms of the strength of the interaction between two atoms. The strength of the bond can be in turn measured in terms of dissociation energy, a quantity often regarded as the most accurate gauge of the chemical bond stability, but experimentally obtained for very simple molecules only. However its value cannot be directly related to the bond order, which is a quantity of much intuitive sense for chemists. Therefore the use of the effective bond order should be preferred, as it can give a very good flavour of the multiple bond strength when used properly, that is, when applied to the molecules belonging to the same class of compounds. In addition to be intuitive and easy to calculate, the effective bond order can be somehow related to the reactivity of the multiple bonded species. The reactivity can be related in turn to the degree of overlap between the orbitals forming the bond. The δ orbitals are good candidates for such purpose, as their overlap is lower than the one featured by σ and π bonds. Thus, in the cases studied above, a low EBO can be associated generally with a weak interaction between the orbitals forming the two δ bonds, which could be able to interact with external compounds or with the ligand itself. The latter possibility was reported in 2007 [**32**] and was based on metal-ligand charge transfer involving the δ orbital. The former possibility was highlighted very recently [**33**], by the direct carboalumination of a dichromium multiple bond.

Bibliography

[1] Kauffman, G.B. 1973, *Coord. Chem. Rev.* 9, p. 339.

[2] Bertrand, J.A., Cotton, F.A. and Dollase, W.A. 1963, *J. Am. Chem. Soc.* 85, p. 1349.

[3] Bertrand, J.A., Cotton, F.A. and Dollase, W.A. 1963, *Inorg. Chem.* 2, p. 1166.

[4] Cotton, F.A. 1965, *Inorg. Chem.* 4, p. 334.

[5] Cotton, F.A., Curtis, N.F., Harris, C.B., Johnson, B.F.G., Lippard, S.J., Mague, J.T., Robinson, W.R. and Wood, J.S. 1964, *Science* 145, p. 1305.

[6] Cotton, F.A., Curtis, N.F., Johnson, B.F.G. and Robinson, W.R. 1965, *Inorg. Chem.* 4, p. 326.

[7] Cotton, F.A. and Harris, C.B. 1965, *Inorg. Chem.* 4, p. 330.

[8] Cotton, F.A., Murillo, C.A. and Walton, R.A. Multiple bond between metal atoms 3rd ed. Berlin: Springer, 2005.

[9] Nguyen, T., Sutton, A.D., Brynda, M., Fettinger, J.C., Long, G.J. and Power, P.P. 2005, *Science* 310, p. 844.

[10] Cotton, F.A., Koch, S.A. and Millar, M. 1978, *Inorg. Chem.* 17, p. 2084.

[11] Kreisel, K.A., Yap, G.P.A., Dmitrenko, O., Landis, C.R. and Theopold, K.H. 2007, *J. Am. Chem. Soc.* 129, p. 14162.

[12] Hsu, C.-W., Yu, J.-S.K., Yen, C.-H., Lee, G.-H., Wang, Y. and Tsai, Y.-C. 2008, *Angew. Chem. Int. Ed.* 47, p. 9933.

[13] Tsai, Y.-C., Hsu, C.-W., Yu, J.-S.K., Lee, G.-H., Wang, Y. and Kuo, T.-S. 2008, *Angew. Chem. Int. Ed.* 47, p. 7250.

[14] Noor, A., Wagner, F.R. and Kempe, R. 2008, *Angew. Chem. Int. Ed.* 47, p. 7246.

[15] Noor, A., Glatz, G., Müller, R., Kaupp, M., Demeshko, S. and Kempe, R. 2009, *Z. Anorg. Allg. Chem.* 635, p. 1149.

[16] Horvath, S., Gorelsky, S.I., Gambarotta, S. and Korobkov, I. 2008, *Angew. Chem. Int. Ed.* 47, p. 9937.

[17] Brynda, M., Gagliardi, L., Widmark, P.-O., Power, P.P. and Roos, B.O. 2006, *Angew. Chem. Int. Ed.* 45, p. 3804.

[18] La Macchia, G., Gagliardi, L., Power, P.P. and Brynda, M. 2008, *J. Am. Chem. Soc.* 130, p. 5104.

[19] La Macchia, G., Aquilante, F., Veryazov, V., Roos, B.O. and Gagliardi L. 2008, *Inorg. Chem.* 47, p. 11455.

[20] Turbomole v6.0 1989-2007. A development of University of Karlsruhe and Forschungzentrum Karlsruhe GmbH.

[21] Karlstrom, G., Lindh, R., Malmqvist, P.A., Roos, B.O., Ryde, U., Veryazov, V., Widmark, P.O., Cossi, M., Schimmelpfennig, B., Neogrady, P. and Seijo, L. 2003, *Comput. Mater. Sci.* 28, p. 222.

[22] Roos, B.O., Lindh, R., Malmqvist, P.A., Veryazov, V. and Widmark, P.O. 2005, *J. Phys. Chem. A* 109, p. 6575.

[23] Roos, B.O., Lindh, R., Malmqvist, P.A., Veryazov, V. and Widmark, P.O. 2005, *J. Phys. Chem A* 108, p. 2851.

[24] Widmark, P.O., Malmqvist, P.A. and Roos, B.O. 1990, *Theor. Chim. Acta* 77, p. 291.

[25] Hess, B.A. 1986, *Physical Review A* 33, p. 3742.

[26] Aquilante, F., Malmqvist, P.A., Pedersen, T.B., Gosh, A. and Roos, B.O. 2008, *J. Chem. Theory Comp.* 4, p. 694.

[27] Aquilante, F., Pedersen, T.B., Sanchez de Meras, A., Koch, H., Lindh, R. and Roos, B.O. 2008, *J. Chem. Phys.* 129, p. 24113.

[28] Aquilante, F., Pedersen, T.B. and Lindh, R. 2007, *J. Chem. Phys.* 126, p. 194106.

[29] Aquilante, F., Todorova, T.K., Gagliardi, L., Pedersen, T.B. and Roos, B.O. 2009, *J. Chem. Phys.* 131, p. 34113.

[30] Tsai, Y.-C., Lin, Y.-M, Yu, J.-S.K. and Hwang, J.-K. 2006, *J. Am. Chem. Soc.* 128, p. 13980.

[31] Tsai, Y.-C., Chen, H.-Z., Chang, C.-C., Yu, J.-S.K., Lee, G.-H., Wang, Y. and Kuo, T.-S. 2009, *J. Am. Chem. Soc.* 131, p. 12534.

[32] Chisholm, M.H. 2007, *PNAS* 104, p. 2563.

[33] Noor, A., Glatz, G., Müller, R., Kaupp, M., Demeshko, S. and Kempe, R. 2009, *Nature Chem.* 1, p. 322.

Paper IV: Quantum Chemical Calculations Predict the Diphenyl Diuranium Compound [PhUUPh] To Have a Stable ^1A_g Ground State

Quantum Chemical Calculations Predict the Diphenyl Diuranium Compound [PhUUPh] To Have a Stable ^1A_g Ground State

G. La Macchia, M. Brynda and L. Gagliardi

Department of Chemistry, University of Geneva, 30 quai E. Ansermet, Geneva 1211, Switzerland

Published in Angew. Chem. Int. Ed. 2006 (45), 6210 –6213

Abstract

The [PhUUPh] molecule has been studied by multiconfigurational quantum chemical methods. It was found that a quintuple bond is formed between the two uranium atoms with a U-U bond length of 2.29 Å. The phenyl ligand was used to mimic a bulky terphenyl ligand, which could be a promising candidate for the stabilization of multiply bonded uranium compounds.

1. Introduction

Use of sterically hindered ligands to maintain the integrity of normally unstable chemical entities is a widespread technique in modern synthetic chemistry. Bulky aryl and alkyl substituents have been designed to stabilize sensitive compounds, such as main-group-element dimers with multiple bonds [**1**], including the alkyne analogues of heavier Group 14 elements [**2, 3**]. This methodology was recently employed in the generation of a new stable low-valent chromium dimer that, according to experimental and theoretical evidence, exhibited a CrCr quintuple bond [**4, 5**]. The synthesis and characterization of this crystalline compound, [Ar'CrCrAr'](Ar '= C_6H_3-2,6(C_6H_3-2,6-*i*Pr_2)$_2$), has renewed interest in metalmetal multiple bonding. A subsequent computational study [**5**] on a simplified model for [Ar'CrCrAr'], [PhCrCrPh], predicted a fivefold bonding picture with filled bonding orbitals ($\sigma^2\pi^4\delta^4$) as the predominant electronic configuration in the singlet ground state.

In contrast to the multiple bonding between early transition metals, like, for example, the quadruple bond in $K_2[Re_2Cl_8]\bullet 2H_2O$ [**6**], only rare examples of direct MM interactions are known in actinide chemistry. The only known bonds of such type occur in the hydride [H_2UUH_2] [**7**] or in the U_2 species, experimentally trapped in argon matrices [**8**], which we have previously described through high-level calculations [**9**]. In the U_2 dimer [**9**], two uranium atoms bind to form a quintuple bond, thus suggesting that this U_2 unit could form the framework for the development of more diverse diuranium chemistry. The U_2^{2+} cation [**10**] was also found to be metastable, exhibiting a large number of low-lying electronic states with a short bond length of about 2.30 Å, compared to 2.43 Å in the neutral U_2 molecule.

The natural tendency of a uranium atom to be preferentially complexed by a ligand, rather than to explicitly form a direct U-U bond, has to date precluded the isolation of stable uranium species exhibiting direct metal–metal bonding. From the experimental point of view, the synthesis of multiply bonded uranium compounds poses many challenges. Although the uranium ionic radius is not exceedingly large, the presence of many electrons combined with the preference for certain coordination modes with common ligands make the task of stabilizing the hypothetical U-U bond difficult. With the relatively low first ionization energies of 584 ($M \rightarrow M^+$) and 1420 kJmol^{-1} ($M^+ \rightarrow M^{2+}$) and the ground-state electron configuration

corresponding to $[Rn]5f^36d^17s^2$, uranium seems nevertheless to be a promising candidate to form multiply bonded species in actinide chemistry. Despite the fact that this most common actinide exhibits a large range of oxidation states (the most common is U^{+6}, but less common oxidation states such as U^{+2}, U^{+3}, U^{+4}, and U^{+5} are also known), monovalent uranium ions have not yet been formally identified [**11**].

Light atoms that are present in various organic ligands are known to bind tightly to uranium ions [**12-15**]. Furthermore, hexa- or tetrafluoro complexes with U^{6+} and U^{4+} are easily formed [**16**], and tetravalent uranium is also stable in hydroxides, hydrated fluorides, and phosphates [**17**]. Hexavalent uranium is the most stable oxidation state, and the most commonly occurring uranium oxide is U_3O_8. Experimental studies taking advantage of the complex behavior of the f orbitals of uranium result in new variations of the already known moieties described above. For example, recent reports of uranium rings containing bimetallic nitride linkages [**15**] or of an ammonium salt of uranium polyazide, $[U(N_3)_7]^{3-}$ [**14**], show that more can be done in this quickly expanding field.

To obtain direct metal–metal bonds, at least two conditions must be fulfilled. A proper supporting ligand has to be prepared, and one has to control the oxidation state of the dimeric metal moiety. To maximize the bonding interactions between metal centers, the number of orbitals engaged in metal–ligand bonding should be reduced, and each metal center should have a maximum number of valence electrons to fill the remaining bonding orbitals. These criteria can be achieved if the metal is in a low oxidation state and bound to a monodentate ligand. The ligand, in turn, must be sufficiently bulky as to stabilize the metal center and prevent further reaction. In the case of uranium, however, the tendency for the higher oxidation states would suggest that if a multiple bond is to be formed between uranium atoms, such a species would rather bear several ligands on each multivalent U center. We have recently studied computationally such multiply bonded molecules (U_2Cl_6, $[U_2Cl_8]^{2-}$) [**18**]. On the other hand, there is no evidence against formation of a lower oxidation state for uranium, and experimental evidence exists for the formation of several uranium hydrides (UH, UH_2, UH_3, U_2H_2, UH_4, U_2H_4), thus implying that a continuous range of oxidation states is available [**7**].

Although U-O, U-N, and U-C bonds with s character form easily [**19**], several studies indicate that such bonds might already possess a multiple character [**15, 20–24**]. This property is mainly a result of the presence of the 5f and 6d orbitals that can directly participate in the bonding. It is therefore difficult to predict to what extent the bonding between two uranium atoms will be characterized by a higher bond order.

Based on several experimental reports of compounds in which the uranium center is bound to a carbon atom, we have considered the possibility that a {CUUC} core containing two U^{1+} ions could be incorporated between two sterically hindered ligands. Herein, we present the results of a theoretical study of a simplified model for such a hypothetical molecule, namely [PhUUPh]. We have chosen to mimic the bulky terphenyl ligands, which could be potentially promising candidates for the stabilization of multiply bonded uranium compounds, by using the simplest phenyl moiety. We demonstrate that [PhUUPh] could be a stable chemical entity with a singlet ground state.

2. Computational Method

The calculations were performed using the software MOLCAS 6.2 [**25**]. All electron basis sets of atomic natural-orbital type, developed for relativistic calculations with the Douglas–Kroll–Hess Hamiltonian [**26**], were employed for all atoms. For uranium, a primitive set 26s23p17d13f5g3h was contracted to 8s7p5d3f1g. For carbon, the primitive set 14s9p4d3f2g was contracted to 3s2p1d. For hydrogen, the primitive set 8s4p3d1f was contracted to 2s1p. The starting geometries were obtained from DFT geometry optimizations by using the B3LYP exchange correlation functional with the same basis set as described above. The C_{2h} symmetry constraint was imposed during the geometry optimization. Subsequent multiconfigurational wave function calculations, followed by second-order perturbation theory, were performed using the CASSCF/CASPT2 [**27, 28**] method available in MOLCAS 6.2. The active space was formed by 14 molecular orbitals (MOs), which are linear combinations of uranium 7s, 6d, 5f, and carbon (bonded to the U atoms) 2p orbitals. Ten active electrons were distributed in the 14 MOs. In the subsequent CASPT2 calculations the orbitals up to and including the U 5d orbital were kept frozen. Selected bond lengths (U-U, U-C) were reoptimized at the CASPT2 level of theory. Spin–orbit effects were taken into account by using

the RASSCF state interaction method (RASSI) [**29**], which allows CASSCF wave functions for different electronic states to interact under the influence of a spin–orbit Hamiltonian. The CASSCF/CASPT2/RASSI methods and the basis sets used here have been successful in a number of studies on dimetal compounds [**30, 31**]. The effective bond order between the two U atoms in [PhUUPh] was calculated as the sum of the occupation numbers of the bonding orbitals minus the sum of the occupation numbers of the antibonding orbitals, divided by two.

The structures of two isomers were initially optimized using DFT, namely the bent-planar [PhUUPh] isomer **A** and the linear isomer **B** (Figure 1). Starting from a *trans*-bent-planar structure, the geometry optimization for isomer **A** predicted a rhombic structure (a bis(μ-phenyl) structure) belonging to the D_{2h} point group and analogous to the experimentally known species U_2H_2 [**7**]. Linear structure **B** also belongs to the D_{2h} point group. CASPT2 geometry optimizations for several electronic states of various spin multiplicities were performed on selected structural parameters, namely the U-U and U-C bond lengths, while the geometry of the phenyl fragment was kept fixed.

3. Results and Discussion

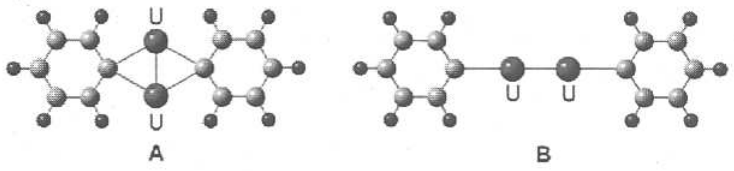

Figure 1. The bent-planar [PhUUPh] isomer (**A**) and the linear [PhUUPh] isomer (**B**).

The most relevant CASPT2 structural parameters for the lowest electronic states of the isomers **A** and **B**, together with the relative CASPT2 energies, are reported in Table 1. The ground state of [PhUUPh] is a ^1A_g singlet with a bis(μ-phenyl) structure (**A**, Figure 1) and an electronic configuration $\sigma^2\sigma^2\pi^4\delta^2$, thus corresponding to a formal U-U quintuple bond. This configuration has a total weight of 49% in the CASSCF wave function. The following occupation numbers are obtained from the CASSCF calculation: σ_g (1.88), σ_u^* (0.06), σ_g (1.65), σ_u^* (0.35), π_u (3.50), π_g^* (0.47), δ_g (1.62), δ_u^* (0.36), thus yielding an effective bond

order of 3.7 between the two uranium atoms.

Table1. Most significant CASPT2 structural parameters and relative energies for the lowest electronic states of isomer **A** and **B** of [PhUUPh].

Isomer	State	d(U-U) [Å]	d(U-C) Å [Å]	U-C-U [°]	C-U-C [°]	ΔE [kcal mol^{-1}]
A	^1A_g	2.286	2.315	59.2	120.8	0
A	^3A_g	2.263	2.325	58.3	121.8	+0.76
A	$^5B_{3g}$	2.537	2.371	64.7	115.3	+4.97
A	$^5B_{3u}$	2.390	2.341	61.4	118.6	+7.00
A	$^3B_{3g}$	2.324	2.368	58.8	121.2	+7.00
A	$^1B_{3g}$	2.349	2.373	59.3	120.7	+7.14
B	$^5B_{2u}$	2.304	2.395		180	+19.67
B	$^3B_{3g}$	2.223	2.430		180	+22.16
B	^3A_g	2.221	2.430		180	+22.69
B	$^1B_{3g}$	2.255	2.416		180	+27.62

It is interesting to compare the electronic configurations of the formal U_2^{2+} moiety in [PhUUPh] and the bare metastable U_2^{2+} cation [**10**]. The U_2^{2+} cation has a singlet ground state with a total orbital angular momentum quantum number (Λ) equal to 10, corresponding to a ^1N_g state. The $^1\Sigma_g^+$ state lies 279 cm^{-1} above the ground state and is degenerate with a triplet state. The ground state of U_2^{2+} has an electronic configuration $\sigma^2\pi^4\delta_g^1\delta_u^1\varphi_g^1\varphi_u^1$, thus corresponding to a triple bond between the two U atoms and four fully localized electrons. In [PhUUPh], the electronic configuration is different, mainly because the molecular environment decreases the coulomb repulsion between the two U^{1+} centers, thus making the U-U bond stronger than in U_2^{2+}. The corresponding U-U bond length (2.29 Å) is also slightly shorter than in U_2^{2+} (2.30 Å). A single bond is present between the U and C atoms. The molecular orbitals that form the chemical bond between the U-U and U-C atoms are represented in Figure 2.

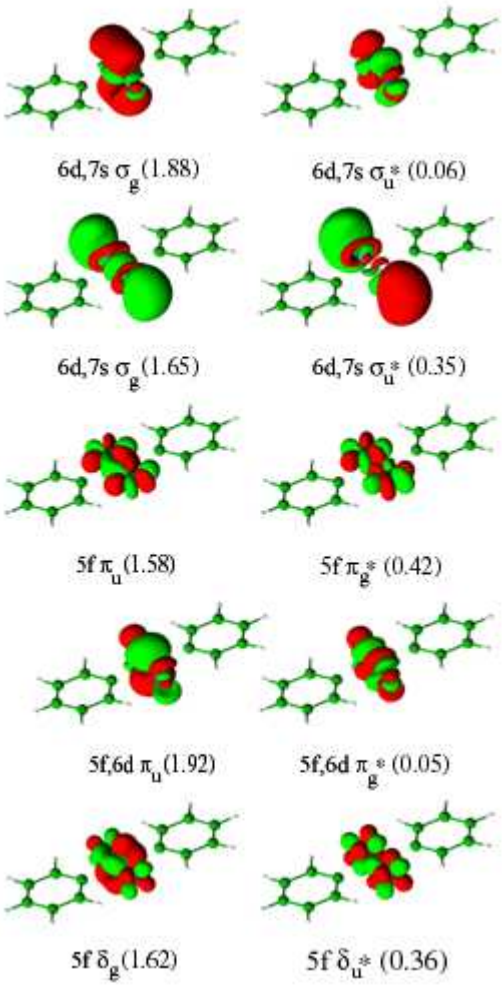

Figure 2. Active molecular orbitals of the bent-planar isomer ^1A_g.

Inspection of Table 1 shows that the lowest triplet state, ^3A_g, is almost degenerate with the ground state (0.76 kcal mol^{-1} higher). Several triplet and quintet states lie 5– 7 kcal mol^{-1} above the ground state. The lowest electronic states of the linear structure lie about 20 kcal mol^{-1} above the ground state of the bis(μ-phenyl) structure.

Since the ^1A_g and the ^3A_g states are close in energy, they may interact through the spin–orbit coupling operator. To evaluate the impact of such an interaction, the spin–orbit coupling between several singlet and triplet states was computed at the ground-state (^1A_g) geometry. First, the ordering of the electronic states is not affected by the inclusion of spin–orbit coupling. Analogous computation with the geometry of the ^3A_g state yields the singlet as the lowest state. The only difference concerns the energy difference $\triangle E_{S1-S2}$ between the two lowest spin states (^1A_g and ^3A_g), which is reduced to 0.3 kcal mol^{-1}.

To assess the strength of the U-U bond in [PhUUPh], its bonding energy was computed as the difference between the energy of [PhUUPh] and those of the two unbound [PhU] fragments. The ground state of [PhU] (with the U, C1, and C2 atoms collinear) was found to be a quartet ($^4B_2$) in C_{2v} symmetry. The CASPT2 Ph-U bond length is 2.38 Å. [PhUUPh] is lower in energy than two [PhU] fragments by about 60 kcal mol^{-1}, with the inclusion of a basis-set superposition error correction.

4. Conclusions

In this work we showed that the diuranium unit could be the framework of a new kind of chemistry exhibiting high bond order. The question that one would like to answer is how to make [PhUUPh] and similar species experimentally. [PhUUPh] could in principle be formed in a matrix—analogous to the already detected diuranium polyhydride species [**7**] by laser ablation of uranium and co-deposition with biphenyl in an inert matrix. The phenyl ligand might however be too large to be made in a matrix, and species such as [CH_3UUCH_3] may be more feasible.

Bibliography

[1] P. Power, *Inorg. Chim. Acta* 1992, 198–200, 443 – 447.

[2] L. Pu, A. D. Phillips, A. F. Richards, M. Stender, R. S. Simons, M. M. Olmstead, P. P. Power, *J. Am. Chem. Soc.* 2003, 125, 11626 – 11 636.

[3] M. Stender, A. D. Phillips, R. J. Wright, P. P. Power, Angew. Chem. 2002, 114, 1863 – 1865; *Angew. Chem. Int. Ed.* 2002, 41, 1785 – 1787.

[4] T. Nguyen, A. D. Sutton, M. Brynda, J. C. Fettinger, G. J. Long, P. P. Power, *Science* 2005, 310, 844 – 847.

[5] M. Brynda, L. Gagliardi, P.-O.Widmark, P. P. Power, B. O. Roos, Angew. Chem. 2006, 118, 3888 – 3891; *Angew. Chem. Int. Ed.* 2006, 45, 3804 – 3807.

[6] F. A. Cotton, N. F. Curtis, C. B. Harris, B. F. G. Johnson, S. J. Lippard, J. T. Mague, W. R. Robinson, J. S. Wood, *Science* 1964, 145, 1305 – 1307.

[7] P . F. Souter, G. P. Kushto, L. Andrews, M. Neurock, *J. Am. Chem. Soc.* 1997, 119, 1682 – 1687.

[8] L. N. Gorokhov, A. M. Emelyanov, Y. S. Khodeev, *Teplofiz. Vys. Temp.* 1974, 12, 1307 – 1309.

[9] L. Gagliardi, B. O. Roos, *Nature* 2005, 433, 848 – 851.

[10] L. Gagliardi, P. PyykkK, B. O. Roos, *Phys. Chem. Chem. Phys.* 2005, 7, 2415 – 2417.

[11] W. J. Evans, S. A. Kozimor, *Coord. Chem. Rev.* 2006, 250, 911 – 935.

[12] T. Arliguie, C. Lescop, L. Ventelon, P. C. Leverd, P. Thuery, M. Nierlich, M. Ephritikhine, *Organometallics* 2001, 20, 3698 – 3703.

[13] M. Brynda, T. A.Wesolowski, K.Wojciechowski, *J. Phys. Chem. A* 2004, 108, 5091 – 5099.

[14] M.-J. Crawford, A. Ellern, P. Mayer, Angew. Chem. 2005, 117, 8086 – 8090; *Angew. Chem. Int. Ed.* 2005, 44, 7874 – 7878.

[15] W. J. Evans, S. A. Kozimor, J. W. Ziller, *Science* 2005, 309, 1835 – 1838.

[16] A. W. Savage, Jr., J. C. Browne, *J. Am. Chem. Soc.* 1960, 82, 4817 – 4821.

[17] V. Vallet, Z. Szabo, I. Grenthe, *Dalton Trans.* 2004, 3799 – 3807.

[18] B. O. Roos, L. Gagliardi, *Inorg. Chem.* 2006, 45, 803 – 807.

[19] J. T. Lyon, L. Andrews, *Inorg. Chem.* 2006, 45, 1847 – 1852.

[20] K. A. N. S. Ariyaratne, R. E. Cramer, J.W. Gilje, *Organometallics* 2002, 21, 5799 – 5802.

[21] R. E. Cramer, J. H. Jeong, J. W. Gilje, *Organometallics* 1987, 6, 2010 – 2012.

[22] R. E. Cramer, R. B. Maynard, J. C. Paw, J.W. Gilje, *J. Am. Chem. Soc.* 1981, 103, 3589 – 3590.

[23] M. Straka, M. Patzschke, P. PyykkK, *Theor. Chem. Acc.* 2003, 109, 332 – 340.

[24] K. Tatsumi, A. Nakamura, *Appl. Quantum Chem. Proc. Nobel Laureate Symp.* 1986, 299 – 311.

[25] G . KarlstrKm, R. Lindh, P.-A. Malmqvist, B. O. Roos,U. Ryde, V. Veryazov, P.-O. Widmark, M. Cossi, B. Schimmelpfennig, P. Neogrady, L. Seijo, *Comput. Mater. Sci.* 2003, 28, 222 – 239.

[26] B . A. Hess, *Phys. Rev. A* 1986, 33, 3742 – 3748.

[27] B . O. Roos in Advances in Chemical Physics, Ab Initio Methods in Quantum Chemistry, Vol. II (Eds.: K. P. Lawley), Wiley, Chichester, 1987, chap. 69, p. 399.

[28] K. Andersson, P.-A. Malmqvist, B. O. Roos, A. J. Sadlej, K. Wolinski, *J. Phys. Chem.* 1990, 94, 5483 – 5488.

[29] B . O. Roos, P.-A. Malmqvist, *Phys. Chem. Chem. Phys.* 2004, 6, 2919 – 2927.

[30] L. Gagliardi, B. O. Roos, *Inorg. Chem.* 2003, 42, 1599 – 1603.

[31] F . Ferrante, L. Gagliardi, B. E. Bursten, A. P. Sattelberger, *Inorg. Chem.* 2005, 44, 8476 – 8480.

Part 4

Summary and concluding Remarks

A lot of work has been achieved since Cotton's discovery of the quadruple bond in $[Re_2Cl_8]^{2-}$. No real breakthrough was performed during 40 years until the discovery of Ar'CrCrAr' in 2005. This compound was featuring a formal quintuple bond although its Cr-Cr bond distance (1.835 Å) was longer than the value of 1.828 Å exhibited by the quadruply bonded Tetrakis (2-methoxy-5-methylphenyl) dichromium compound. The last few years witnessed great progresses in synthesising compounds featuring formal quintuple bonds. The ability of the terphenyl in isolating high order bond multiplicity resurrected the interest in finding new molecules featuring formal quintuple bond and exhibiting Cr-Cr bond length shorter than the one characterizing the previously synthesized compounds.

The discovery that already well known frameworks like amidinates, aminopyridinates and guanidinates were very good candidates for the isolation of increasingly shorter Cr-Cr bond distances resulted in the reduction of the gap with the bare dichromium bond length, reported experimentally to be 1.68 Å. The reason of such shortening is quite intriguing and requires some explanations. The answer can be already found looking at the environment surrounding the bimetallic unit. All the studied ligands are suitable to protect the transition metal core unit. Since the performed computational studies mentioned in this work were performed in gas phase, such property was not investigated. Although we are not describing the solvent effects, were are however able to point out the effects of the ligands on the dichromium unit. The terphenyl ligand, when chromium is involved, has no real influences on the dichromium bond length and his role is limited to protect the inner part of the molecule against external interactions. The ligands containing nitrogen are more useful, since in addition to their shielding function they can apply pressure on the bimetallic unit. Such feature is the consequence of their architecture. Contrary to the terphenyl, amidinates, aminopyridinates, diazadienes and guanidinates are bridging ligands. Indeed, each ligand is coordinated to the two metallic centers. It appears therefore obvious that playing with the N-R-N fragment, that is varying the N-N distance, will allow to change the Cr-Cr bond length. For such purpose, guanidinates seem to be the best candidate since the substitution of the outer residues has more effect in bending the N-R-N fragment. The latter can be associated to a pincer forcing the two chromiums to get closer. The ligand has to be able as well to keep a relatively long Cr-N bond length since the shortening of the Cr-N bond is directly correlated to the

lengthening of the Cr-Cr distance.

Nowadays the strategy for isolating quintuple bond featuring very short Cr-Cr bond length is well defined. However, finding an application to the aforementioned compounds is not an easy task and up to now only few examples of reactivity, such as carboalumination, were reported. This issue make the synthesis of such compounds more complicate and one has to decide what is the ultimate target: isolating very short Cr-Cr bond distances or finding some applications to these compounds. Both objectives seem to be mutually excluded and therefore some choice will have to be done.

Nowadays, the research on d-block transition metal dimers seems finally to provide some reactivity for such kind of compounds. Unlike for transition metals, the investigations on heavy elements such as di-actinides are still at the embryonal stage, mainly due to difficulties in experimental manipulations. Nonetheless, the work on PhUUPh and the analysis of its electronic configuration are signals that a chemistry based on such framework is possible.

Part 5

List of publications of G. La Macchia

(1) *Quantum Chemical Calculations Predict the Dipheny Diuranium Compound [PhU-UPh] to have a stable ^1A_g ground state*
G. La Macchia, M. Brynda and L. Gagliardi
Angewandte Chemie International Edition, 45(37), 2006, p6210-6213

(2) *Theoretical Prediction of linear free energy relationships using proton nucleomers*
G. La Macchia, L. Gagliardi, G.S. Carlson, A.N. Jay, E. Davis and C.J. Cramer
Journal of Physical Organic Chemistry, 21(2), 2008, p136-145

(3) *Large Differences in secondary metal-arene interactions in the transition metal dimers ArMMAr (Ar=Terphenyl; M=Cr,Fe or Co): Implication for Cr-Cr quintuple bonding*
G. La Macchia, L. Gagliardi, P.P. Power and M. Brynda
Journal of the American Chemical Society, 130(15), 2008, 5104-5114

(4) A theoretical study of the ground state and lowest excited states of $PuO^{0/+/+2}$ and $PuO_2{}^{0/+/+2}$
G. La Macchia, I. Infante, J. Raab, J.K. Gibson and L. Gagliardi
Physical Chemistry Chemical Physics, 10 (2008), p7278-7283

(5) Bond Length and Bond Order in One of the Shortest Cr—Cr Bonds
G. La Macchia, F. Aquilante, V. Veryazov, B.O. Roos and L. Gagliardi
Inorganic Chemistry 47 (24) (2008), p11455-11457

(6) *Amidinato– and Guanidinato–Cobalt(I) Complexes : Characterization of Exceptionally Short Co–Co Interactions*
C. Jones, C. Schulten, R.P. Rose, A. Stasch, S. Aldridge, W.D. Woodul, K.S. Murray, B. Moubaraki, M. Brynda, G. La Macchia and L. Gagliardi
Angewandte Chemie International Edition, 48 (40) (2009)

(7) *Correlation between the effective bond order (EBO) and a Cr-Cr bond distance in different classes of compounds*
G. La Macchia, G. Li Manni, T. K. Todorova, M. Brynda, B.O. Roos and L. Gagliardi
submission stage

(8) *Ionization Potentials of neutral and cationic actinide mono- and di-oxydes: a theoretical investigation*
Ivan Infante, Attila Kovacs, Giovanni La Macchia, Abdul Rehaman Moughal Shahi, and Laura Gagliardi
submission stage